Characterization and Patterned Polymer Films from a Novel Self-Assembly Process

by

Yanjing Liu

Dissertation submitted to the Faculty of the

Virginia Polytechnic Institute and State University

in partial fulfillment of the requirements for the degree of:

DOCTOR OF PHILOSOPHY

IN

CHEMISTRY

APPROVED:

G. Alan Schick, Chairman

Mark R. Anderson

Seshu B. Desu

John C. Schug

James P. Wightman

May 3, 1996

Blacksburg, Virginia

Keywords: Self-Assembly, Photolithography, Organic Thin Films, Multilayers, Pattern.

CHARACTERIZATION AND PATTERNED POLYMER FILMS FROM A NOVEL SELF-ASSEMBLY PROCESS

by

Yanjing Liu

Committee Chairman: Dr. Alan G. Schick

Chemistry

(ABSTRACT)

The layer-by-layer molecular-level manipulation of ionic polymer have been utilized to fabricate ultrathin multilayer films (SAMp). In this process, monolayers of polycations and polyanions are sequentially adsorbed onto a substrate surface by alternately dipping the substrate into aqueous solutions of poly(vinylamine) backbone azo (PDYE), poly(sodium 4-styrenesulfonate) (PSS), and poly(allylamine hydrochloride) (PAH). The ionic attractions developed between the oppositely charged polymers promote strong interlayer adhesion and a uniform and linear multilayer deposition process. UV/Vis absorbance, contact angle, and ellipsometry measurements revealed that in all cases the bilayer deposition process was linear and highly producible from layer to layer and film thickness of up to 1 μm can be easily obtained by repeating the deposition process. The typical thickness of bilayer film depend on the solution concentration. Contact angle and UV/Vis spectroscopy measurements demonstrated that the deposition time for a full monolayer coverage of azo dye and PAH was about 20 seconds. Our results showed that the mechanical stability of these SAMp films was remarkable, and SAMp films can only be removed from the substrate by scraping. SAMp films are stable in the common organic solvents and even in the high acidic media (6M HCl aqueous solution). The conformation of these films are thermally stable at high temperature.

In an attempt to develop patterned surfaces of sulfonate and thiol functionality, close-packed, well-ordered (3-mercaptopropyl)trimethoxysilane (MPS) monolayer were formed on the surfaces of single crystal silicon, quartz, and glass by allowing hydrolyzed silane to self-assemble from a dilute hydrocarbon solution. The films of MPS were irradiated with an ozone-producing UV light source results in efficient conversion of the surface-localized thiol groups to sulfonated groups, a complete photo-oxidation of the thiol surface was obtained and characterized by x-ray photoelectron spectroscopy (XPS) and contact angle measurements. Sulfonated self-assembled films can be used as good organic templates for the deposition of SAMp films and for micropatterning of organic surfaces based on our results. Such results significantly extend the application of SAMp films since the sulfonate-functionalized surface can be introduced into the surfaces of aromatic polymers, metals, ceramics, semiconductors, and plastics. So that the process of SAMp deposition can be carried out onto many different substrate surfaces.

The novel self-assembly technique combined with photolithography was used to develop three different methods of micropatterning fabrication in an attempt to achieve the goal of full-color flat-panel display. The characteristic of distinguishing our methods from the existed ones is that the patterning is done first and then the vertical multilayers were built-up on the patterned areas. Moreover, in this process, SAMp films were used as active species. Scanning Electron Microscopy (SEM) was employed to confirm the patterning technique. In order to block the further growth of the second film type on the sites of first film type, several molecules with inert function groups were tried. UV/Vis absorbance and contact angle measurements revealed that dodecyltrimethylammonium bromide (DTAB) atop the PAH/PSS SAMp film could prevent further adsorption of the ionic polymers.

ACKNOWLEDGEMENTS

First of all, I would like to sincerely thank my research advisor, Dr. G. Alan Schick, for his excellent scientific guidance, inspiration, confidence and financial support. Throughout my Ph.D. work, he has always provided encouragement and allowed me to pursue my own ideas and directions. I would also like to thank my committee members - Dr. Mark R. Anderson, Dr. Seshu B. Desu, Dr. John C. Schug and Dr. James P. Wightman, for their invaluable advice, continued assistance and interdisciplinary discussion.

Deepest appreciation specially goes to Dr. James P. Wightman - with whom I always obtained the generous support and the easy access to his lab equipment such as contact angle Goniometer, ellipsometer, and computer. Without his support, I could never finish this project in this period. Sincere gratitude is expressed to Dr. Seshu B. Desu for his continuous and invaluable aid from his kind donation of the silicon and ITO samples to allow me to use his equipment such as spin-coater, sputter. Sincere appreciation also goes to Dr. Mark R. Anderson and those people in his group for continuous providing me with invaluable assistance in carrying out my research, I sincerely value your friendship and support.

Many thanks go to Dr. Youxong Wang, Dr. Wei Pan, Dr. Limin Dong, Dr. Qing Ji, Dr. Hideko T. Oyama, Dr. Shu Liu, Dr. Xiaowei Sun, Frank Cromer, Hong Zhuang, Donghang Xie, Heng Shi,. Minghui Zhang, Yuwen Wang, Lance Wang, and Mingfei Chen for your technical assistance in carrying out my research.

Thanks also go out to my fellow group members, both past and present - Rajesh K. Tiwari, Zigi, Sun, Robin Wood, Doug Moses, and Tod Hucheson. I sincerely appreciate your friendship as well as assistantship in the lab.

I would like to express my most cordial appreciation to my wife, Wei Sun, for her love, constant support, understanding and the sacrifice of her job as a doctor. This degree belongs to you, too. I also thank my son, Zhao, for his love, support, and hard work to adopt a completely different atmosphere here. Finally, the utmost appreciation are sent to my beloved parents and parents-in-law, for their continued encouragement, support, and love throughout graduate school.

TABLE OF CONTENTS

LIST OF FIGURES

Chapter 1

Introduction

1.1 General

Ultrathin films and multilayered structures have gained increasing interest during the last decade due to their potential applications in a variety of areas, including x-ray optics [1], nonlinear optics [2], waveguides, microstructural electronics, optical and biological sensors [3-5], material protection (corrosion resistance) and coating techniques [6]. Most of these tasks require the preparation of well defined films composed of molecules with appropriate properties in a unique geometrical arrangement with respect to each other and to the substrate. Molecularly thin films offer the possibility to construct multilayer assemblies in which the distance between two molecules along the layer normal can be controlled in the Angstrom range [7].

Today there exists four principal methods for the preparation of ultrathin organic multilayer films: the Langmuir-Blodgett (LB) technique [8-10], spin coating [11-13], self-assembly monolayers (SAMs) through chemisorption [14-16], and self-assembly monolayers through physisorption [17-18]. The preparation method can influence the properties of the films by affecting the structure and degree of order in the films. Langmuir-Blodgett deposition of performed monolayers from a gas-liquid interface to a solid planar substrate can provide well-ordered, densely packed mono- and multilayered systems, but rather inconvenient for automation and large scale application. LB multilayers are also mechanically unstable, and held together primarily by van der Waals force [4,9]. Spontaneous self-assembly monolayers (SAMs) adsorbates onto solid substrates can provide densely packed monolayers and has recently been extended to the formation of multilayers in selected systems [19-20], the presence of covalent bonds or ionic attraction between layers provide additional stability not seen in LB systems. However, each layer is

grafted onto the previous one, requiring chemical reactions with a high yield in order to preserve the surface density of functional groups in each layer, in many SAMs systems, adsorption of multilayers displaying structural order has proven difficult. The method of solution spin casting yields layered structures and is often used to deposit the photoresist films used in the lithographic stages of microelectronic manufacturing process. The flow of the liquid is governed by a balance between centrifugal driving force and viscous resisting force [19]. But there are radial variations in film thickness and concentration, and the film thickness and uniform rely on the solvent concentration, viscosity, spin rates and diffusion. Recently the self-assembly monolayers through physisorption has been explored by Decher [17] and others [18]. Self-assembly via physical adsorption is a particularly simple means of creating films containing both polymers and surfactants. It needs neither performance of oriented films nor special equipment. Electrostatically attractive interaction between the anionic, cationic molecules or appropriated substrates forces molecules to pack closely on the substrate. Thus, organic molecules and inorganic molecules can spontaneously form highly ordered and oriented multilayers.

On the other hand, there has been substantial interest recently in the potential use of organic polymers for advanced display technologies from full-color flat screens for portable computers to equipment for high-definition television images. The interest in polymer dyes for such applications is derived from their high emission quantum efficiencies, broad range of available emission wavelengths, high thermal stability, simplicity to manufacture and the ability to prepare large areas. For technologists, designing and building flat-panel and projection displays are still stiff challenges, many activities such as materials processing and lithography need to be developed in order that blue, green and red color molecules pixels can be aligned on the substrates. Conventional spin-coated photoresist materials exhibit large pinhole densities and variations in thickness.

SAMs are two-dimensional, layered, and dense-packed films, but unfortunately cannot provide thick films. Related investigations are limited to maximum layer numbers of 8 to 12. Thus, SAMs are commonly used as resist films for patterning applications [20-21]. In contrast, LB films are two-dimensional, layered, crystalline solids that provide high control of film thickness and are impermeable to plasma to depths of 40 nm [22]. Although LB films have proven to be excellent resist materials capable of a line resolution of submicron, they cannot be used as the candidates for active full-color light-emitting pixels due to their vital and inconvenient deposition process.

Up to now, all the existing patterning methods of thin films have a common process: first, the films are deposited as resists, then the spatial pattern are formed by selectively etching the films. The major challenge towards development of a flat full-color display is that the patterns need to be formed first. Different color light-emitting pixels then, combined with some endcapping techniques, can be alternatively deposited and aligned on the 2-dimensional substrates one by one.

The ultimate goal of this work is the development of advanced display technologies with the novel self-assembly films and photolithography. The objective of this study was three-fold. The first objective was to confirm and characterize the build up of multilayer polymer thin films on silicon by the molecular self-assembly process through physisorption so that a better understanding of the technique may be obtained. Here, the stepwise growth process, the monolayer and multilayered structures with the different concentrations, deposition times, and chemical- and heat-resistant treatments were studied in chapter 3. Next, a complete photo-oxidization of the thiols surface has been first obtained and characterized. The sulfonate ($-SO_3H$) groups provide both a high degree of local (surface) acidity and of net negative charge, thus promoting the hydrolysis and surface attachment of the polycation molecules. Selective deposition of multilayer polymer

films via photopatterning using sulfonate- and thiol-functionalized self-assembled monolayers (SAMs) as the new organic template has been studied discussed in chapters 4 and 5. The final objective was to develop novel methods of patterning ultrathin ionic polymer films by the self-assembly process and photolithography. The distinguishing characteristic of our methods is that the patterns are formed first, then the thick multilayer films selectively are adsorbed on the open regions without using any etchants. In order to selectively grow the second system of polymer film only on the bare silicon regions, the blocking effects of several surfactants on the atop of the first system of polymer film were studied in chapter 6.

1.2 References

1. T. W. Barbee Jr., *Proc. Soc. Photo-Opt. Instrum. Eng.*, **563**, 2 (1985); E. Spiller, in *Physics, Fabrication, and Application of Multilayered Structures*, P. Dhez and C. Weisbuch, Eds. Plenum, New York, pp.271-309, 1988.
2. H. E. Katz et. al., *Science* **254**, 1485 (1991).
3. H. E. Katz and M. L. Schilling, *Chem. Mater.* **5**, 1162 (1993).
4. A. Ulman, *An Introduction to Ultrathin Organic Film From Langmuir-Blodgett to Self-Assembly*, Academic Press, Boston, MA, 1991.
5. W. Gopel, and Ch. Ziegler, eds., *Nanostructures Based on Molecular Materials*, VCH Publishers Inc., New York, NY, 1992.
6. J. D. Swalen, D. L. Allara, J. D. Andrade, E. A. Chandross, S. Garoff, J. Iaraelachvili, T. J. McCarthy, R. Murray, R. F. Pease, J. F. Rabolt, K. J. Wynne, and H. Yu, *Langmuir*, **3**, 932 (1987). H. Shin, R. J. Collins, M. R. De Guire, A. H. Heuer, and C. N. Sukenik, *J. Mater. Res.*, **10**, 3, 692 (1995).

7. G. Decher, and J. D. Hong, *Makromol. Chem., Macromol. Symp.*, **46**, 321 (1991).

8. K. B. Blodgett, *J. Am. Chem. Soc.*, **57**, 1007 (1935).

9. G. L. Gaines, Jr. *Insoluble Monolayers at Liquid-Gas Interface*, Interscience Publishers, New York, 1966. H. Fuchs, H. Ohst, and W. Prass, *Adv. Mater.*, **3**, 10 (1991).

10. G. A. Schick, I. C. Schreiman, R. W. Wagner, J. S. Lindsey, and D. F. Bocian, *J. Am. Chem. Soc.*, **111**, 1344 (1989).

11. G. Coulon, Macromolecules, 22, 2581 (1989).

12. G. Gustafsson, Y. Cao, G. M. Treacy, F. Klavetter, N. Colaneri, and A. J. Heeger, *Nature*, **357**, 477 (1992).

13. P. L. Burn, A. B. Holmes, A. Kraft, D. D. C. Bradley, A. R. Brown, R. H. Friend, and R. W. Gymer, *Nature*, **356**, 47 (1992).

14. J. Sagiv, *J. Am. Chem. Soc.*, **102**, 92 (1980).

15. M. Gatin, and M. R. Anderson, Vibration Spectroscopy, 5, 255 (1993).

16. C. D. Bain, E. B. Troughton, Y. T. Tao, J. Evall, G. M. Whitesides, and R. G. Nuzzo, *J. Am. Chem. Soc.*, **111**, 321 (1989).

17. G. Decher, and J. D. Hong, *Ber. Bunsen-Ges. Phys. Chem.*, **95**, 1430 (1991); G. Decher, J. D. Hong, and J. Smith, *Thin Solid Films*, **210/211**, 504 (1992); Y. Lvov, F. Essler, and G. Decher, *J. Phys. Chem.*, **97**, 13773 (1993).

18. M. Ferreira, J. H. cheung, and M. F. Rubner, *Thin Solid Films*, **244**, 806 (1994); D. Ingersoll, P. J. Kulesza, and L. R. Faulkner, *J. Electrochem. Soc.*, **141** 140 (1994).

19. N. Tillman, A. Ulman, and T. L Penner, *Langmuir*, **5**, 101 (1989).

20. H. Lee, L. J. Kepley, H. G. Hong, and T. E. Mallouk, *J. Am. Chem. Soc.*, **110**, 618 (1988). S. D. Evans, A. Ulman, K. E. Goppert-Berarducci, L. J. Gerenser, *J. Am. Chem. Soc.*, **113**, 5866 (1991).

19. D. E. Bornside, C. W. Macosko, and L. E. Scriven, *J. Appl. Phys.*, **66**, 11, 5185 (1989).

20. G. P. Lopez, H. A. Biebuyck, and G. M. Whitesides, *Langmuir*, **9**, 1513 (1993).

21. W. J. Dressickm and J. M. Calvert, *Jpn. J. Appl. Phys.*, **32**, 5829 (1993).

22. A. Barraud, *Thin Solid Films*, **99**, 317 (1983).

Chapter 2
Literature Review

This chapter will provide some perspective for the orignial work in the areas of organic ultrathin film fabrication and patterning technologies which will be presented in the chapters to follow. First, a general review about the preparation methods of ultrathin organic films ·such as Langmuir-Blodgett (LB) technique, self-assembled monolayers through chemisorption (SAMs) and self-assembly multilayers through physisorption (SAMp) will be addressed. Then a background in the areas of fabrication of various patterns using ultrathin films, photochemistry and lithography techniques will be presented. A comprehensive review dealing all aspects of this work would be very extensive. Therefore, only relevant SAMp and patterns based on lithography will be throughly reviewed.

2.1 Preparation Methods of Ultrathin Organic Films

2.1.1 Langmuir-Blodgett Films

Langmuir-Blodgett (LB) is the first technique to provide us with th practical capability to construct ordered molecular assemblies base on the interlayer interaction of van der Waals force, The L-B technique makes use of amphiphilic (or semiamphiphilic) molecules (*i.e.* molecules which have both a hydrophilic head and an hydrophobic chain) to make a monomolecular film on the surface of water, and then transfer it to a solid substrate in the form of superimposed monomolecular layers (Fig. 1.1), such films have either hydrophobic or hydrophilic surfaces, depending upon which direction the substrates last moved through the surfaces. These lamellar structures are usually highly organiczed in

which the hydrophilic heads form double polar planes separatedly by a double hydrophobic inert plane [1]. These built-up films can be made to consist of as many as hundred layers.

The history of L-B technique may date back to as early as Aristotle when he spoke on the subject of "spreading oil on troubled water" [2]. However, it seems that Benjamin Franklin carried out the first preparation of such film when he showed that a layer of oil had a calming influence on the water in the Clapham ponds [2]. It was in the 19th century that Agnes Pockels prepared the first monolayers at the water-air interface [3-4]. After Langmuir carried out the first systematic study of monolayers of amphiphilic molecules at the water-air interface [5], Blodgett first studied the deposition of multilayers of long-chain carboxylic acid onto a solid substrate [6-7]. Only after Kuhn illustrated us his fantastic stride in molecular architecture in the 1960s [8-9], the field of L-B films has developed steadily. In the last 15 years, it has literally exploded [2, 10-15], owning to the use of L-B method as a molecular ordering method in quite a large range of disciplines: nonlinear optics [16], novel organic conducting materials [17], biology [18], molecular electronics [19], sensors [20], surface catalysis [21], resist [22], solid-state chemistry and physics [23].

2.1.2 Self-Assembled Monolayers (Chemisorption)

Self-assembled monolayers (SAMs) are molecular assemblies that are formed spontaneously by the immersion of an appropriate substrate into a solution of an activel surfactant in an organic solvent [a1]. The pioneer studies were carried out by Sagiv [24], Hubbard [25], and Allara [26] in the early 1980s. There are several types of self-assembly methods which yield organic monolayers. These include organosilicon on hydroxylated surfaces (SiO_2 on Si, Al_2O_3 on Al, glass) [24,27-28]. Alkanethiols on gold [29-30], silver

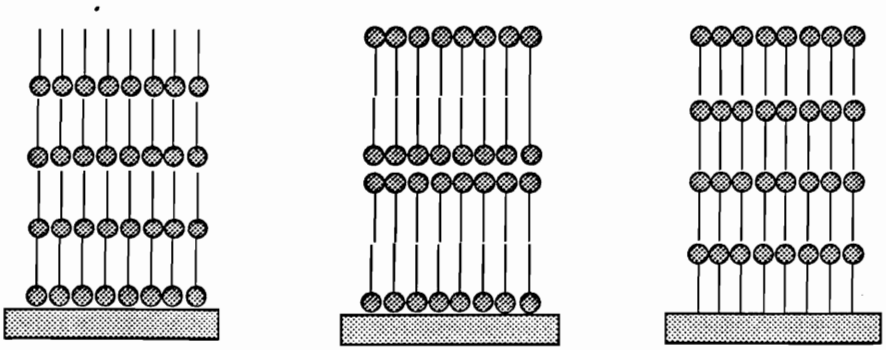

Fig. 2.1 Schematic representation of Langmuir-Blodgett films.

[31], amd copper [32]; dialkyl sulfides and disulfides on gold [33-34]; alcohols and amines on platinum [35]; carboxylic acids on aluminum oxides [36] and silver [37].

A self-assembled monolayers are prepared by submerging a substrate into a solution of active self-assembling surfactant molecules. The very strong interaction between the head group e.g., alkylsilane derivatives $RSiX_3$, $-R_2SiX_2$ or R_3SiX (where X is chloride or alkoxy and R is a hydrocarbon group) and the substrate, (e.g., SiO_2, TiO_2), result in head group pinned to a specific surface site through a chemical bond with the rest of the molecule pendant. The monolayer formation is spontaneous and the process may take from several seconds to hours depending on the adsorbing species, the surface and solvent conditions.

Extensive literature exists on reaction of organosilane derivatiives with hydroxylated surfaces, primarily silica substrates. During the adsotpion, Si-Cl bonds react with the OH groups present on the surface of the substrate and with trace water [38], to form a network of Si-O-Si bonds [39]. Thus, a monolayer is formed in which the molecules are connected both to each other and to the surface by strong chemical bonds. A schematic view of a monolayer is shown in Fig. 2.2. The construction of self-assembled multilayers requires that the monolayer surface be modified to provide a terminating functional group so that a subsequent monolayer can be adsorbed on the "activated" monolayer, thus, densely packed SA multilayer films may be built up by repeating this process (Fig. 2.3). However, since each layer is grafted onto the previous one, requiring chemical reactions with a high yield in order to preserve the surface density of functional groups in each layer, the quality of the monolayers rapidly degrades as the thickness of the films increases [40-43], in some cases, such tendency of disorder occurs even the films grow only a few layers.

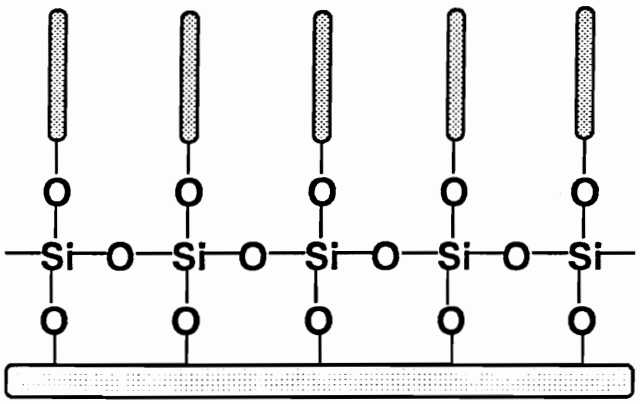

Fig. 2.2 Schematic representation of an self-assembled monolayer of alkyltrichlorosilane on a hydroxylated surface [2].

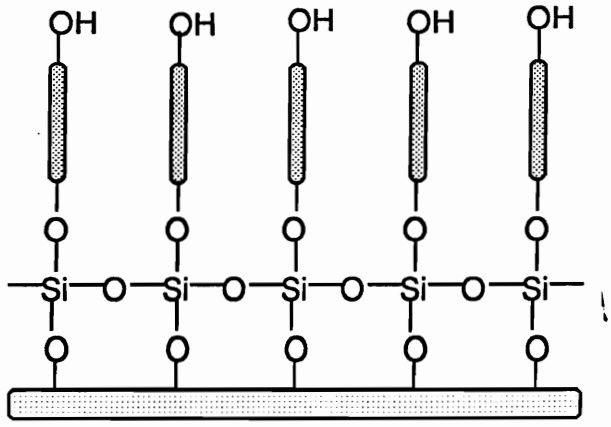

Fig. 2.3. (a) A hydroxy-terminated self-assembled monolayer.

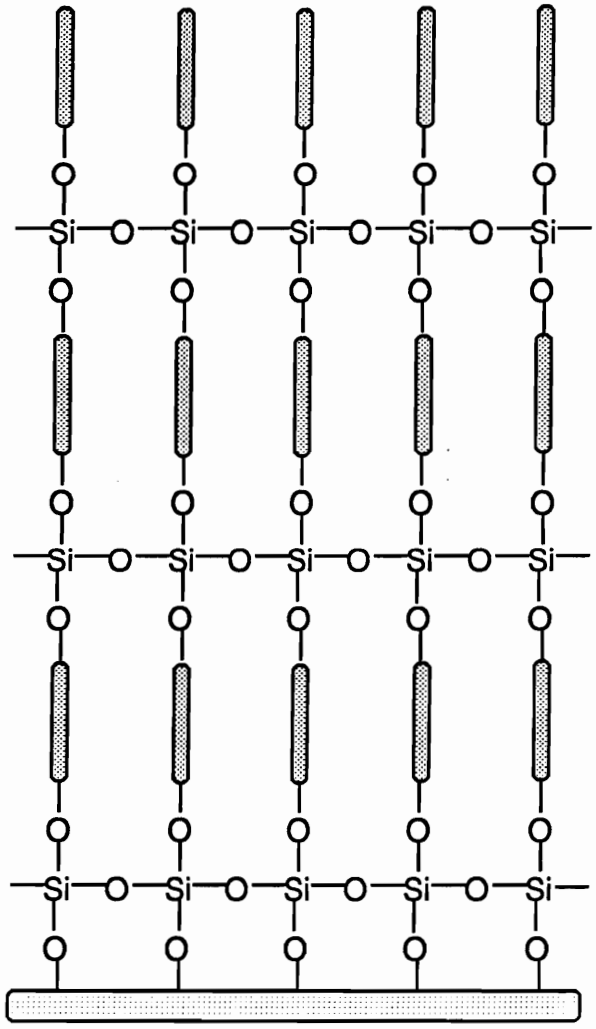

Fig. 2.3. (b) Schematic representation of self-assembled multilayers.

In short, self-assembled, chemisorbed monolayers open exciting new possibilities of engineering smooth surfaces with their chemical properties fine-tuned at the molecular level [25]. They have found many applications in the engineering of surface properties or as resist for pattern technology [44-46], adhesion layers for catalysts, biomolecules [47], and functional substrate for the deposition of metal oxides [48].

2.1.3 Self-Assembled Monolayers (Physisorption)

Films containing both polymers and surfactants offer many interesting possibilities for manipulating their structure and properties. A few years ago, a technique based on the alternate adsorption of oppositely charged polyelectrolytes was explored by Decher and his collaborators [49]. Self-assembly via physical adsorption is a particularly simple means of creating such films. It needs neither special equipment, temperature and pressure control, nor preformation of oriented films. Electrostatically attractive interaction of the hydrophilic and appropriate substrates, such as most mineral solids (mica, silica etc.), forces molecules to pack closely on the substrate. Thus, organic molecules can spontaneously be adsorbed and form highly ordered and oriented layers on the substrate. Then, consecutively alternating adsorption of anionic and cationic polyelectrolytes leads to the formation of multilayer assemblies as shown in Fig. 2.4. The ionic attraction developed between the oppositely charged polymers promote strong interlayer adhesion and a uniform and linear multilayer deposition process.

Self-assembly by physical adsorption of dipolar cationic/cationic amphiphilies and cationic/ anionic polymers and mixed systems of both dipolar amphiphilies and polymers were described by Decher et al [49], regular and stepwise multilayers were thus prepared on a chemically modified silicon surface from solutions of the amphiphiles or polymers, by alternate deposition of anionic and cationic molecules. Build-up of more than 100 layers

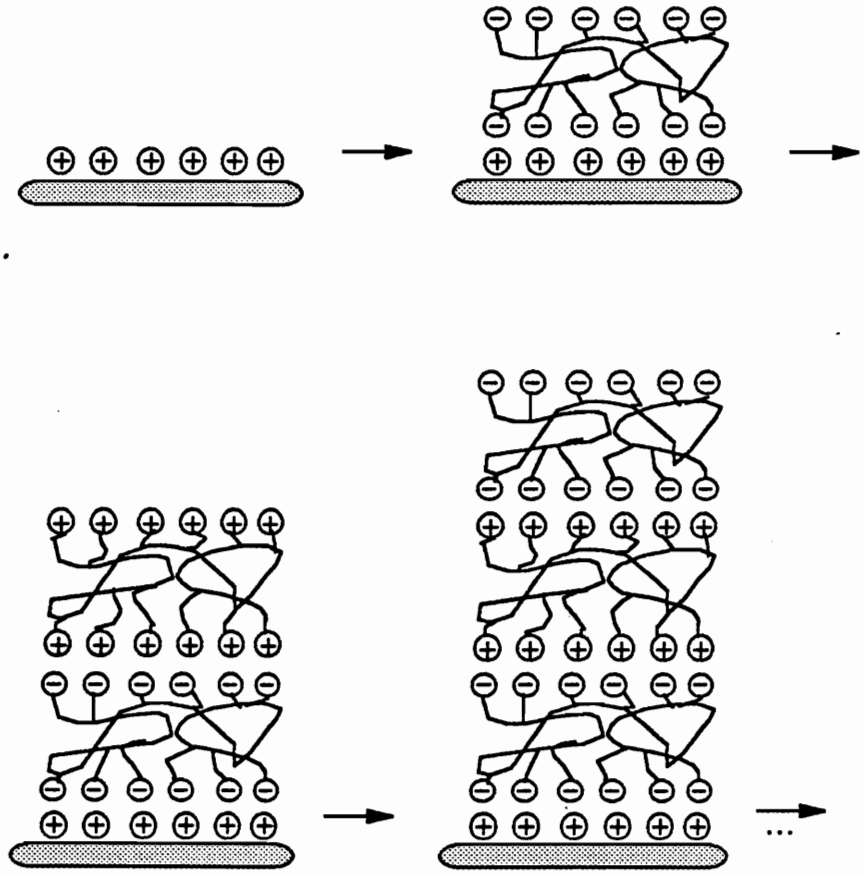

Fig. 2.4. Schematic representation of the buildup of self-assembled multilayers through physisorption [49].

were reported [49]. The film thickness is strongly dependent on the ionic strength of the solution from which the polyelectrolyte was adsorbed , therefore, by addition of molar quantities of electrolyte the average thickness of each oppositely charged layer pair can be adjusted with a precision of 0.05 nm [49]. On the other hand, since the L-B transfer of amphiphilic monolayers from the air/water interface onto solid supports is a powerful tool to create periodic lattice in many composed of bilayers. SAMp method can be exployed to provide uniform molecular films with very fine thickness adustment, the combination of polycation/polyanion SAMp and the conventional L-B technique to fabricate superlattice films with predetermined alternation of lipid and polyelectrolyte layers was reported [49], such superlattice was realized in a multicomponent film, in which additional polyelectrolyte sheets were inserted between the amphiphile headgroups, variation of the repeat unit of superlattice results in a linear increase of the superlattice layer spacing of 0.4 nm per additional inserted polycation/polyanion pair.

The SAMp technique has recently emerged as a powerful tool of processing conjugated polymers into ultrathin multilayer films with controlled thickness and controlled molecular architecture [50]. Rubner et al. demonstrated that this new approach can be used to manipulate electroactive polymers through the use of conjugated or non-conjugated polymers such as poly(thiophene acetic acid), polypyrrole, and sulfonated polyaniline, conductivity as high as 40 S cm^{-1} was obtained [50]. The fabrication of light emitting diodes (LED) based on self-assembled heterostructures containing poly(ρ-phenylene vinylene) (PPV) was reported a few months ago [51]. These LED devices show bright emission under ac voltage which is clearly visible in daylight. Moreover, such LED devices also exhibit relatively small threshold voltages (in the vicinity of 3 Volts) and relatively large stability probably due to defect-free films.

SAMp technique was also utilized to form nanoparticles between self-assembled films in which to incorporate a range of crystallites. Alternate layers of a cationic polyelectrolyte and such anionic solid nanoparticles as montmorillonite clay platelets [51] and exfoliated α-$Zr(HPO_4)_2$, $Ti_2NbO_7^-$, etc. [52] were prepared on silicon substrates. Because the hectorite sheets or α-$Zr(HPO_4)_2$ in a single adsorbed layer will have packing imperfections which eliminates interlayer penetration and thus, increase the structure integrity of the nanostructured films, while retaining the ease and generality of the polyelectrolyte adsorption process.

Polymerization of appropriate polyeletrolyte layers in the film provides an additional means of stability and permeability control. Mao et al. described that photoactive bolaform amphiphile multilayers prepared by SAMp can be photopolymerized, such polymerization changes the apparent electrostatic properties of the layer interface and undoubtedly increase the lateral strength of the film while maintaing and maybe increasing its uniformity [53].

Self-assembly through physical adsorption has advantages over chemisorption in that it does not require 100% reaction at each stage so that micron thick multilayer films can be easily fabricated by repeating the deposition process, and the film molecules are free to adjust their positions to improve the overall packing since they are not covalently bound to the substrate. Self-assembly through physical adsorption also has advantages over th Langmuir-Blodgett technique in that a solution process is independent of the substrate size and topology and that the process is suitable for automation and large-scale or nano-scale applications. Self-assembly through physical adsorption has advantages over the spin-coating technique in that more uniform and ordered structured film with the homogeneous thickness can be formed.

This spontaneous, layer-by-layer self-assmbly method offers a potentially powerful strategy for fabricating ordered inorganic-organic, inorganic-inorganic or organic-organic nano-structured films with controled thickness and controlled molecular architecture on many modified substrates such as plastics, ceramics, composites, metals, semiconductors at room temperature and ambient condition. Judicious selection of components and their layer-by-layer self-assembly will result in nanostructured films with the desired mechnaical, optical, electrical, magnetic, electro-optical, electromagnetic, and chemical properties.

2.2 Pattern Techniques

2.2.1 LB Films and SAMs in Resist Applications

The unrelenting pursuit of further miniaturization of electronic circuits and optoelectronic devices has made high resolution patterns a crucial element in future computer and display technologies. Since spin-coated photoresist materials have large pinhole densities and variations of thickness, among the existed methods of ultrathin film fabrication, other methods of ultrathin films fabrication have long been employed for resist application due to their two-dimensional, layered, crystalline solids that provide high control of films thickness and are impermeable to various treatments such as plasmam, X-ray, electron beam and UV irradiation.

The first reports on electron lithography utilizing LB films as resists was issued by Barraud *et al.* in 1980, who exhibited that LB films of ω-tricosenoic acid are excellent resist materials capable of a line resolution of 60 nm with a film 100 nm thick [55]. Fariss *et al.* used ω-octadecylacrylic acid LB multilayers both as positive and negative electron beam resist, they showed that resolution about 50 nm in the positive resist mode [56]. Miyashita *et al.* reported that resolution of 100 nm has been obtained when LB films of *N*-octadecyl acrylamide were used as ultrathin resist materials for electron beam lithography

[57]. Kuan *et al.* used LB films of poly(methyl methacrylate) (PMMA) as resist films for microlithography [58].

In an attempt to prepare good photoresist LB films, Barraud *et al.* tried to use polymerization both in the hydrophilic and hydrophobic parts in order to maintain the good mechanical properties, but the polymerized films swelled and the spacial resolution was very poor [59]. Other groups such as Wegner and Messier used fatty acids with diyne groups for the photoresist also through the polymerization, but the results have not been found useful [60].

2.2.2 SAMs in Resist Applications

On the other hand, patterns of SAMs has been traditionally successful for the serial fabrication of small pattern structures even though the history is very short. It may date back in 1986, when Calvert *et al.* found that SAMs used as adhesion promoters for LB techniques for integrated circuit (IC) were themselves capable of functioning as ultrathin film photoresists due to their excellent quality of films [61]. Two primary routes exist for the preparation of patterning of self-assembled films which chemically interact with a substrate surface. The first method exploits the adsorption of functioalized organothiols on gold surfaces for SAMs formation. A coordinative interaction betweeen the thiol group and the gold surface leads to film assembly, Whitesides' group at Harvard University has prepared most of the patterns based on this type of SAMs. An alternate approach involves the chemisorption of organosilane compounds at surface possessing polar -OH groups to form strong Si-O-substrate (siloxane) bonds, which permits functionalization of a wide varity of substrates not readily accessible with other SAMs systems. Calvert et al. at the Naval Research Laboratory's (NRL) Center focused on their patterning work on the latter systems.

Up to now optical lithography has been the most imposrtant technique for the generation of patterns in which SAMs serve as resists. Fig. 2.5 shows the basic principle of pattern generation in a thin film by means of optical lithography [65]. A photoresist deposited on the thin film is exposed to UV light incident through a mask. The exposed positive or unexposed negative photoresist is removed in a developing process. The resist pattern can be used as a mask for the following etch process. Another approach is using SAMs as photoresist directly as shown in Fig. 2.6 [62-66]. A SAM film is directly exposed to UV light which induces polymerization in the unmasked regions of the SAM film. Then the unpolymerized portion of the resist is selectively desorbed using an electrochemical reductive stripping method. Resist removal results in a negative image of the mask which can be used as a mask for the following etch process.

For a number of reasons there has been considerable recent interest in using ultrathin SAMs resists for patterning surfaces [66]. First, since such resist consist of single, small molecules, the theoretical resolution of lithographically defined features can be as small as a few nanometers if the resist is patterned with an appropriate tool, such as the tip of a scanning tunneling microscope (STM) [67-68]. Second, SAMs are extremely dense and in some cases their structure approaches that of a two-dimensional crystal even when the SAM is formed by vapor-phase dosing [69]. This insures low defect density and simplified resist application and stripping. Finally the terminal groups of SAMs can be varied to enhance selective chemical or physical vapor deposition of materials [69].

2.2.3 Other Pattern Techniques of SAMs

Direct patterning of SAMs may also be accomplished by direct writing, oxidation, photochemistry or other lithographic techniques. The examples of the writing includes processes involving mechanical scraping or machining of a surface to form a pattern by

selectively removing the SAMs [67]: Whitesides et al. used an ultrafine "pen" (made from PMMA) to "write" patterns on a gold surface using an organothiol "ink" [67]; A lot of research results of patterning based on the oxidation of SAMs by UV exposure [71-75], oxidants [76-77] have been reported recently. Lithography is one of the dominative technique of patterning of SAMs today, photolithography, electron beam and X-ray lithography have been successfully used in the patterns of SAMs. The NRL has a number of innovative research programs to fabricate and characterize novel nanostructure of SAMs. Lithographic techniques with electrons on very thin layer and monomolecular resists show promise for high resolution [63, 78-79], the resolution of these procedures may be enhanced by reducing the backscatter with a strategically-located dielectric layer which serves to reduce the number of backscattered electrons reaching the resist [79]. Patterns of SAMs formed with 14 nm X-rays using a projection arrangement was reported [80]. These patterns indicate a resolution of appromixately 0.15 micron. More recently patterns of SAMs with STM have attracted much interest [81-83], the patterns was written by exposing a monolayer (about 1 nm) with STM and modified by the action of the STM tip. Subsequent development of the image took place by selective electroless deposition of nickel onto the unexposed regions of the film. Expermentally the resolution increase with decreasing voltage, approaching an apparent limit of 5 nm.

Another approach is based on the photochemistry of the terminal groups of the SAMs, Calvert et al. at NRL have focused on the studies emphasizing the photochemistry of various aromatic organosilane and electroless metallization of SAMs on silicon [71-74], their approach combined the concepts of surface reactivity and molecular self-assembly with advanced lithographic tools such as excimer laser and UV lamp has enabled them to fabricate surfaces with procise positional control at submicron resolutions. Similar methods to pattern polypyrrole, polythiophene, and polyaniline derivatives by selective

oxidation of the corresponding monomer were also reported [84-87], including demonstration of selective polymer deposition by use of a chemically patterned SAM surface [88-89]. Wrighton et al. recently demonstrated that conducting polymers can be selectively deposited on photochemically patterned disulfide SAMs on Au. Irradiation through a mask produces a patterned SAM: the nonirradiated regions terminate in aryl azide, and the irradiated regions terminate in a functioalized amine, then the conducting polymers can be electrodeposited from either aqueous or organic solution.

In this review, we have emphasized the pattern methods using LB films and SAMs as resist in order to illustrate the basic features and the current development of these approaches. The relative success of SAMs over LB films results from the fact that the SAMs resist is highly organized, thin, and largely defect free. Although significant progress has been made, the future holds many challenges for these technologies, as we have mentioned in Chapter 1, the existed patterning methods have a common process: form the films firs, then remove some to form patterns. Moreover, such techniques employ thin films only as passive resists, they can not meet the challange toward the advanced flat full-color display and 2-dimensional microelectronic devices by themselves. For example, Fig. 2.7 is a schematic representation of flat full-color pixels, several molecule pixels emitting different colors align on the patterned planar surface with high resolution, the thickness of each pixels should be thick enough to emit the bright light. Such technique not only needs the multi-color photolithography with precise control but also the novel preparation method of thin films which have highly ordered structure, no size limit (in order to form patterned film of large screen with high resolution) and some distinguished characteristics such as endcapping. SAMp might be the possible solution since it possesses many of the basic features as a good candidate.

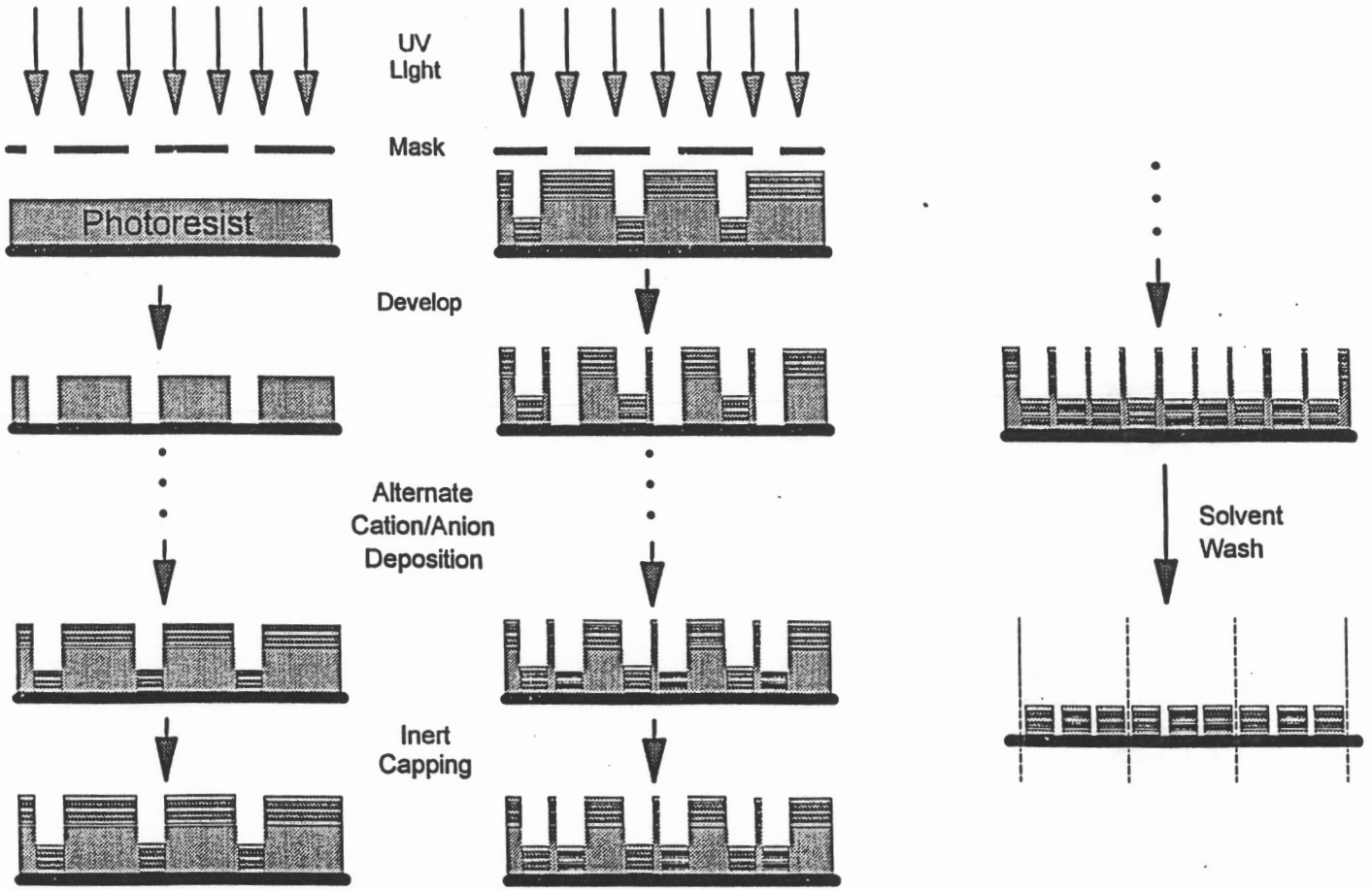

Fig. 2.7. Schematic represention of fabrication of full color pixels.

2.4 References

1. A. Barraud, *Thin Solid Films* **178**, 73 (1989).
2. A. Ulman, *An Introduction to Ultrathin Organic Film From Langmuir-Blodgett to Self-Assembly*, Academic Press, Boston, MA, 1991.
3. B. Franklin, *Phil. Trans. R. Soc.* **64**, 445 (1774).
4. A. Pockels, *Nature*, **43**, 437 (1891). A. Pockels, *Nature* **46**, 418 (1892).
5. I. Langmuir, *J. Am. Chem. Soc.* **39**, 1848 (1917).
6. K. A. Blodgett, *J. Am. Chem. Soc.* **57**, 1007 (1935).
7. K. A. Blodgett, *Phys. Rev.* **51**, 964 (1937).
8. H. Kuhn, D. Mobius, and H. Bucher, *Techniques of Chemistry*, Weissberger, A.; B. W. Rositer Eds.; Wiley, New York, 1973 Part 3B, Vol.1.
9. H. Kuhn, *Verh. Schweiz Naturforsch. Ges.* 245, 1965.
10. J. H. Cheung, and M. F. Rubner, *Thin Solid Film* **244**, 990 (1994).
11. A. D. Dhindsa, M. R. Bryce, J. P. Lloyd, and M. C. Petty, *Synthetic Metals* **22**, 185 (1987).
12. M. Sugi, *Thin Solid Film* **152**, 305 (1987).
13. K. Hong, and M. F. Rubner, *Thin Solid Film,* **160**, 187 (1988).
14. D. V. Paranjape, M. Sastry, and P. Ganguly, *Appl. Phys. Lett.* **63**, 18 (1993).
15. N. A. Kotov, F. C. Meldrum, and J. H. Fendler, *J. Phys. Chem.* **98**, 2735 (1994).
16. F. Kajzar, and J. Messier, *Opt. comm.*, **45**, 133 (1983); P. N. Prasad, *Thin Solid Film,* **152**, 275 (1987).
17. A. Barraud, Le Vide, 40, 359 (1985); A. Barraud, C. Rosilio, and A. Ruaudel-Teixier, *Thin Solid Film* **68**, 91 (1980).

18. C. Lecomte, C. Baudin, F. Berleur, A. Ruaudel-Teixier, A. Barraud, and M. Momenteau, *Thin Solid Film* **133**, 103 (1985).

19. *ARAGO7: Electronique Moleculaire. Perspectives en Traitement Moleculaire de l'Information*, Masson, Paris, 1988; M. Sugi, *Thin Solid Film,* **152**, 305 (1987).

20. J. Anzai, K. Furuya, C. Chen, T. Osa, and T. Matsuo, *Anal. Sci.* **3**, 271 (1987); A. Arya, U. J. Krull, M. Thompaon, and H. E. Wong, *Anal. Chim. Acta.* **173**, 331 (1985). .

21. J. H. Fendler, *Membrane-Mimetic Approach to Advanced Materials*, Springer-Verlag, Berlin, 1994.

22. A. Barraud, C. Rosilio, and A. Ruaudel-Teixier, *Thin Solid Film,* **99**, 317 (1983); A. Barraud, C. Rosilio, and A. Ruaudel-Teixier, *Polym. Prepr., Am. Chem. Soc., Div. Polym. Chem.* 19, 179 (1978).

23. G. J. Kovacs, P. S. Vincett, and J. H. Sharp, Can. J. Phys. 63, 346 (1985).

24. W. A. Zisman, *Adv. Chem. Ser.* **43**, 1 (1964).

25. J. Sagiv, *J. Am. Chem. Soc.* **102**, 92 (1980).

26. A. T. Hubbard, *Acc. Chem. Res.* **13**, 177 (1980). M. P. Soriaga and A. T. Hubbard, *J. Am. Chem. Soc.* 104, 3937 (1982).

27. R. G. Nuzzo, and D. L. Allara, *J. Am. Chem. Soc.* **105**, 4481 (1983).

28. N. Tillman, A. Ulman, and T. L. Penner, *Langmuir* **5**, 101 (1989).

29. L. Netzer, R. Iscovici, and J. Sagiv, *Thin Solid Films* **99** 235 (1983).

30. M. Anderson, and M. Gatin, *Langmuir* **10**, 1638 (1994).

31. C. D. Bain, and G. M. Whitesides, *J. Am. Chem. Soc.* **110**, 3665 (1988).

32. I. Rubinstein, S. Steinberg, Y. Tor, A. Shanzer, and J. Sagiv, *Nature* **332**, 426 (1988).

33. A. Ulman, *J. Mat. Ed.*, **11**, 205 (1989).

34. L. C. F. Blackman, and M. J. S. Dewar, *J. Chem. Soc.* 171 (1988).

35. E. B. Troughton, C. D. Bain, G. M. Whitesides, R. G. Nuzzo, D. L. Allara, and M. D. Porter, *Langmuir* **4**, 365 (1988).

36. R. G. Nuzzo, F. A. Fusco, D. L. Allara, *J. Am. Chem. Soc.* **109**, 2358 (1987).

37. D. L. Allara, R. G. Nuzzo, *Langmuir* **1**, 45 (1985).

38. N. E. Schlotter, M. D. Porter, T. B. Bright, and D. L. Allara, *Chem. Phys. Lett.* **132**, 93 (1986).

39. E. W. Abel, g. H. Pollard, P. C. Uden, and G. Nickless, *J. Chromatogr.* **22**, 23 (1966).

40. K. M. R. Kallury, U. J. Krull, and M. Thompson, *Anal. Chem.* **60**, 169 (1988).

41. L. Netzer, R. Iscovici, and J. Sagiv, *Thin Solid Films* **99**, 235 (1983).

42. L. Netzer, R. Iscovici, and J. Sagiv, *Thin Solid Films* **100**, 67 (1983).

43. L. Netzer, and J. Sagiv, *J. Am. Chem. Soc.* **105**, 674 (1983).

44. S. R. Wasserman, G. M. Whitesides, I. M. Tidswell, B. M. Ocko, P. S. Pershan, and J. D. Axe, *J. Am. Chem. Soc.* **111**, 5852 (1989).

45. A. Kumar, and G. M. Whitesides, Science 263, 60 (1994).

46. D. Kang, and M. S. Wrighton, Langmuir 7, 2169 (1991).

47. S. K. Bhatia, J. J. Hickman, and F. S. Ligler, *J. Am. Chem. Soc.* **114**, 4432 (1992).

48. H. Shin, R. J. Collins, M. R. De Guire, A. H. Heuer, and C. N. Sukenik, *J. Mater. Res.* **10**, 692 (1995).

49. G. Decher, and J. D. Hong, *Makromol. Chem., Macromol. Symp.* **46**, 321 (1991). G. Decher, and J. D. Hong, European Patent, application number 91 113 464.1; G. Decher, and J. D. Hong, *Ber. Bunsenges. Phys. Chem.* **95**, 1430 (1991); Y. Lvov, G. Decher, and H. Mohwald, *Langmui,* **9**, 481 (1993); Y. Lvov, G. Decher, and

G. Sukhoorukov, *Macromolecule,* **26**, 5396 (1993); Y. Lvov, f. Essler, and G. Decher, *J. Phys. Chem.* **97**, 13773 (1993); J. Schmitt, T. Grunewald, K. Kuaer, P. Pershan, G. Decher, and M. Losche, *Macromolecules* **26**, 7058 (1993); G. Decher, and J. Schmitt, *Prog. Colloid Polym. Sci.* **89**, 160 (1992); G. Decher, J.D. Hong, and J. Schmitt, *Thin Solid Films* **210/211**, 504 (1992); G. Decher, and J. Schmitt, *Prog. in Colloid & Polymer Sci.*, **89** 160 (1992);

50. D. Ingersoll, P. J. Kuleza, and L. R. Faulkner, *J. E.ectorchem. Soc.*, **141**, 140 (1994); M. Ferreira, J. H. Cheung, and M. F. Rubner, *Thin Solid Films* **244**, 806 (1992); J. H. Cheung, A. F. Fou, and M. F. Rubner, *Thin Solid Films* **244**, 985 (1992);

51. H. P. Hong, D. Davidov, Y. Avny, H. jchayet, E. Z. Faraggi, and R. Neumann, *Adv. Mater.* **7**, 846 (1995).

52. R. E. Kleinfeld, and G. S. Ferguson, *Science* **265**, 370 (1994).

53. W. S. keller, H. N. Kim, and T. E. Mallouk, *J. Am. Chem. Soc.* **116**, 8817 (1994);

54. G. Mao, Y. Tsao, M. Tirrell, H. T. Davis, V. Hessel, and H. Ringsdorf, *Langmuir* **9**, 3461 (1993);

55. A. Barraud, C. Rosilio, and A. Ruaudel-Teixier, *Thin Solid Films* **68**, 91 (1980).

56 G. Rariss, J. Lando, and S. Rickert, *Thin Solid Films* **99**, 305 (1983).

57 T. Miyashita, H. Yoshida, and M. Matsuda, *Thin Solid Films* **155**, L11 (1987).

58 S. W. Kuan, C. W. Frank, Y. Lee, T. Eimori, D. R. Allee, R. F. W. Pease, and R. Browning, *J. Vac. Sci. Tech.* **B7**, 1745 (1989).

59 A. Barraud, C. Rosilio, and A. Ruaudel-Teixier, *Polym. Prepr., Am. Chem. Soc., Div. Polym. Chem.* **19**, 179 (1979).

60 B. Teike, G. Lieser, and G. Wegner, *J. Polym. Sci.* **17**, 1631 (1979); F. Kajzar, J. Messier, J. Zyss, I. Ledoux, *Opt. Comm.* **45**, 133 (1983).

61 J. M. Schnur, P. E. Schoen, P. Yager, J. M. Calvert, J. Georger, and A. Singh, *Thin Solid Films* **152**, 181 (1987).

62 K. C. Chan, T. Kim, J. K. Schoer, and R. M. Crooks, *J. Am. Chem. Soc.* **117**, 5875 (1995).

63 W. Dressick, J. M. Calvert, *Jpn. J. Appl. Phys.* Part 1, **32**, 5829 (1993).

64 N. A. Abbott, J. P. Folkers and G. M. Whitesides, *Science* **257**, 1380 (1992).

65 D. Kleinfeld, K. H. Kahler, and P. E. Hockberger, *J. Neurosci.* **8**, 4098 (1988); N. A. Abbott, J. P. Folkers, and G. M. Whitesides, *Science* **257**, 1380 (1992).

66 K. C. Chan, T. Kim, J. K. Schoer, and R. M. Crooks, *J. Am. Chem. Soc.* **117**, 5875 (1995).

67 J. M. Calvert, T. S. Koloski, W. J. Dressick, C. S. Dulcey, M. C. Peckerar, F. Cerrina, J. W. Taylor, D. Suh, O. R. Wood II, A. A. MacDowell, and R. D'Souza, *Soc. Phot. Inst. Eng.* **1924**, 30 (1993).

68 C. B. Ross, L. Sun, and R. M. Crooks, *Langmuir* **10**, 3383 (1994); T. Kim, R.M. Crooks, M. Tsen, and L. Sun, *J. Am. Chem. Soc.* **117**, 3963 (1995); T. Kim, and R.M. Crooks, Tetrahedronl Lett. 35, 9501 (1994).

69 O. Chailapakul, L. Sun, C. Xu, and R. M. Crooks, *J. Am. Chem. Soc.* **115**, 12459 (1993).

70 D. S. Y. Hsu, and H. F. Gray, *Appl. Phys. Lett.* **63**, 159 (1993)

71 J. M. Scunur, M. C. Peckerar, C. R. K. Marrian, P. E. Schoen, J. M. Calvert, and J. H. Gorger, U. S. Patent 5, 079,600 (1992).

72 J. M. Calvert, M. S. Chen, C. S. Dulcey, J. H. Gorger, M. C. Peckerar, J. M. Scunur, and P. E. Schoen, *J. Electrochem. Soc.* **139**, 1677 (1992).

73 J. M. Calvert, M. S. Chen, C. S. Dulcey, J. H. Gorger, M. C. Peckerar, J. M. Scunur, and P. E. Schoen, *J. Vac. Sci. Tech.* **B 9**, 3477 (1991).

74 J. M. Calvert, P. E. Pehrsson, C. S. Dulcey, and M. C. Peckerar, *Mat. Res. Soc. Proc.* **260**, 905 (1992).

75 S. K. Bhatia, J. Hickman, and F. S. Ligler, *J. Am. Chem. Soc.* **114**, 4432 (1992).

76 N. Balachander, and C. N. Sukenic, *Langmuir* **6**, 1621 (1990).

77 S. K. Bhatia, J. L. Teixeira, M. Anderson, L. C. Shriver-lake, J. M. Calvert, J. H. Georger, J. J. Hickman, C. S. Dulcey, P. E. Schoen, and F. S. Ligler, *Anal. Biochem.* **208**, 197 (1993).

78 C. R. K. Marrian, E. A. Dobisz, and M. C. Peckerar, *Proc. IEEE*, **79**, 1149 (1991).

79 K. W. Rhee, and M. C. Peckerar, *Appl. Phys. Lett.* **62**, 533 (1993).

80 C. R. K. Marrian, and E. A. Dobisz, *J. Vac. Sci. Technol.* B **10**, 2877 (1992); C. R. K. Marrian, and E. A. Dobisz, *Ultramicroscopy*, Elsevier Science Publishers 42, 1993.

81 G. P. Lopez, H. A. Biebuyck, and G. M. Whitesides, *Langmuir* **9**, 1513 (1993).

82 R. F. Leonard, and W. F. Cordes, *Optical Microlithography II,* H. L. Stover, Ed., *SPIE* 1983, P125.

83 M. J. Hampden-Smith, and T. T. Kodas, Chem. Vap. Deposition, 1, 39 (1995).

84 H. Yoneyama, and M. Kitayama, Chem. Lett. 657 (1986).

85 M. Okano, K. Itoh, and A. Fujishima, *J. E.ectrochem. Soc.* **134**, 837 (1987).

86 Y. M. Wuu, F. R. F. Fan, and A. J. Bard, *J. E.ectrochem. Soc.* **136**, 885 (1989).

87 M. S. A. Abdou, Z. W. Xie, A. M. Leung, and S. Holdcroft, *Synth. Met.* **52**, 159 (1992).

88 M. Nishizawa, M. Shibuya, T. Sawaguchi, T. Matsue, and I. Uchida, *J. Phys. Chem.* ***95***, 9042 (1991).

89 L. F. Rozsnuai, and M. S. Wrighton, *J. Am. Chem. Soc.* **116**, 5993 (1994).

Chapter 3

Molecular Self-Assembly of Polyionic Polymers: A New Process for Fabrication Ultrathin Multilayer Thin Films

3.1 Abstract

Multilayer ultrathin films comprised of poly(vinylamine) backbone azo and poly(allylamine chloride) have been deposited on bare single crystal silicon, quartz, and glass substrates by a self-assembly process. The process involves the alternate dipping of a substrate into aqueous an solution of a polycation followed by dipping an aqueous solution of polyanion. The growth process and the structure are probed with UV/Vis spectroscopy, contact angle and ellipsometry measurements. The results suggest that well-ordered uniform multilayer films have been formed and film thicknesses of up to 1 μm can be easily obtained by repeating the deposition process. The thickness of the monolayer films depends on the solution concentration. The self-assembled multilayers can only be removed from the substrate by scraping and show remarkable chemical stability. The deposition time for a full monolayer coverage of azo dye and PAH is about 20 seconds. The conformation of the films are thermally stable up to at least 150 ^{0}C.

3.2 Introduction

Research on organic ultrathin films consisting of Langmuir-Blodgett (L-B) films and self-assembled monolayer (SAM) films are of interest for practical and scientific applications in areas ranging from microelectronics processing to biomedicine [1-6]. LB films, formed by the amphiphilic molecules which have hydrophilic and hydrophobic portions, are generally limited to small fabrication areas and periodically alternating layered systems and are subject to post deposition relaxation since they are fabricated under high surface pressures [7-10].

SAM films, monolayers chemisorbed spontaneously from solution onto solid substrates, represent another prospect for organic ultrathin films [11-14]. However, SAM films have not been employed toward the preparation of the thick films, because sequential chemisorption strategies are difficult to design. Recently, Decher et al.[15-18] demonstrated that it is possible to buildup multilayer ultrathin films of polymers onto modified single crystal Si surfaces. In these cases, the adsorption is based on the electrostatic attraction of interlayer charges, and is therefore also self-limiting. Alternating adsorption of anionic and cationic polyelectrolytes leads to the formation of multilayer assemblies. This new method of creating ultrathin films is really very interesting, since the process is simple, easy to handle, and there is effectively no limit to the number of layers that can be easily deposited. This approach to multilayer film fabrication offers great promise when combined with the patterning technology.

This chapter will demonstrate that poly(vinylamine) polymer backbone azo containing chromophores can be spontaneously co-adsorbed with poly(allylmine hydrochloride) in a alternating fashion with a polyanion on bare single crystal Si, quartz and glass substrates. UV/Vis absorption spectroscopy and contact angle and ellipsometry measurements are employed to follow the deposition process. Well-ordered uniform multilayer films have been formed, where the deposited film thickness is determined by solution concentration. The film structure is stable to high temperature treatments, and contact angle measurements and UV/Vis spectroscopy suggest that the deposition time for a full monolayer coverage of azo dye is about 20 seconds.

3.3 EXPERIMENTAL

3.3.1 Materials

Poly(sodium 4-styrenesulfonate) (NaPSS, MW=70,000), and Poly(allylamine hydrochloride) (PAH, MW=50,000-65,000) were obtained from Aldrich. N-2-Aminoethyl-3-Aminopropyltrimethoxysilane (APS) was purchased from Huls America Inc. The Poly(Vinylamine) backbone containing azo chromophores, Poly s.119 (PDYE), was obtained from Sigma (MW=70,000). All the above materials were used without further purification. Their chemical structures are shown in Fig. 3.1.

Single-crystal p-111 silicon wafers were kindly supplied by Prof. Desu (Department of Material Science, Virginia Tech), quartz slides were purchased from G. M. Associates Inc.(Oakland, CA) and glasses substrates were obtained from Fisher for the adsorption experiments.

The ultrapure water used for all experiments and for all cleaning steps was obtained from a Barnstead Nanopure II bioresearch grade deionization/ultrafiltration unit. The product water resistivity was 18 megohm-cm.

3.3.2 Procedures

3.3.2.1 Substrate Surfaces Cleaning

In our study, glass, quartz and single crystal silicon with hydrophilic and positively charged surfaces were used as substrates for the adsorption process. It is very important that a surface is clean and free from impurities in order for the first monolayer to spontaneously deposit onto the substrate surface in a regular and uniform manner. Greasy materials were removed by rubbing the surfaces with filter paper saturated with Micro Detergent (International Products Corp.), followed by a rinse in ultrapure water. Then the

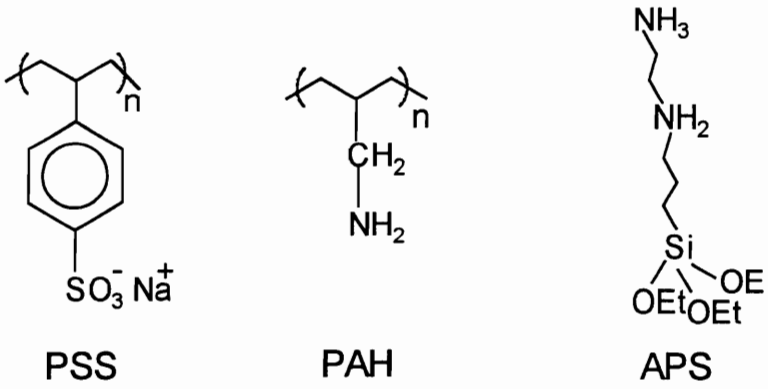

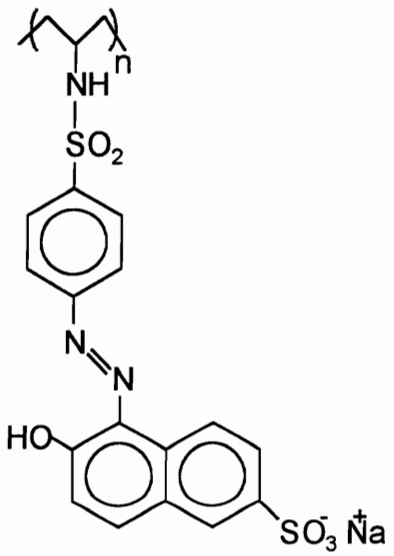

Fig. 3.1 Chemical structures of the polyelectrolytes used for the fabrication of polyionic films.

substrates were cleaned again based on the RCA cleaning procedures [19]. First, the substrates were immersed in a mixture of H_2O/H_2O_2 (30%)/NH_4OH (29 w/w% as NH_3) (5:1:1) at 70 ^{0}C for 10 minutes and washed with water. Afterwards the substrates were immersed in a mixture of H_2O/H_2O_2/HCl (37 w/w%) (6:1:1) for 15 minutes, followed by rinsing with water. The substrates were baked in a drying oven for 60 minutes at 130 ^{0}C. The above procedure produces hydrophilic substrates surface. Positively charged surfaces were made . by treating the hydrophilic surfaces with N-(2-aminoethyl-3-aminopropyl)trimethoxysilane (APS) solution.

3.3.2.2 Deposition of the APS Monolayer

Once the substrates have been thoroughly cleaned and dried, the APS monolayer can be deposited to form the positively charged surfaces. 0.5 mL of APS were added to 80 ml. of toluene containing $1.3x10^{-3}$ mol/dm^3 glacial acetic acid. After mixing, the substrates were dipped into the solution and heated in an oven at 46 ^{0}C for 1 hour. Afterwards the substrates were ultrasonically agitated for 2 minutes each in pure toluene, a toluene/methanol (1:1) mixture twice, and finally in pure methanol twice. The freshly prepared substrates were used within 1 hour for the adsorption experiments.

3.3.2.3 Construction of a Multilayer System

Solutions of polycation (PAH) and polyanions (PSS and PDYE) were made by dissolving the polymers in HCl solutions. Solutions with pH values of 4, 7, and 10 were investigated.

For the hydrophilic slides which have a negatively charged planar surfaces, the multilayers were fabricated by first immersing the substrates in the polycation solution (PAH) to adsorb and a monolayer of the polycation. After washing with ultrapure water

the substrates were dipped into the polyanion (either PSS or PDYE) solution. A monolayer of polyanion molecules was adsorbed, and the surface was restored to its original negative charge. By repeating the above steps in an alternating fashion, multilayer assemblies of polymers were obtained as shown schematically in Fig. 3.2. For the APS-modified slides, which have positively charged surfaces, the substrates were first immersed in the polyanion solution and then in the polycation solution (For structures see Fig. 2.4).

After each deposition and cleaning step the samples were either air dried or without air dried. The drying effects on the quality of the SAMp films were followed by contact angle measurements and UV/Vis spectroscopy.

In order to protonate the amino groups, acidic solutions of all the compounds were used. Typical adsorption times were 15 minutes per layer at ambient temperature. The surfaces of the films were washed 20 times with ultrapure water after adsorption of each layer.

3.3.2.4 Stability of SAMp

A. Chemical Stability

The SAMp films systems (5 bilayers) of PAH/PSS and PAH/PDYE were ultrasonically agitated in pure solvents of acetone, methanol, chloroform, hexadecane and toluene for 60 min, respectively. Then, they were rinsed with methanol/acetone and ultrapure water, followed by second ultrasonic agitation in pure solvents for another 30 min. and washed with methanol/acetone and ultrapure water again. After the samples were air-dried, contact angle measurements were employed to check for changes of surface structure before and after the first and second agitation.

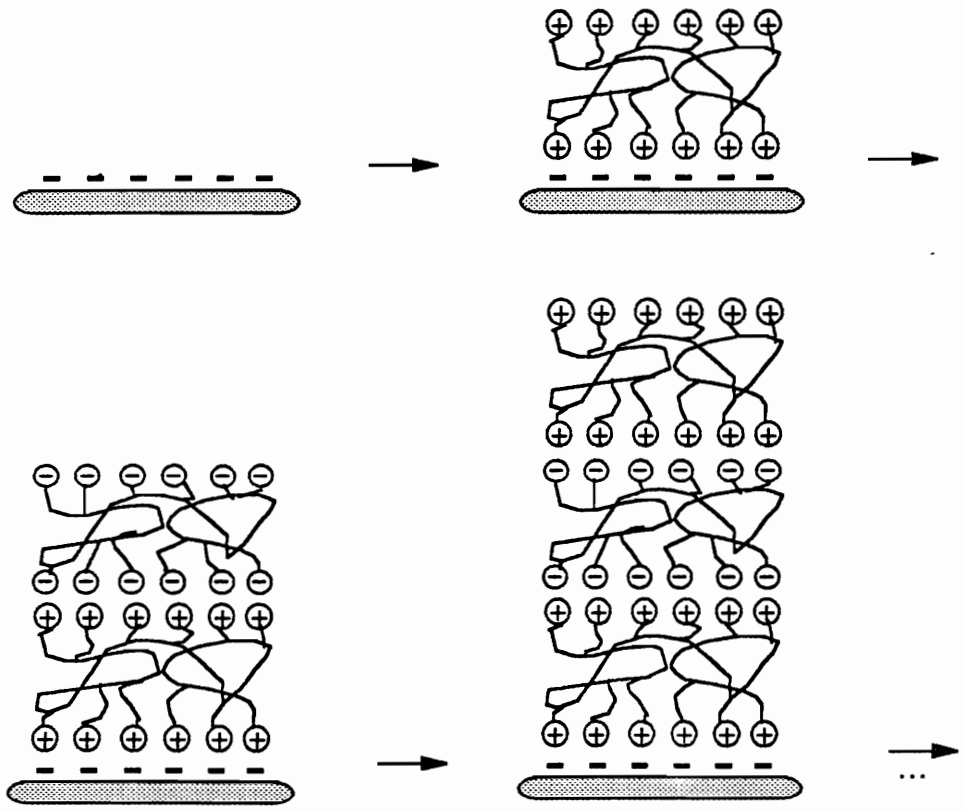

Fig. 3.2. Schematic representation for the spontaneous self-assembled multilayers deposited on silica through the physical attraction.

The SAMp film systems of PAH (1 layer) and PAH/PSS (1 bilayer) was immersed in 6M aqueous HCl solution containing TiO_2 nanocolloids at room temperature for 20 min. Water contact angle measurements and XPS were employed to monitor the adsorption process and the chemical stability at this very high acidic condition.

The samples were also subjected to carry out the abrasion resist test, in which the surface of the SAMp films were rubbed vigorously with cotton swab saturated with acetone, ultrapure water, ethanol and ultrapure water each for 10 min, and was twice repeated. The chemical abrasion treatments of the SAMp films were probed by contact angle measurements and UV/Vis spectroscopy.

B. Thermal Stability

The seven samples of the PAH/PSS SAMp films deposited on glass slides were subjected to a test of thermal stability. The samples were heated for two hours in an oven at 40°C, 50°C, 90°C, 115°C, 130°C, and 150°C, respectively, and then cooled back to room temperature. Contact angle measurements were employed to examine thermally induced effects on SAMp structural stability prior to and after a heating process

3.3.3 Characterization of the Multilayer Film Systems

3.3.3.1 UV/Vis Spectroscopy Measurements

Multilayer assemblies containing azo chromophores were characterized by a Perkin Elmer Lambda 6 UV/Vis spectrophotometer. The amount of material deposited per layer as determined by optical absorption measurements was found to correlate directly with the thickness of the layer as determined by profilometry and ellipsometry measurement. Therefore, plots of optical absorbance with the number of layers provide useful information about the quality and the reproducibility of the multilayer deposition process.

3.3.3.2 Contact Angle Measurements

Wettability is a property of surfaces that is both theoretically and practically important [20]. Whitesides et al. [21] and others [22] have shown qualitatively the wettability of a solid is determined by the structure of its outermost few angstroms. In order to assess the water wettability of the self-assembly films, advancing contact angle measurements were carried out by the sessile drop method with a Rame-Hart 100-00 115 NRL contact, angle goniometer equipped with a video camera and monitor. The temperature was not controlled so it varied from 20 to 25 ^{0}C. The volume of a drop was 5 μL; the observed contact angle was independent of the volume of the drop over the range 1-20 μL. The sessile drops of nanopure water were carefully placed on the film surfaces with a microliter syringe held in an upright position. Contact angles were determined within 1 min of applying the drops to the film. The tangent to the drop at its intersection with the surface was estimated visually. All reported values are the average of at least six measurements taken on both sides of at least three drops.

3.3.3.3 Ellipsometry Measurements

Ellipsometric measurements of SAMp films on *p*-111 silicon wafers were made using a variable angle spectroscopic ellipsometric (J. A. Woollam Co.) with a xenon source and a 1 mm spot. The instrument was always calibrated against 25 nm SiO_2 on Si. Data was collected at takeoff angles of 75-77^0 (10 increments) and at wavelengths of 300-800 nm (10 nm increments). Each data point was averaged over five revolutions of the analyzer. Data were processed using V.A.S.E. software version 1.1 (J. A. Woollam). Each set of analyzer and polarizer angles was the average of at least four measurements taken at different location (separated by about 0.5 cm) on the sample. Thickness measurement accuracy was ±0.1 nm. Ellipsometrically determined thicknesses were comparable to

theoretical values calculated using the simplifying assumption that the monolayer was deposited normal to the substrate with all alkyl chains in extended, all-trans conformations.

3.4 Results and Discussion

3.4.1 Nature of Quartz Substrates

Quartz is generally characterized as having high surface energies and tends to be hydrophilic in nature. In the absence of adsorbed thin films, it usually is wettable by water and in most cases yields very low contact angles. When quartz is suspended in aqueous solution, adsorption of ions takes place, imparting a surface charge on the quartz surface. The sign of the charge depends on the pH of the aqueous media. Thus, above the pH for zero charge (isoelectric point), quartz surfaces are negatively charged, while at lower pH values, net positive charges result. Schubert and Baldauf [23] postulated that the charge of the quartz surface originated from the breaking of Si-O bonds during pulverization. This results in positive surface charges on the quartz, which is considered to interact with water as follows:

$$\equiv Si^{+} + H_2O \Leftrightarrow \equiv Si\text{-}OH_2 \Leftrightarrow \equiv Si\text{-}OH + H^{+} \qquad (3.1)$$

$$\equiv Si\text{-}OH + H^{+} \Leftrightarrow \equiv Si\text{-}O^{-} + 2\,H^{+} \qquad (3.2)$$

Cationic surfactants and polymers are considered to be adsorbed by silica surface through ion exchange [23]. Ter Minassian-Saraga [24] suggests the ion exchange process for long-chain cations as follows:

$$\equiv Si\text{-}OH \Leftrightarrow \equiv Si\text{-}O^{-} + H^{+} \qquad (3.3)$$

$$\equiv Si\text{-}OM \Leftrightarrow \equiv Si\text{-}O^{-} + M^{+} \qquad (3.4)$$

$$\equiv Si\text{-}OH + RN(CH3)_3{}^{+} + Br^{-} \Leftrightarrow (\equiv Si\text{-}O^{-})[RN^{+}(CH_3)_3] + H^{+} + Br^{-} \qquad (3.5)$$

$$\equiv Si\text{-}OM + RN(CH3)_3{}^{+} + Br^{-} \Leftrightarrow (\equiv Si\text{-}O^{-})[RN^{+}(CH_3)_3] + M^{+} + Br^{-} \qquad (3.6)$$

Tamamushi et al. [25] have shown that the relative adsorption of anionic and cationic surfactants by polar solids can be reversed by alternating pH. Cations tend to be adsorbed to a greater extent at high pH's (surfaces negatively charged) while anionic surfactants are adsorbed more at low pH values (surfaces positively charged).

Therefore, in a weak acidic aqueous environment of pH 4, well above quartz's isoelectric point of 1.5 [23], the quartz surface carries a negative charge, and it is ready to adsorb polycation molecules. Furthermore, since the pKa of RNH_2 is 10.8, the amino groups of APS are protonated in the acidic aqueous solution. Therefore, the APS modified surface has a positively charged surface.

3.4.2 Strategy for and Realization of Multilayer Buildup

The process of the consecutively alternating adsorption of polycations and polyanions is schematically depicted in Fig. 3.2. The illustration shows the buildup of a multilayer assembly using a cationic polyelectrolyte and a anionic polyelectrolyte.

In step I, a hydrophilic substrate which has a negatively charged surface is immersed in the aqueous solution of the polycation (PAH), and a monolayer of the polycation is adsorbed. Since the adsorption is carried out at relatively high concentrations of polyelectrolytes, many ionic groups remain exposed to the interface with the solution and thus the surface charge is concerted to positive [16]. After washing with ultrapure water to remove adhering solution of the excess polycation the substrate is dipped into the polyanion (either PSS or PDYE) solution, and rinsed a second time. Again a monolayer of polyanion molecules is adsorbed but the surface charge is restored to negative. By repeating the above steps in an alternating fashion, multilayer assemblies of polymers were obtained.

During the buildup of multilayer assemblies, the substrates could be stored for several days without apparent deterioration of the surface following deposition. If the washing steps were omitted, an adhering layer of one solution would be left on the surface of the substrate. This would result in a contamination of the next solution and eventually to co-precipitation of both compounds and to the undesired incorporation of precipitated particles into the following layer.

Self-assembly via physical adsorption is based on the attraction of opposite charges. Electrostatically attraction between the substrate and polyelectrolytes forces molecules to pack closely and form highly ordered and oriented layers on the substrate. The ionic attraction between the oppositely charged polymers promotes strong interlayer adhesion and consecutively alternating adsorption of polyanions and polycations leads to the buildup of multilayer assemblies. Consequently, one is able to build up micron-thick films just by repeating the alternating deposition steps as many times as desired. Moreover, one is also able to incorporate more than two molecules into the multilayer simply by immersing the substrate in as many polyelectrolyte solutions as desired. Even aperiodic multilayer assemblies can easily be prepared.

Fig. 3.3 displays the optical absorbtance spectrum of a solution of the poly s.119. A peak at 475 nm is observed, with a molar absorption coefficient of 1.25x10-4 (L/mol)/cm [24]. The 475 nm band is attributed to a π-π^* transition of the azo group and a coincident charge transfer transition from a π orbital of the phenyl ring to a π^* orbital of the 2-hydroxynalphthalene [24]. UV/Vis spectra following the deposition process and growth of the (PDYE)/PAH multilayer films on glass are shown in Fig. 3.4. Two absorption bands are observed at 410 nm and 471 nm. No shift in maximum absorption is observed as the number of layers of the multilayer film increases, which means that there is no molecular aggregation between adjacent layers. The absorption peak at 475 nm in

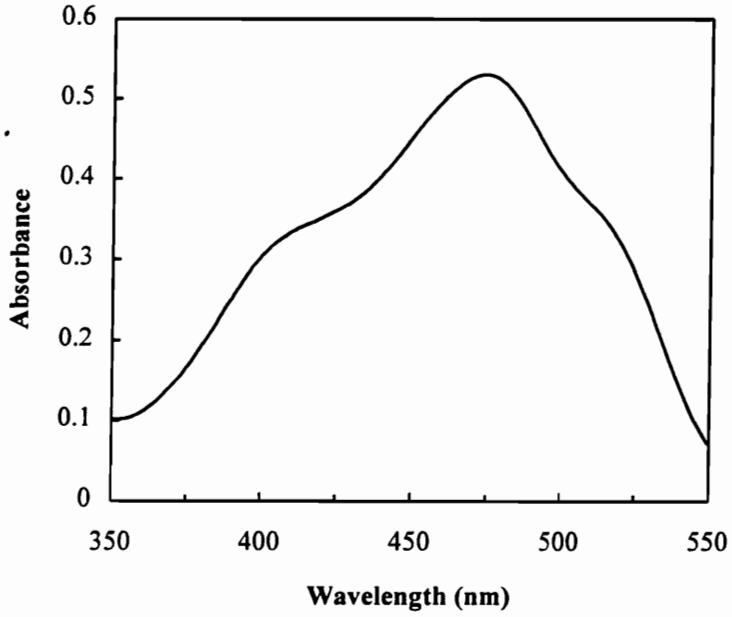

Fig. 3.3. Absorption spectrum of the poly s.119 (PDYE) solution in water.

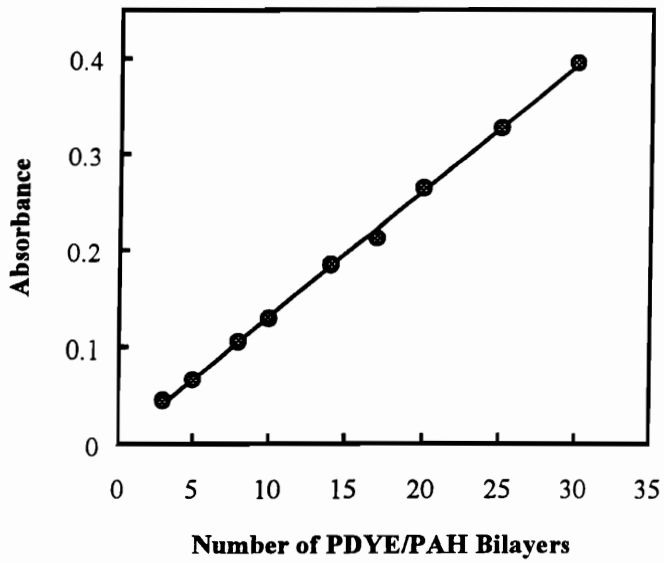

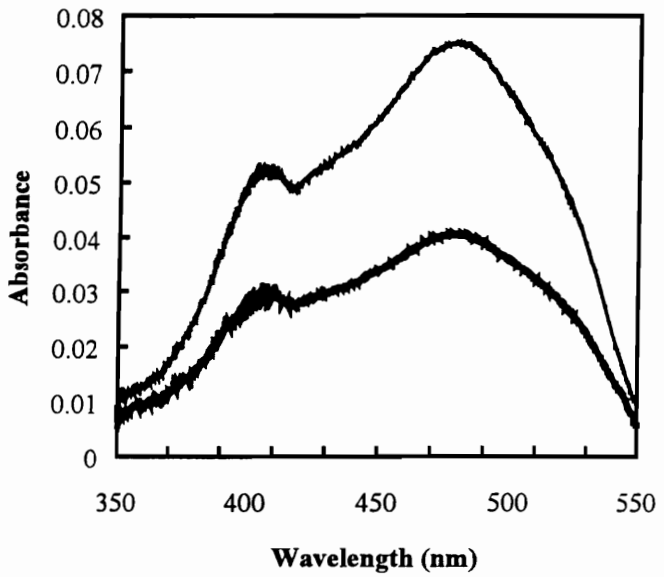

Fig. 3.4. (a) Dependence of optical absorbance of the poly s.119 (PDYE) multilayer films (at 471 nm) on the number of deposited bilayers. (b) Absorbance spectra of poly s.119 (PDYE) films (3 and 6 bilayers) on glasses.

solution shifted to 471 nm in films is explained by molecular exciton theory as being due to the formation of H aggregates in the monolayer films [25]. The absorption peak at 410 nm is attributed to an aggregate of azo dye in the monolayer [26]. Fig. 3.4 also displays the optical absorbance at 471 nm for up to a 30 layers (15 layers of each compound), composed of the PDYE with PAH on the hydrophilic quartz substrate. In this case, the concentration of the polymer dye and PAH solutions are $1.0x10^{-3}$ mol L^{-1} and $5x10^{-3}$ mol L^{-1}, respectively. From Fig. 3.4, we can clearly see that the consecutive adsorption of layers is stepwise and the deposition process is very consistent from layer to layer. The set of points in Fig. 3.3 were fitted with a linear least-squares line, yielding an average optical density of 0.0130±0.0002 per bilayer at 471 nm. The linear nature of these plots again suggests that each layer adsorbed contributes an equal amount of material to the thin film.

We have also repeated the work done by Decher et al.[15-17]. In this case, the positively charged APS modified silicon and quartz substrates were used. The polycation used was poly(allylamine chloride) (PAH), the polyanion was poly(styrene sodium). The absorption spectra of water solution of PSS and PAH are shown in Fig. 3.5. Two peaks are found for PSS solution spectrum at 192 nm and 225 nm. The very strong absorption of PAH solution at $\lambda<190$ nm is also observed. The multilayer adsorption of the compounds PAH and PSS onto quartz slide has been followed by UV/Vis spectroscopy and is depicted schematically in Fig. 3.6. In the same fashion, a multilayer assembly of 20 layers (10 layers of each compound) was built. The UV/Vis absorbance spectrum of a PAH/PSS film system is also shown in Fig. 3.6. The maximum adsorption occurs at about 202 nm, which contributes the overlap of PSS and PAH absorptions. The dependence of optical absorption at 200nm on number of bilayers is also shown in Fig. 3.6. A straight line relation is observed, the set of points yields an average optical density of 0.0110±0.0003

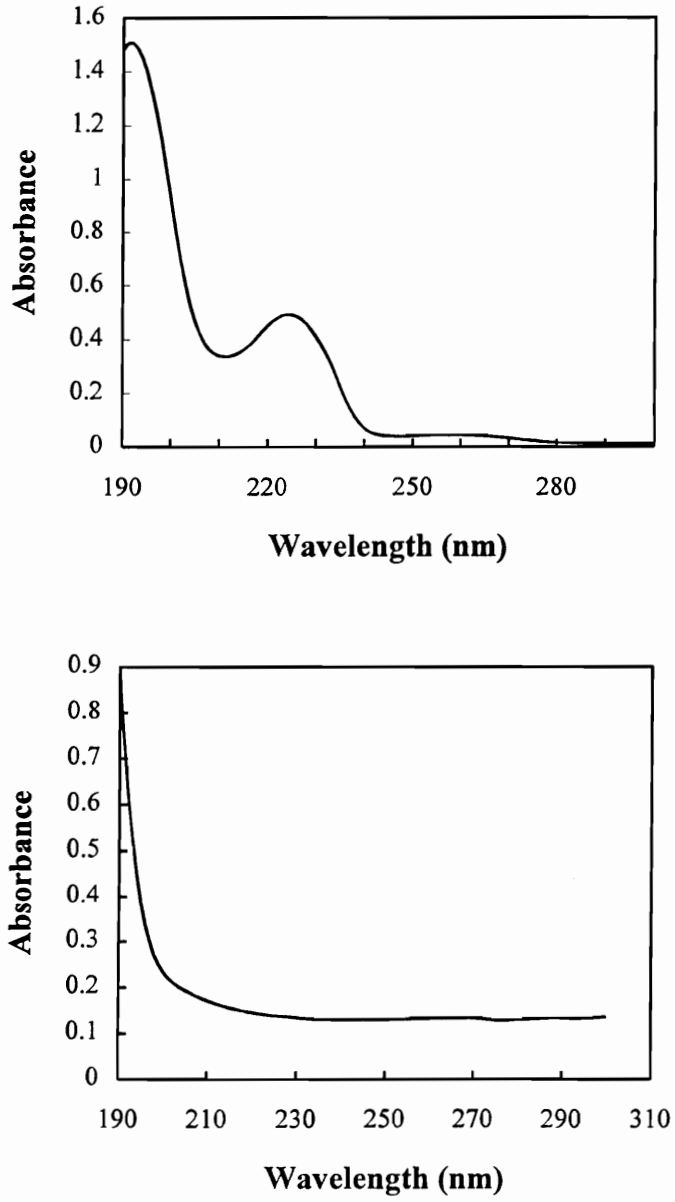

Fig. 3.5 (a) Optical absorbance of PSS in water; (b) Optical absorbance of PAH in water.

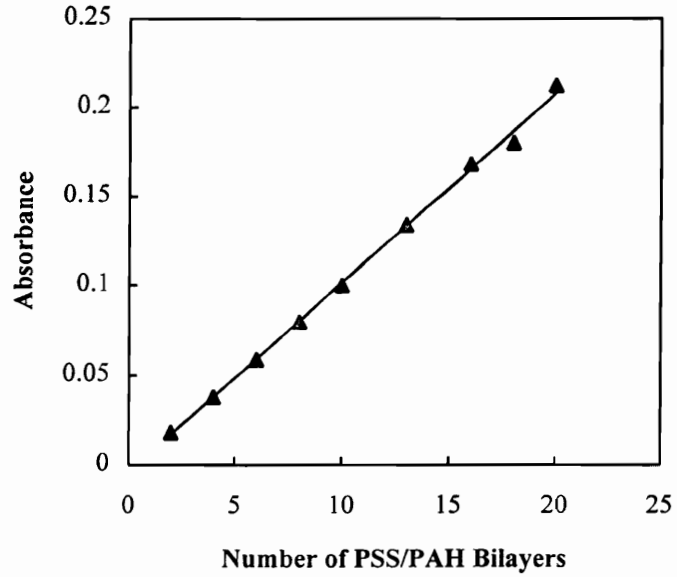

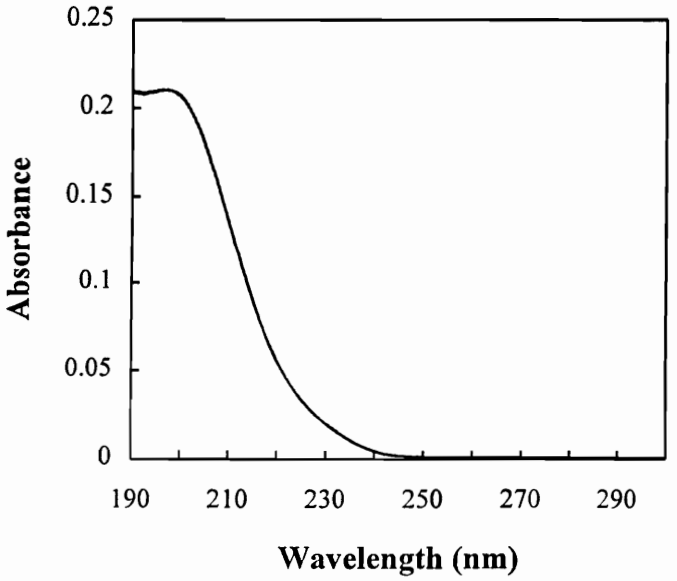

Fig. 3.6. (a) Optical absorbance (at 200 nm) vs. numer of bilayers of PSS/PAH deposited on quartzs; (b) Optical absorbance spectrum of 20 bilayers of PSS/PAH film on quartz.

per bilayer at 200 nm. The results are similar to Decher's. These data emphasize again that this novel method of fabricating multilayer films is reliable and feasible.

Ellipsometry measurements are also employed to probe the deposition process. Fig. 3.7 shows the Ellipsometrically determined thickness of the film fabricated on single crystal silicon with alternating 10 layers of PAH and PDYE. The monomer concentrations of PAH and PDYE were $1.5x10^{-3}$ mol L^{-1} and $1.0x10^{-3}$ mol L^{-1}, respectively. The thickness of the first layer of PAH is 0.7 nm, whereas the first bilayer has a thickness of 1.2 nm. The total thickness of the 10 bilayer films is 12.8 nm. Fig. 3.8 displays the ellipsometry spectrum of a film fabricated on single crystal silicon of alternating 10 layers of PAH and PSS (for structures see Fig. 3.2). The monomer concentration of PAH and PSS were $1.5x10^{-3}$ mol L^{-1} and $1.0x10^{-3}$ mol L^{-1}, respectively. The thickness of PAH (first layer) is the same as the above, 0.7 nm, and that of the first bilayer of PSS/PAH is 1.3 nm. The total thickness of the 10 bilayer film is 12.8 nm. From both Figs. 3.7 and 3.8, a linear relation of the thickness vs. number of the layers clearly shows us each layer adsorbed contributes an equal amount of material to the thin film. Highly ordered and uniform films have been fabricated on the substrates.

3.4.3 Concentration Dependence of the Thickness of Monolayer

The dependence of absorbance of self-assembly adsorption on the concentration was studied with the help of UV/Vis spectroscopy, contact angle measurements and ellipsometry. Fig. 3.9 shows UV/Vis absorption spectra of two thin films deposited on glass, with three alternating bilayers of poly(allylamine hydrochloride) (PAH) and poly s.119 (PDYE) (for structures see Fig. 3.2). The monomer concentration of PAH in the deposition solution is $1.5x10^{-3}$ mol L^{-1} for both a and b. However, in case a, the monomer

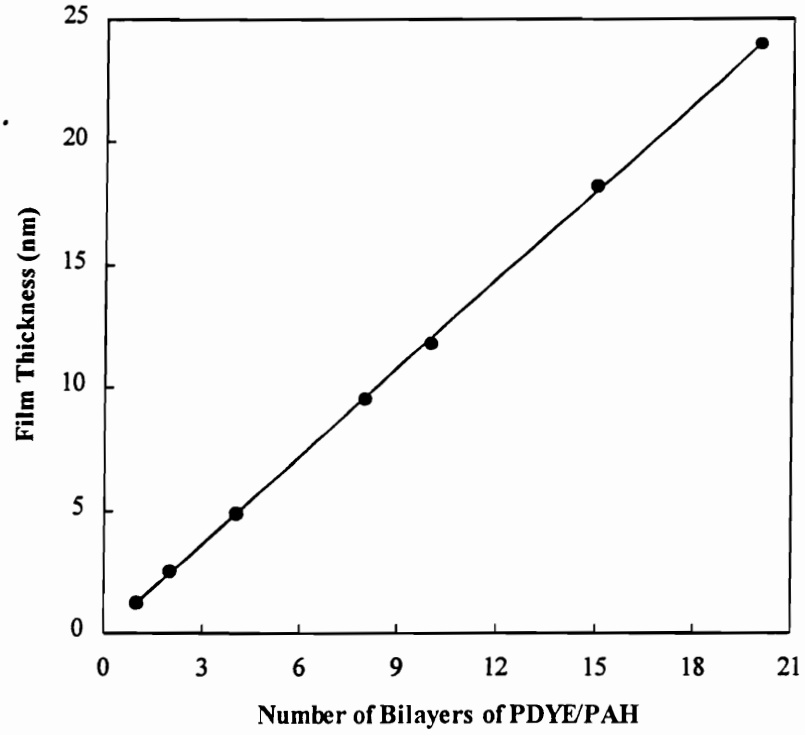

Fig. 3.7. Dependence of ellipsometric thickness of the adsorbed PDYE/PAH multilayer films on the layer number.

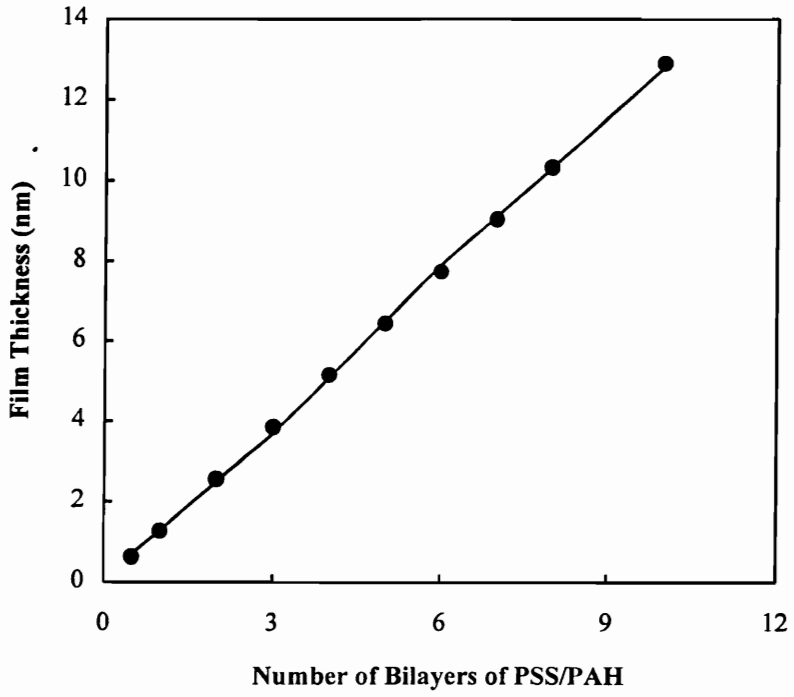

Fig. 3.8. Dependence of ellipsometric thickness of PSS/PAH multilayer films on the number of deposited bilayers.

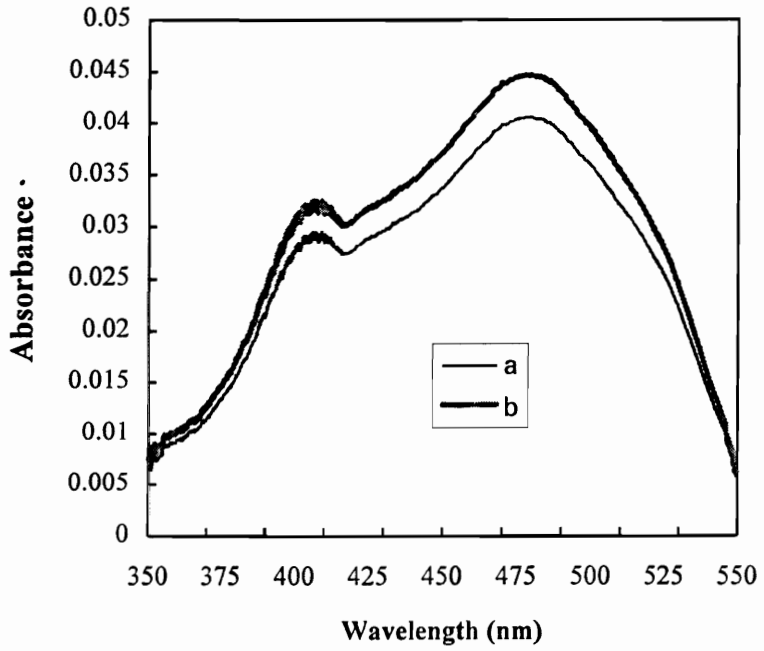

Fig. 3.9. Optical absorbance of PDYE/PAH multilayer films. (a). Deposited using 1.0 $x10^{-3}$ M solution of PDYE; (b) Deposited using $1.0x10^{-2}$ M solution of PDYE.

concentration of the PDYE solution was about $1.0x10^{-3}$ mol L^{-1}, whereas in the other it was $1.3x10^{-2}$ mol L^{-1}.

From Fig. 3.9, the stronger optical absorption per layer means that the more poly s.119 molecules have been adsorbed even though the number of the layers is equal for both cases a and b. This suggests that the solution of higher monomer concentration deposited a thicker monolayer. Contact Angle and ellipsometry measurements can be used to confirm this possibility.

Water contact angles measured on glass supported films deposited from the same solution concentrations is shown in Fig. 3.10. For the multilayer films of PDYE/PAH, the contact angles show steady increase with the number of bilayers of film. In pure water, the silicon surface is wetted and gives zero contact angle. Cationic surfactant PAH adsorbs on the Si surface and increases the contact angle. The increased contact angles are attributable to the adsorption of cations with polar head groups attached to the negatively charged surface with the nonpolar hydrocarbon chains oriented upward toward the bulk portion of the droplet. With the alternation of PDYE and PAH adsorption, for the first 3 bilayers, the contact angles increase with the number of multilayers, and then level off for the following layers. In addition to the steady increase and leveling, there is also a striking trend in contact angle with the solution concentration without the addition of any salts. The higher the concentration, the greater the contact angles. The data suggest that a thicker film is formed with a higher concentration and that the contact angle remains low due to the hydrophilic head groups of PDYE and PAH being oriented at the bilayer/solution interface.

Gaudin [27] concluded that there is a relationship between the magnitude of the contact angles and the density of the adsorbed coating of a surface-active substance. Ottewill and Rastogi [28] found that, as with glass and other negatively charged

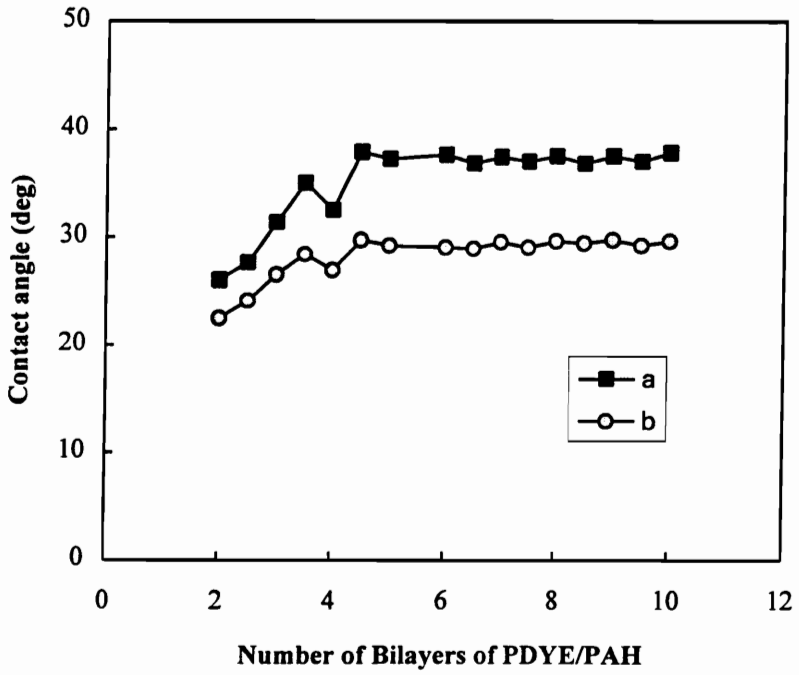

Fig. 3.10. Contact angle on the surfaceof PDYE/PAH multilayer film as a function of number of bilayers. (a) Deposited using $1.0x10^{-2}$ M solution of PDYE; (b) Deposited using $1.0x10^{-4}$ M solution of PDYE.

substances, the zeta potentials of negative AgI solutions generally increased in positive volume as the cationic concentration increase. Their results are similar to our contact angle measurements.

In order to further confirm the concentration-sensitive thickness, we turn to the ellipsometry technique. Film thickness measured by ellipsometry is depicted in Fig. 3.11. The total thickness of the 10 bilayers of PAH/PDYE film fabricated on single crystal silicon substrates from the lower concentration is 12.0 nm, the average thickness of each bilayer is 1.2 nm. Since the first layer of PAH has a thickness of 0.7 nm, then the thickness of PDYE monolayer is about 0.5 nm. Whereas in the other the total thickness is 13.5 nm for the 10 bilayer film and the average thickness of each PDYE monolayer is about 0.65 nm.

It is known that the polyelectrolyte adsorption on different surfaces is affected by salts [29] and Decher and Schmitt [17] have reported that the average thickness of oppositely charged layer pairs can be changed by the concentration of the added NaCl. However, in the absence of salts, the adsorption of the polyionic molecules is indeed influenced by their concentration. Therefore, in the low concentration solution, the ionic polymer tends to exist in an extended chain conformation and adsorbs "flat" on the surface, whereas in the high concentration solution, the ionic polymer conformation tends to be more "loopy" due to the very strong electrostatic repulsion of the ionic groups. Thus, the polymer adsorbs in a looped conformation and a thicker film is deposited. In principle, therefore, it is possible to adjust the total film thickness by varying both or either of the concentrations of the polycation and polyanion.

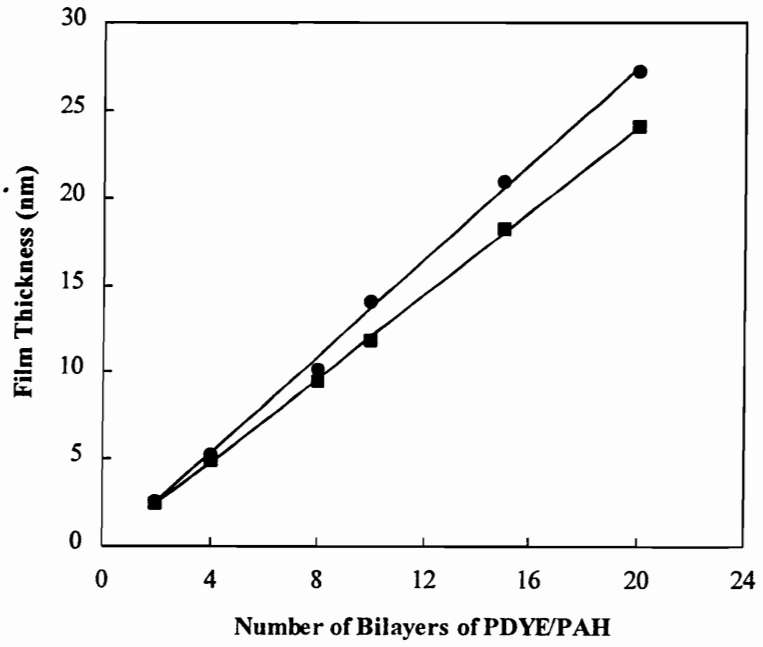

Fig. 3.11. Ellipsometric thickness of the PDYE/PAH multilayer films as a function of number of bilayers.

3.4.4 Temperature Behavior of the Self-Assembly Films

The temperature behavior of the self-assembled films was followed by the contact angle measurement. The seven samples of the films were fabricated on glass slides with alternating layers of poly(allylamine hydrochloride) (PAH) and polymer s.119 (PDYE) (for structures see Fig. 3.2). The concentration of PAH was $1.5x10^{-3}$ mol L^{-1} and that of PDYE was $1.0x10^{-3}$ mol L^{-1}. The number of the bilayers in each film is five. Table 3.1 shows the temperature behavior of the self-assembled films. The contact angle of the films of PAH/PDYE (concentrations) is about 41^0 at the room temperature. When heated to various temperatures, the contact angles rise to the same value of 60^0. After cooling to room temperature, the contact angle is decreased to around 48^0, not to the original 41^0. But after cooling overnight the initial contact angle is restored. The change of the contact angles upon temperature is completely reversible and reproducible.

Decher and coworkers [18] reported using small angle X-ray scatting that the total film thickness of such self-assembled films is reduced as the temperature increases, exhibiting a nonlinear negative expansion coefficient . After cooling to room temperature the spacing is reduced, but after storing overnight the initial length of the repeat unit is almost restored.

The temperature dependence of contact angle of film thickness can be interpreted as follows: At room temperature, some water penetrates into the film and physisorbs to the film surface. When the film contains some water, the contact angle is 41^0. As the temperature is increased to 35 ^{0}C, the film expels most of the water, and the film is more compact and the surface is hydrophobic as the contact angle increases to 60^0. At higher temperatures, the film does not expel water any more, so the contact angle stays unchanged, but the conformations of the films continue to change. When cooled to room temperature, the film regains some water to form a swollen structure, therefore, the

Table 3.1. Dependence of contact angle of the multilayer film of PDYE/PAH on temperature.

Temperature (^{0}C)	25	40	50	90	115	130	150
Contact Ancle (^{0}) heat for 2 hours	41±2	59±2	58±2	60±1	60±1	60±1	60±1
Contact Ancle (^{0}) cool for 2 hours	41±2	48±2	48±2	47±2	48±2	49±2	47±2
Contact Ancle (^{0}) cool for overnight	41±2	40±2	39±2	38±3	40±2	41±2	40±2

contact angle decreases to 48^0. After an overnight cooling, the film adsorbs almost all the water it has expelled, so the contact angle returns to 41^0 and the conformation of the film expands to the original form.

Temperature sensitivity of swelling has been observed in both macroscopic and microscopic colloidal microgels [30-31], and the volume phase transition temperature (i.e., the temperature corresponding to the greatest change in volume) is in the range 31-35 ^{0}C. It is reasonable to expect that the sulfonate end groups contribute to the swelling and expansion of the polymer chains.

As we have shown, the conformation of the polyelectrolyte films are indeed influenced by the change of the temperature, and the changes are completely reversible. This suggests that the layer structure stays stable up to a temperature of 150 ^{0}C.

3.4.5 Chemical, Mechanical Stability of Self-Assembled Films

As was discussed earlier, SAMp monolayers of PAH/PSS essentially are ionic macromolecules packed closed by strong electrostatic attraction between the substrate and the first monolayer and interlayers. Therefore, it can be expected that the stability of these SAMp will be much higher than that of any LB films. Indeed, we have found that SAMp of PAH/PSS are stable with respect to ultrasonic agitation with solvents of acetone, methanol, chloroform, hexadecane and toluene at room temperature as shown in Table 3.2. The water contact angles of PAH/PSS films were 41 ± 2^0 before exposured to the organic solvents. However, it remained unchanged after ultrasonic treatments in the various solvents for 90 min each.

The stability of SAMp films in acidic media is remarkable. When the SAMp film of PAH monolayer was immersed in 6M HCl at room temperature for 20 min, water contact angle remains unchanged (20 ± 2^0) and XPS spectrum indicates that no apparent change

Table 3.2. Advanced contact angles (deg.) measured before, and after PAH/PSS SAMp were ultrasonically agitated with organic solvents.

	Before	After (first 60 min)	After (second 30 min)
Chemicals	Contact Angles	Contact Angles	Contact Angles
Acetone	41 ± 2	41 ± 2	41 ± 2
Methanol	41 ± 2	41 ± 2	41 ± 2
Chloroform	41 ± 2	41 ± 2	41 ± 2
Hexadecane	41 ± 2	41 ± 2	41 ± 2
Toluene	41 ± 2	41 ± 2	41 ± 2

for the photopeak of N1s as shown in Fig. 3.12. As expected, there is no adsorption of TiO_2 atop the PAH SAMp film, due to the electrostatic repulsion between the cationic complexes of TiO_2 and PAH. These results also indicate that SAMp film of PAH is very dense and efficient to prevent the adsorption of cations. While in the condition of PAH/PSS system, aqueous contact angle drops from 29 ± 2° to 11 ± 2° due to the adsorption of TiO_2 nanoparticles. Fig. 3.13 shows XPS survey spectrum of this adsorption, the titanium peak locations at 464.5 ($2p_{1/2}$) and 458.6 ev ($2p_{3/2}$) agree with reference values [32] for bulk TiO_2.

SAMp could only be removed by scraping and showed remarkable mechanical and structural stability. Table 3.3 shows the results of abrasion/chemical treatment of PAH/PSS films. SAMp films were rubbed vigorously with cotton swabs saturated with acetone, ultrapure water, ethanol and ultrapure water, each for 10 min. This sequence was repeated twice more. The absorbance spectra and contact angle measurements have clearly shown that there was no apparent degradation in the SAMp films. Therefore, the ultrahigh chemical and mechanical stability of SAMp, combined with other remarkable characteristics as have mentioned in Chapter I and II, make SAMp films good candidates for both the active and passive units in photolithographically processed devices, where acetone and ethanol are widely used as developing and stripping solvents.

Another remarkable property of SAMp is durability. They remained unaltered for at least 6 months when they were stored in covered containers, as was evidenced by their appearance, absorption spectra, and contact angle measurements. Furthermore, another system of SAMp with highly ordered structures could be built up on the 6-month-old SAMp as though it were a freshly prepared substrate.

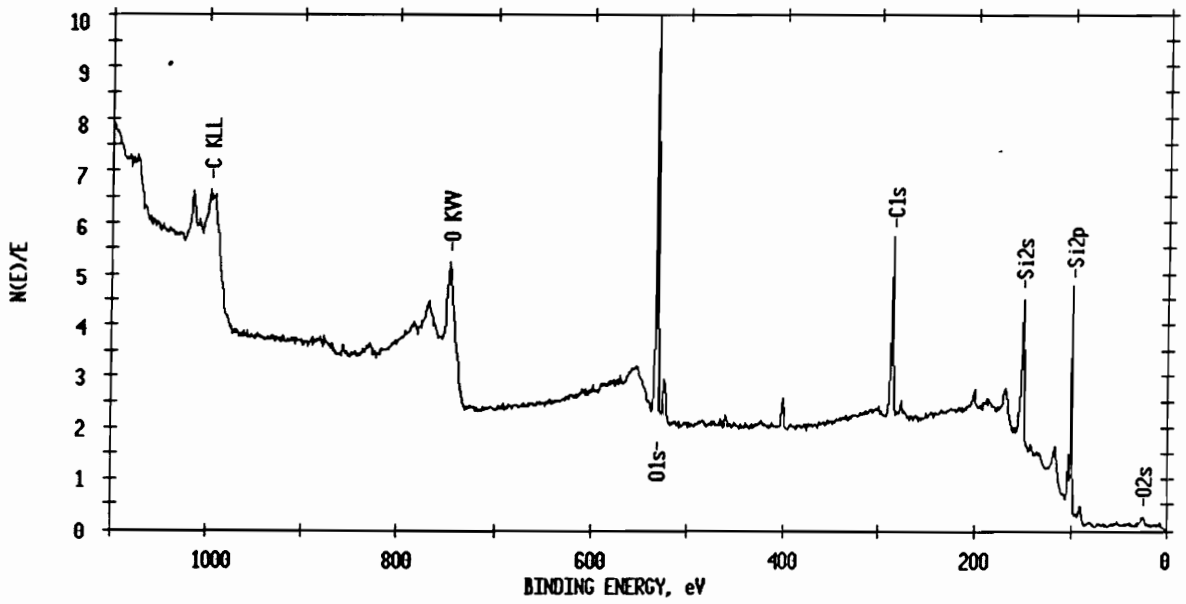

Fig. 3.12. The survey scan XPS spectrum of PAH SAMp film on single crystal silicon substrate after immersing in 6M HCl aqueous solution containing TiO_2.colloids for 20 min at room temperature.

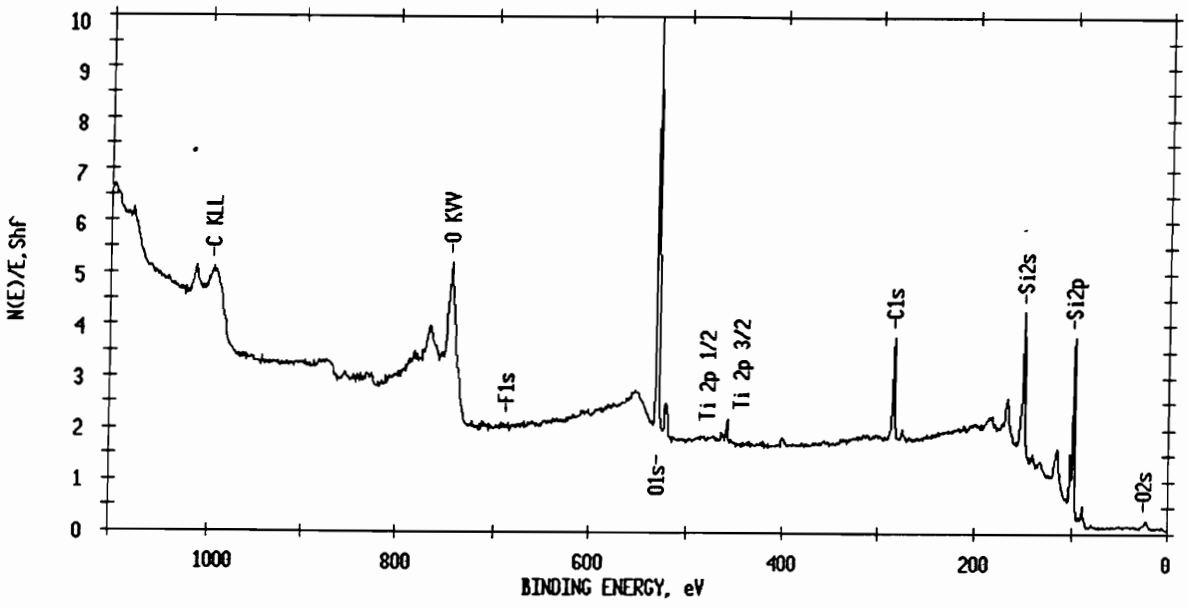

Fig. 3.13. The survey scan XPS spectrum of PAH/PSS (1 bilayer) SAMp film on single crystal silicon substrate after immersing in 6M HCl aqueous solution containing TiO_2.colloids for 20 min at room temperature.

Table 3.3. Advanced contact angles (deg.) and UV/Vis spectra measured before and after the chemical abrasion treatments of PAH/PSS SAMp.

	Before		After	
Chemicals	Contact Angle	Absorbance	Contact Angle	Absorbance
Acetone	41 ± 2	0.042	41 ± 2	0.041
Ethanol	41 ± 2	0.040	41 ± 2	0.041

3.4.6 Determination of the Adsorption Time

The typical time of adsorption of polyions used by Decher's group is about 15 min [16-18]. Since the adsorption is based on the attraction of the opposite charges, from the view point of the electrostatistics the adsorption process may be finished in a very short time.

When discussing the relation between the monolayer coverage of an adsorbed polymer layer and the dipping time, one must also consider kinetic effects. The equilibrium conformation of an adsorbed polymer is not necessary the same as the conformation of the polymer in solution. This means that one has to consider the reconformation time. A few experiments have been done to investigate the kinetics of reconformation of the adsorbed layer [33]. Odberg and Sandberg studied the reconformation time of high molecular weight polyelectrolyte with the help of ellipsometry measurement, their results suggest that, assuming an exponential process, the reconformation time constant of the high molecular weight polymer layer perpendicular to the surface, is in the order of 20-30 s.

Contact angle measurements were employed to determine the deposition time. PAH monolayer films were deposited on bare optical glass substrates, the concentration of PAH was 1.13×10^{-3} mol L^{-1}. Twelve samples were prepared for the contact angle measurements. The deposition times were chosen as 5, 10, 20, and up to 1200 seconds. The results of contact angle measurements of PAH monolayer films on glasses as a function of deposition time is shown in Table 3.4. At first, the contact angles increase as the deposition time increases. After 20 seconds, the contact angle reaches a constant value at 23^0 and no longer increases even through the deposition time is as long as 120 minutes. Although a partial monolayer is sufficient to produce a contact angle which is about the same as that of a full monolayer coverage [34-35], the results show that a full monolayer

Table 3.4. Contact angles of PAH monolayer adsorption on glasses as a function of the deposited time.

Samples	Time (sec.)	Contact Angle (deg.)
1	5	10 ± 2
2	10	15 ± 2
3	20	23 ± 2
4	40	23 ± 2
5	60	23 ± 2
6	90	24 ± 2
7	120	23 ± 2
8	240	22 ± 2
9	300	24 ± 2
10	600	24 ± 2
11	900	23 ± 2
12	1200	23 ± 2

adsorption of PAH at the given concentration is reached in a very short time. If it is true, 20 layers of polyelectrolyte film can be easily deposited in one hour. That would be a great advantage when compared to any other methods of film fabrication (L-B techniques and SAM methods). We repeated the above measurements several time and the results proved to be reproducible.

In order to quantitatively determine the deposition time, UV/Vis spectroscopy was also used. The samples were prepared as follows: First, monolayer films of PAH were deposited on optical glass slides from a 1.13×10^{-3} mol L^{-1} solution, followed by a complete wash with copious quantities of high-purity water. Then PDYE monolayer films were deposited with the different times. Optical absorbance measurements were performed to monitor the quantity deposited. The deposition times for the PDYE monolayers ranged from 5 seconds to 600 seconds. The absorption intensity of PDYE monolayer/PAH on glass at 471 nm for different deposition times are listed in Table 3.5 The results show the same trends as were reported in the contact angle measurements. When the dipping time is less than 20 seconds, only partial adsorption occurs. After about 20-25 seconds, the absorption intensity increases to 78×10^{-3}, then as the dipping time increases, the optical intensity stays unchanged, and no further increase in adsorption is observed for the increase of the dipping time. The results suggest again that a monolayer coverage of PAH has been reached in a very short time (within about 30 seconds).

3.5 Conclusions

Ionic polymer films comprised of an azo dye-containing poly(vinylamine) (PDYE), poly(styrene sodium) (PSS), and poly(allylamine chloride) (PAH) have been buildup on positively- and negatively- charged quartz, glasses, and single crystal silicon surfaces by a self-assembly process. The basic process used to create multilayer thin film involves the

Table 3.5. Summerization of the optical absobance intensity of PDYE monolayer adosobed on the PAH monolayer (at 471 nm) at a given time.

Samples	Time (sec.)	Absorbance ($1x10^{-3}$)
1	5	4
2	10	50
3	20	78
4	30	70
5	60	76
6	150	79
7	240	81
8	600	78

alternate dipping of a substrate into an aqueous solution of a polycation followed by dipping an aqueous solution of polyanion. The deposition process is performed at ambient temperature and pressure. The process was studied by using UV/Vis absorption spectroscopy, contact angle measurements, and variable angle spectroscopic ellipsometry. The results suggest that well-ordered and uniform multilayer thin films have been formed on these substrates, and desired thicker films for the applications in electroluminescence, microelectronics and optics can be easily reached by just repeating the deposition process. There is no theoretical limit to the size of the substrates. A striking observation is that the thickness of a deposited monolayer depends on electrolyte concentration without addition of salts. When the concentration of PDYE is $1.0x10^{-3}$ mol L^{-1}, the average thickness of one monolayer of PDYE is 0.5 nm, whereas when the concentration increases to $1.0x10^{-2}$ mol L^{-1}, the average thickness rises to 0.65 nm. The ionic polymer films contain some water at room temperature, when heated, the physisorbed moisture can be easily desorbed. After a sufficiently long time of cooling at room temperature, the water again physisorbs on the surface of the film. The self-assembled multilayers have shown us their remarkable chemical and abrasion-resistive stabilities in common organic solvents and in very high acidic media. The conformations of the self-assembled multilayer films are thermally stable up to 150 ^{0}C, so this kind of films can be used for special high temperature applications. From UV/Vis absorption and water contact angle measurements, the deposition time of one monolayer of ionic polymer is estimated to be about 20-30 s, which is a great advantage compared to any other method of fabrication of multilayer thin films.

3.6 References

1. H. Rnigsdoff, *Angew. Chem. Int. Edn. Engl.*, **29**, 1269 (1990).
2. L. Netzer, R. Iscovici, and J. Sagiv, *Thin Solid Films*, **99**, 233 (1983).
3. F. L. Carter, R. E. Siatkowski, and H. Wohhltjen, *Molecular Electronics Devices III,* North-Holland, Amsterdam, 1988.
4. H. Kuhn, *J. Photochem.* **10**, 111 (1981).
5. W. Gopel, and Ch. Ziegler ed. *Nanostructures based on Molecular Materials*, Weinheim, New York, 1992.
6. R. J. Collins, and C. N. Sukenik, *Langmuir*, **11**, 2322 (1995).
7. K. B. Blodgett, J. Am. Chem. Soc. 56, 495 (1934).
8. A. Barraud, C. Rosilio, and A. Ruaudel-Teixier, *Thin Solid Films*, **68**, 7 (1980).
9. G. Roberts ed. *Langmuir-Blodgett Films*, Plenum Publishing Corp., New York, 1992.
10. K. Sakai, M. Saito, M. Sugi, and S. Iizima, *Jpn, J. Appl. Phys.*, **24**, 865 (1985).
11. J. D. Swalen, D. L.Allara, J. D. Andrade, E. A. Chandross, S. Garoff, J. Israelachvill, T. J. McVarthy, R. W. Murray, R. F. Rease, J. F. Rabolt, K. J. Wynne, and H. Yu, *Langmuir*, **3**, 932 (1987)
12. D. L. Allara, and J. D. Swalen, J. Phys. Chem., 86, 2700 (1982).
13. R. Moaz, and J. Sagiv, Langmuir, 3, 1034 (1987).
14. C. D. Bain, and G. M. Whitesides, J. Am. Chem. Soc., 110, 5897 (1988).
15. G. Decher, and J. D. Hong, European Patent, application number 91 113 464.1.
16. G. Decher, and J. D. Hong, *Ber. Bunsenges. Phys. Chem.*, **95**, 1430 (1991).
17. G. Decher, and J. Schmitt, *Prog. in Colloid & Polymer Sci.*, **89**, 160 (1992).
18. G. Decher, Y. Lvov, and J. Schmitt, *Thin Solid Films*, **244**, 772 (1994).

19. W. Kern, *Semicond. Int.*, 94 (1984).

20. F. M. Fowkes, Ed., *Contact Angles, Wettability, and Adhesion*, Advances in Chemistry 43, American Chemical Society, Washington D.C., 1964; D. H. Kaelble, Physical chemistry of Adhesion, Wiley, New York, 1971. F. P. Bowden, and D. Tabor, *The Friction and Lubrication of Solids, Part II*, Oxford University Press, London, 1969.

21. E. B. Troughton, C. D. Bain, G. M. Whitesides, R. G. Nuzzo, D. L. Allara, and M. D. Porter, *Langmuir*, **4**, 365 (1988); C. D. Bain, and G. M. Whitesides, *Science*, **240**, 62 (1988); S.R. Holmes-Farley, and G. M. Whitesides, *Langmuir*, **3**, 62 (1987); S. R. Holmes-Farley, R. H. Reamey, R. G. Nuzzo, T. J. McCarthy, and G. M. Whitesides, *Langmuir*, **3**, 799 (1987).

22. W. A. Zisman, In *Contact Angles, Wettability, and Adhesion*, F. M. Fowkes, Ed., Advances in Chemistry 43, American Chemical Society, Washing D.C., 1, 1964.; J. M. McBride, B. E. Segmuller, M. D. Hollingsworth, D. E. Mills, and B. A. Weber, *Science*, **234**, 830 (1986).

23. H. Schubert, and H. Baldauf, *Tenside*, **4**, 6, 172 (1967). M. M. Allingham, J. M. Cullen, C. H. Giles, S. K. Jain, and J. S. Woods, *J. Appl. Chem.* (London), **8**, 108 (1958).

24. K. Asano, K. Miyano, and H. Ui, *Langmuir*, **9**, 3587 (1993). L.Ter Minassian-Saraga, *J. Chim. Phys.*, **57**, 10 (1960).

25. K. Shinoda, T. Nakagawa, B. Tamamushi, and T. Isemura, *Colloidal Surfactants*, Academic, New York, 1963, p.179.

26. J. Heesemann, *J. Am. Che. Soc.*, **102**, 2167 (1980).

27. E. G. McRae, and M. Kasha, *Physical Processes in Radiation Biology*. Academic Press, New York, 1964, p.23.

28. Gaudin, A.M., *Flotatation*, 2nd Ed., McGraw-Hill, New York, Vols. 1-3, 1957.

29. Ottewill, R.H., and Rastogi, M.C., *Trans. Faraday Soc.*, **56,** 866, (1960).

30. H. A. Van der Schee, and J. Lyklema, *J. Phys. Chem.*, **88**, 6661 (1984).

31. J. Zhang, R. Pelton, and Y. Deng, *Langmuir*, **11**, 2301 (1995).

32. C. D. Wagner, W. M. Riggs, L. E. Davis, J. F. Moulder, and G. E. Muilenberg, eds. *Handbook for X-ray Photoelectron Spectroscoopy*, Perkin-Elmer, Eden Prairie, MN, 1978.

33. L. Odberg, and S. Sandberg, *Langmuir*, **11**, 2621 (1995).

34. N. Yamada, T. Okano, H. sakai, F. Karikusa, U. Sawasaki, and Y. Sakurai, *Makromol. Chem., Rapid Commun.*, **11**, 571 (1990)

35. P. F. Brode, *Langmuir*, **4**, 176 (1988).

Chapter 4
Characterizing and Developing Sulfonate-Functionalized Self-Assembled Monolayers

4.1 Abstract

Monolayer films of (3-mercaptopropyl)trimethoxysilane (MPS) were prepared on single crystal silicon, quartz, and glass substrates by allowing the silane to spontaneously adsorb from a dilute hydrocarbon solution. Treatment of this type of monolayer with an ozone-producing mercury lamp results in efficient conversion of the surface-localized thiol groups to a sulfonate groups. With the help of X-ray photoelectron spectroscopy and contact angle measurement, a complete photo-oxidization of the thiols surface has been characterized.

4.2 Introduction

Intense research efforts are currently being directed toward developing processing techniques that produce high-quality ceramics and high-performance and conducting polymers under conditions that are compatible with a wide range of other materials and composites. Conducting, nonlinear optical, electroluminescent, magnetic, impermeable, hard, soft, active, abrasion and corrosion resistant coating all represent growing markets for ceramics and polymers deposited on plastics. For many of the above applications, the processing needs a functionalized interface to bridge the different materials. For example, sulfonate groups can be introduced into the surfaces of aromatic polymers such as polystyrene and polycarbonate through room temperature exposure to sulfuric acid liquid or vapor [1-2]. Amino, carboxylate, hydroxyl and phosphate groups can be bonded to polyethylene [3]. By the nucleation and growth on aqueous system, a thin ceramic film of

γ-Fe_2O_3 and FeOOH can be formed on sulfonated polystyrene substrates. Functionalized, siloxane-anchored, self-assembled monolayers (SAMs) have been shown to provide homogeneous, stable and versatile surface modification of oxide/hydroxide-bearing substrates [4-11].

Since sulfonated surfaces have found extensive applications, an efficient creation of RSO_3H-bearing surfaces is of particular importance. Sukenik *et al.* have reported the in situ creation of surface bearing CH_2SO_3H groups based on the oxidation of the CH_2SH group using H_2O_2/CH_3COOH [12]. Calvert and co-workers have shown in a closely related system that Sukenik's procedure produces incomplete oxidation [9]. As a superior oxidation procedure, Hickman and coworkers have reported the photo-oxidation of siloxane-anchored thiols [13]. Ichinose *et al.* have introduced a phenylthiol group to enhance the benzene-like adsorption (ε= 10^4 mol^{-1} dm^3 cm^{-1}) around 248 nm to the film, which is much larger that those of alkylsulfides (ε= 10^2-10^3 mol^{-1} dm^3 cm^{-1}) and thiol (ε< 100 mol^{-1} dm^3 cm^{-1}). However, none of the reported chemical conversions provide surfaces which show the complete wetting that would be expected for a truly uniform, hydrophilic, sulfonated surface [4]. On the other hand, the sulfonated SAM surface may provide more uniform and complete array of anionic reaction centers as organic templates for the buildup of self-assembled multilayer through physisorption in comparison to bare Si substrates, leading to adherent films with uniform thicknesses.

In this chapter, we show that close-packed, well-ordered 3-mercaptopropyl)trimethxysilane (MPS) monolayer can be formed on the surfaces of single crystal silicon, quartz, and glass by allowing hydrolyzed silane to self-assemble from a dilute hydrocarbon solution. The films of MPS were irradiated with the UV output of an ozone-producing Hg pencil lamp in order to photo-oxidize thiols to sulfonate. From contact angle measurements and X-ray photoelectron spectroscopy, a complete oxidation

of the thiols on a silane-anchored surface can be seen to occur, and a complete wetting of the sulfonated substrate can be achieved.

4.3 Experimental

4.3.1 Materials

(3-mercaptopropyl)trimethoxysilane (MPS), hydrogen peroxide (30%), toluene, ethanol, and methanol were obtained from Aldrich. Hydrogen chloride (37.9%) was purchased from Fisher. All the above materials were used without further purification. *p*-Silicon substrates were standard semiconductor grade silicon wafers (3-in. diameter) from Monsanto. The ultrafine glass slides were obtained from Fisher.

Ultrapure water was obtained from a Barnstead Nanopure II deionization/ultrafiltration unit. The resistivity of water was above 18 MΩ-cm.

4.3.2 Methods

4.3.2.1. Preparation of Silanization Substrates.

The silicon wafers (0.015-0.2 in. thick) were cut into strips 4 cm x1.5 cm. The quartz, and glass slides were rubbed with filter paper saturated with Micro Detergent (International Products Corp.), followed by a rinse in ultrapure water. The slides were then hand-wiped with acetone followed by sonication in acetone (2x10 min each) and ethanol (2x10 min each). After drying the surface, the slides were placed in a slide-staining jar and exposed to a piranha solution [30:70 mixture of hydrogen peroxide (30%) and hydrogen chloride (36%)] at 70 ^{0}C for 1 hour. After the mixture was cooled to room temperature, the liquid was poured off. The slides were immediately rinsed with nanopure water. The washing process was repeated at least 4 times. Then the slides were baked in an oven at 120 ^{0}C for 2 hours. The above procedure yields a surface which is totally

wetted by water. Preparation of the single crystal silicon slides is accomplished using the procedures discussed in Chapter III.

4.3.2.2. Formation of Self-Assembled Monolayer of MPS.

Once the slides have been thoroughly cleaned and dried, the MPS monolayer can be deposited. In this process, a moisture free atmosphere must be maintained. 0.5 mL of MPS were added to 80 mL of toluene which contained 1.3×10^{-2} mol L^{-1} of glacial acetic acid. After mixing well in a vial that had been thoroughly rinsed with piranha solution and ultrapure water, the solution was transferred into a slide-staining jar. The slides were then put into the slide-staining jar and were allowed to stand in solution with no agitation. The above process was performed in a nitrogen atmosphere. The slide-staining jar was then placed in an oven and heated at 46^0C. After 1 hour, the slides were removed from the deposition solution, rinsed with pure toluene twice, and ultrasonically agitated for 2 min each in pure toluene, a toluene/methanol (1:1) twice, and finally pure methanol twice. The slides were then allowed to dry either in air or under a nitrogen stream. No difference in the results were observed between the two drying methods.

4.3.2.3. Photo-Oxidation Procedures

MPS self-assembled films were exposed directly or through a contact mask to the light from a low pressure mercury lamp (Spectroline Ozone-producing lamp). The pencil lamp (length 1 1/8", outside diameter 1/4") was held about 5-10 cm above the slide surface. The power of the mercury lamp was about 2 W. The orientation of the slide was set parallel to the pencil lamp which results in an approximately even distribution of radiation along the slide length.

4.3.3 Surface Characterization

X-ray photoelectron spectroscopy (XPS), ellipsometry and contact angle measurements were employed to characterize the photo-oxidation of thiol surfaces and the deposition process of SAMp films on sulfonated-functionalized SAM surfaces. Contact angle measurements have been described in Chapter 3.

4.3.3.1 X-Ray Photoelectron Spectroscopy (XPS)

XPS is an ideal instrument for the surface analysis of chemical change as a result of photo-oxidation of thiol molecules due to its high sensitivity, and non-destructive nature [4,13].

XPS analysis was performed on a Perkin-Elmer PHI 5400 spectrometer with a MgKα (1253.6 eV) achromatic X-ray source operated at 15 KeV and an emission current of 20 mA. The vacuum inside the analysis chamber was maintained at $<2 \times 10^{-7}$ torr during the analysis. Samples with dimension of 1 cm x 1 cm were mounted on the sample holder with double-sided tape. Analyses were obtained from the center area of 2 x 2 mm^2. All samples used for XPS measurements were single crystal silicon substrates and were analyzed at ambient temperature. For each sample, a survey scan was taken from 0 to 1000 eV, and narrow multiplex scans were obtained on those significant peaks observed in the survey scan spectra. all spectra were referenced to the Si 2p(3/2) peak at of the silicon substrate [13]. Atomic concentration calculations were performed on an Apollo 3500 computer, using PHI software version 4.0.

4.3.3.3 Ellipsometry Measurements

Ellipsometry measurements were carried out at room temperature with a rotating ellipsometer (Gaertner Scientific Corporation, Chicago). The light source was a He-Ne

laser at a wavelength of 632.8 nm. The angle of incidence was 70^0. The measurements necessary for the calculation of the film thickness consisted of the determination of two sets of polarizer and analyzer readings for the silicon substrate and of the corresponding values for the substrate coated with a monolayer film.

Each set of analyzer and polarizer angles was the average of at least four measurements taken at different positions (separated by about 1 cm) on the sample. The refractive index of each substrate was determined directly from the analyzer and polarizer readings for the uncoated silicon. Refractive indices for the various substrates ranged from 3.84 to 3.87. We have estimated that the oxide layer was about 3.0 nm in thickness. We assumed that the monolayer had a refractive index of 1.45 and was completely transparent to the laser beam [14]. Altering this value by 0.05 resulted in less than 0.1 nm change in the thickness of the monolayer.

4.4 Results and Discussion

4.4.1 Characterization of MPS Monolayer Films

(3-Mercaptopropyl)trimethoxysilane (MPS) is a commercially available, stable silane. MPS is known to readily polymerize in aqueous solution. Therefore, we have to be careful to avoid moisture contamination during the self-assembly process, since pre-deposition polymerization often produces thick and uneven adsorbed films [14]. Monolayers were prepared on clean silicon wafers, whose surface is supposed to be silicon dioxide with 5 x 1014 SiOH groups/cm [15]. For the purpose of contact angle measurements, monolayers were also prepared on clean glass and quartz slides. For the silanation, the slides were allowed to react with the silane in a freshly prepared, unstirred solution of dry toluene (dried with molecule sieve). The reactions took place inside glass containers sealed with nitrogen gas. Then the glass container was put in an oven and

heated at 46° for 1 hour. The substrates were removed from the solution, rinsed with organic solvents, and dried. The ellipsometric angles for the substrate were measured just before immersion.

Due to the susceptibility of the silicon-chloride bond to hydrolysis, it was necessary to limit the amount of water present in the system in order to obtain monolayers of good quality [14]. Although, the surface of a silicon dioxide substrate is not anhydrous, and a thin film of surface-condensed water may be necessary for the formation of the monolayer [16-17]. It is critical to keep the solution of MPS under a nitrogen atmosphere and in an oven (sealed with parafilm) when these monolayers are prepared since the relative humidity may be too high.

To characterize the MPS film surfaces before and after irradiation, contact angle or ellipsometry measurements, and X-ray photoelectron spectroscopy (XPS) were used. The freshly prepared MPS monolayer film gave a measured thickness of 9 ± 1 (n=1.45), which is agreement with the projection of a single layer of extended molecular chains onto the surface normal. Using the sessile drop method, the advancing contact angle of MPS film for water was 57 ± 3^0, confirming previously reported values [13]. This contact angle value is consistent with a moderately polar surface where the mercapto group is oriented upward [18].

The above data show that adsorption from an organic solvent solution of MPS results in layers of approximately monolayer coverage.

The composition of MPS monolayers on single crystal silicon substrates was analyzed by XPS. Figure 4.1 shows the XPS scan spectrum of a freshly prepared MPS self-assembled film on single crystal silicon. From Table 4.1, the observed relative atomic concentrations of C(1s), O(1s), N(1s), Si(2p), and S(2p) are seen to be 18.56, 52.69, 0.11, 26.04, and 2.61, respectively. The large amount of silicon relative to sulfur is

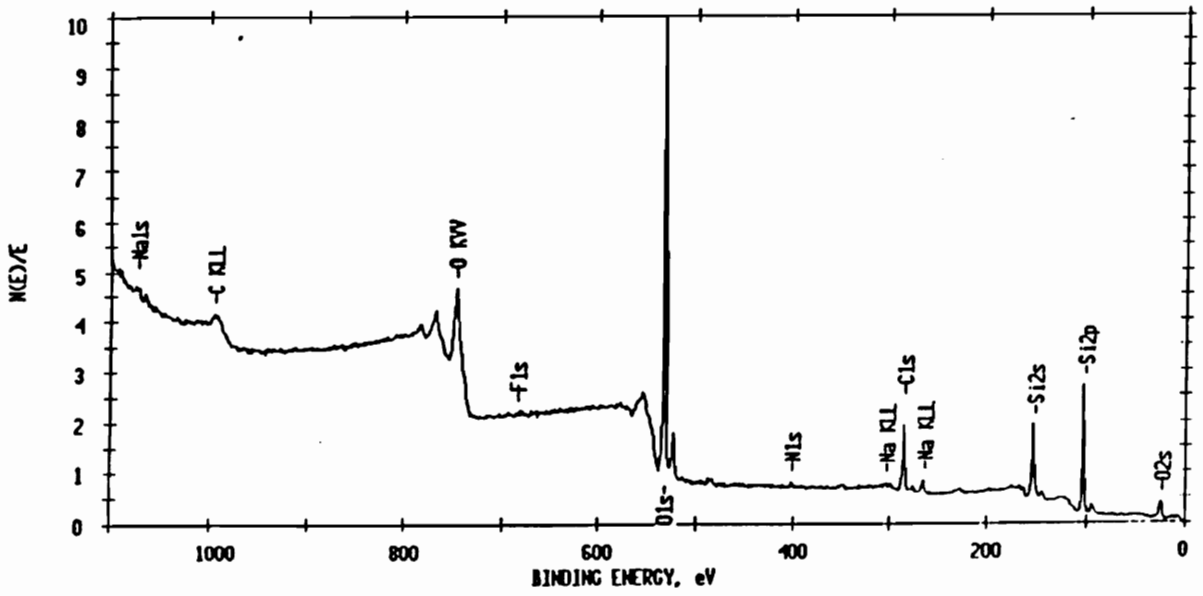

Fig. 4.1. The scan XPS spectrum of MPS monolayer films on single crystal silicon.

Table 4.1. Atomic concentration of elements of MPS monolayer film on single crystal silicon.

Element	Sensitivity Factor	Concentration (%)
C1s	0.296	18.56
O1s	0.711	52.69
N1s	0.477	0.11
Si2p	0.339	26.04
S2p	0.666	2.61

an indication that the silane layer is thin, so a significant level of electron emission is observed from the underlying substrate. If the thickness of the silane film had exceeded the escape depth (less than 10 nm), the stoichiometry of the MPS molecule would have resulted in comparable atomic percentages for silicon and sulfur.

4.4.2 Characterization of Photo-Oxidation of MPS Monolayer

The photochemical patterning of mercapto groups by UV irradiation of MPS film with a low-pressure Hg lamp has been reported recently [13]. The thiol group can be efficiently excited only by the 185 nm line of an ozone-producing lamp because of the low absorptivity of alkyl thiols at typical output of 254 nm ($\varepsilon < 50$ mol^{-1} dm^3 cm^{-1}). Therefore, if the exposure time is not long enough, the conversion cannot reach 100%. In order to evaluate the irradiation effects, contact angle measurements were employed. A MPS-modified glass slide was exposed to a fixed amount of irradiation, and contact angles were recorded for three positions along the length of the slide as shown in Figure 4.2. The figure shows how the contact angle on the photo-oxidized MPS film (3 min irradiation) varies with position of irradiation on the slide. The smaller the contact angle corresponds to the greater the intensity of the irradiation at that position. From the graph, there appears to be some regional variation in intensity, the strongest irradiation area being near the center. The area of weakest irradiation is seen to be far away from the center, although the standard error of $\pm 2^0$ indicates the observed variation is essentially insignificant. Figure 4.3 shows contact angles observed on a MPS monolayer on glass substrates as a function of UV exposure time. The distance of the Hg lamp above the film is about 50 mm. Before the UV irradiation, the contact angle is 57^0. As the sample is exposed to the radiation, the contact angle decreases as the irradiation time increases. After 7 minutes the contact angle is less than 3^0 in all areas of the exposed film, the

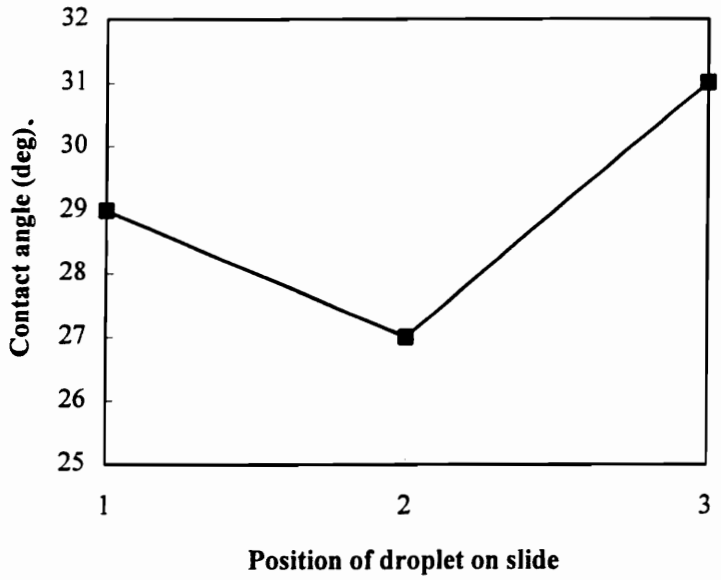

Fig. 4.2 Contact angle (degree) of photo-irradiated (3 min) MPS film as a function of position of droplet on slide.

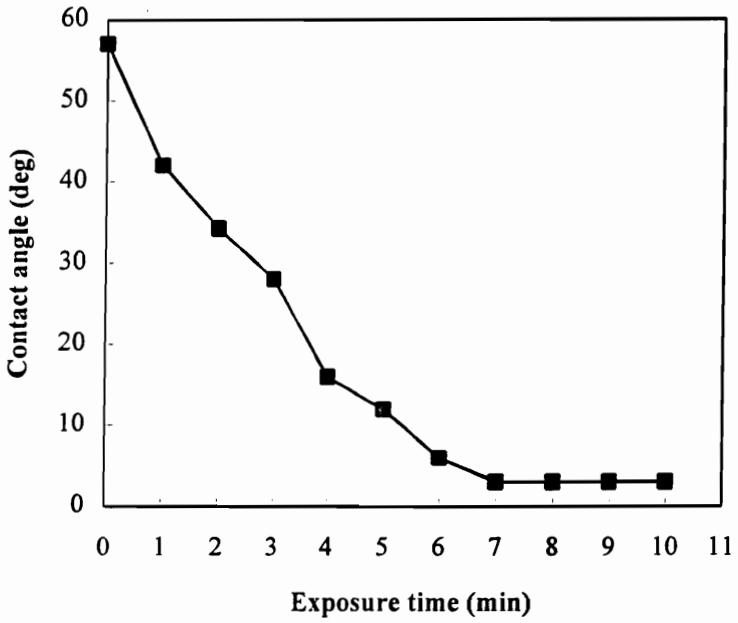

Fig. 4.3 Contact angle of MPS monolayer film deposited on glass substrates as a function of exposure time of UV.

surface is completely wetted. This indicates that most of the thiol groups have been converted to sulfonate groups. If the distance of the lamp from the film is increased, longer exposure times were necessary for the photochemical conversion to be completed. For example, when the distance was about 10 cm, the time for the contact angle to reach 30^0 was about 35 minutes, and the time for the contact angle to reach 3^0 was 75 minutes. If the time of exposure is not long enough, a partial conversion result will be obtained, the film surface displays different contact angle values which depend on the position of the substrates, and there is a large error in the contact angle. We thus expect that the reason for Hickman et al. reporting contact angles of 30 ± 6^0 after UV irradiation [13] is due to incomplete exposure.

The thickness of MPS monolayer determined by ellipsometry measurements shows no change after the monolayer is exposed to the UV light. This clearly demonstrates that such optical treatment does not result in any thiol removal, but rather results in the photochemical reaction of thiols.

Thiol groups can spontaneously be oxidized also in air. XPS was used to investigate the oxidation of thiol groups in air as shown in Figure 4.4., all spectra were referenced to the Si $2p_{3/2}$ peak of the single crystal silicon sample. Part of the figure in Figure 4.4(a) shows the S 2p region for a freshly prepared MPS monolayer. The sulfur S $2p_{3/2}$ photopeak is observed at 163.5 eV, evincing its divalent state as is typical of thiol. A very weak peak at 169 eV indicates that some sulfonate groups exist at a time of about 20 minutes after freshly preparing the sample. After the MPS monolayer was stored in air for 3 days, more thiol groups were oxidized to sulfonate as shown in Figure 4.4 (b) in which both thiol (peak at 163.5 eV) and sulfonate (peak at 169 eV) are clearly observed. After UV irradiation for 15 minutes at a distance 5 cm, the S 2p peak intensities have greatly decreased, and the sulfonate peak at 167.67 eV (S $1p_{3/2}$) and 168.97 eV (S $2p_{1/2}$)

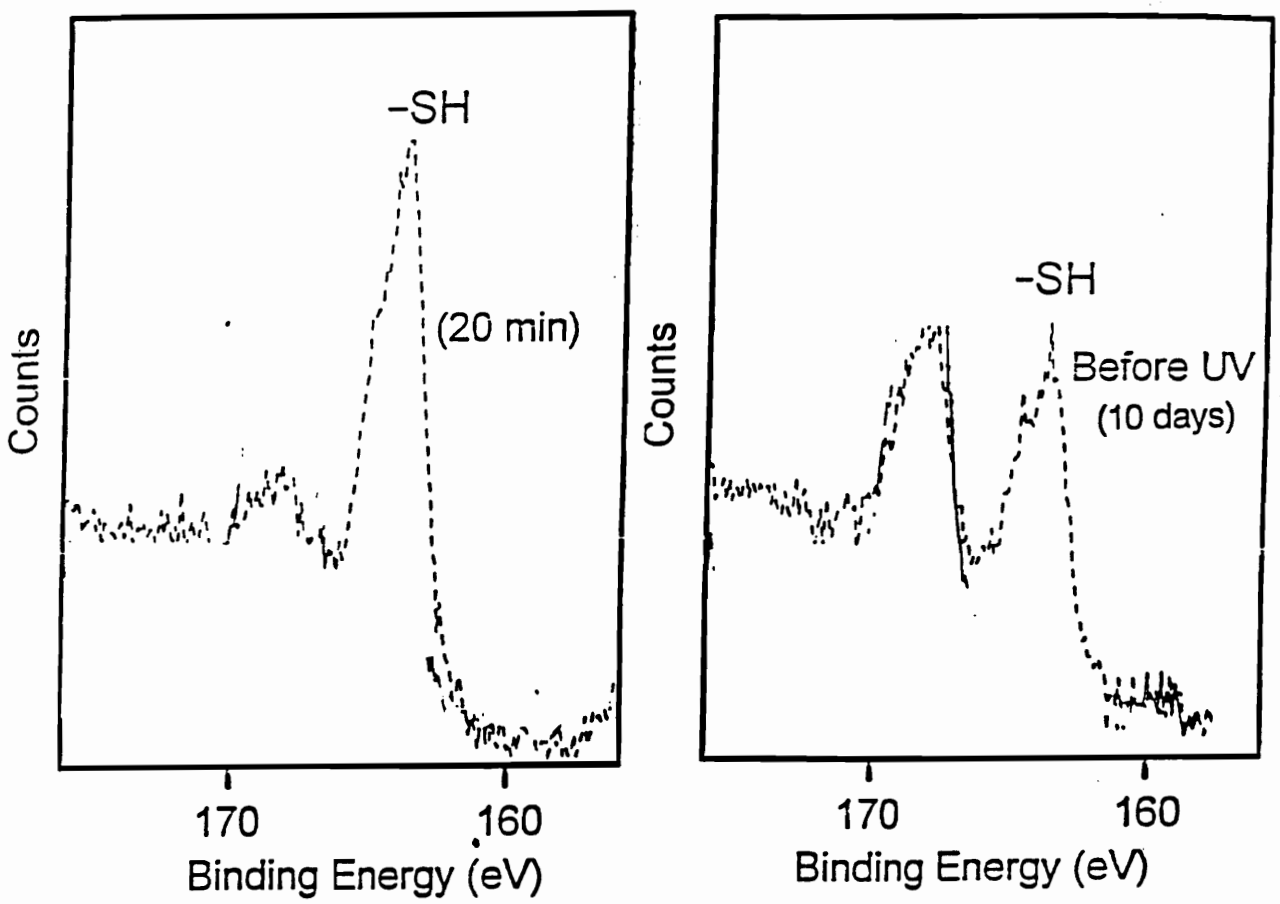

Fig. 4.4. The XPS spectra of MPS monolayer films are shown (a) freshly prepared film 20 min. and (b) film stored in 10 days at ambient condition. All the spectra were referenced to the Si 2p(2/3) peak of the single crystal silicon sample.

[15] have greatly increased. When we increase the irradiation time to 1 hour, a complete oxidation of sulfur to sulfonate is accomplished as evinced in Figure 4.5. Our results of complete oxidation of thiol groups might also due to the use of the ozone-produced mercury lamp. During the UV exposure process, a relatively high density of ozone is produced near the monolayer surface, as a result, the oxidation process is promoted and fully completed.

4.5 Conclusions

The present work has demonstrated that the use of photo-oxidation to transform thiol groups to sulfonate groups is a convenient, effective, and reliable approach. The techniques of ellipsometry, contact angle measurements, and XPS were employed and gained a consistent picture showing the oxidation by photoxidation of thiol groups to sulfonate groups in a monolayer, and the obtained sulfonated functionalized self-assembled monolayer surface is completely wetting. This study demonstrates that useful photochemical methods can be employed on a Self-assembled film to modify a property of interests as we have talked at the begining of this Chapter. Our main interest focus on that a complete wetting, sulfonated self-assembled films can be used as good organic templates for the deposition of self-assembled ionic polymer films, and to micropatternig of organic surfaces. We can use the functionality difference between thiol and sulfonate to direct the adsorption of ionic polymers such as these discussed in Chapter III into specific surface areas, then allowing built-up films to be deposited as patterns with micron-scale features.

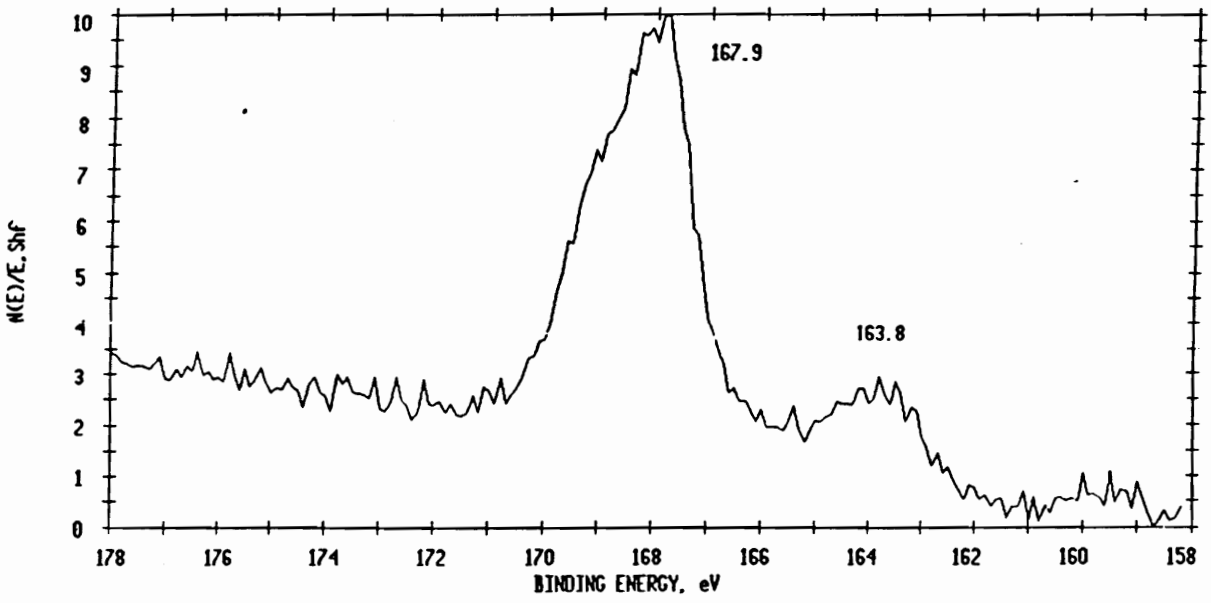

Fig. 4.5. The XPS spectrum of MPS monolayer film after the irradiation with a UV light source for 15 minutes. The spectra was referenced to the Si 2p(2/3) peak of the single crystal silicon sample.

References

1. B. C. Bunker, P. C. Rieke, B. J. Tarasevich, A. A. Campbell, G. E. Fryxell, G. L. Graff, L. Song, J. Liu, J. W. Virden, and G. L. McVay, *Science*, **264**, 48 (1994).
2. E. Dalas, *J. Material Chem.*, **1**, 473 (1991).
3. S. B. Bentjen, D. A. Nelson, B. J. Tarasevich, and P. C. Rieke, *J. Appl. Polym. Sci.* **44**, 965 (1992).
4. R. J. Collins, and C. N. Sukenik, *Langmuir*, **11**, 2322 (1995).
5. Y. W. Lee, J. Reed-Mundell, C. N. Sukenik, and J. E. Zull, *Langmuir*, **9**, 3009 (1993).
6. B. C Bunker, P. C. Rieke, B. J. Tarasevich, A. A. Campbell, G. E. Fryxell, G. L. Graff, L. Song, J. Liu, J. W. Virden, and G. L. McVay, *Science*, **264**, 48 (1994).
7. N. Tillman, A. Ulman, and J. F. Elman, *langmuir*, **5**, 1074 (1989).
8. L. Netzer, and J. Sagiv, *J. Am. Chem. Soc.*, **105**, 674 (1983).
9. S. K. Bhatia, J. L. Teixeira, M. Anderson, L. C. Shriver-lake, J. M. Calvert, J. H. Georger, J. J. Hickman, C. S. Dulcey, P. E. Schoen, and F. S. Ligler, *Anal. Biochem.*, **208**, 197 (1993).
10. J. N. Israelachvili, *Intermolecular and surface Forces*, Academic Press, San Diego, 1991.
11. A. Ulman, *An Introduction to Ultrathin Organic Films from Langmuir-Blodgett to Self-Assembly*, Academic Press, New York, 1991.
12. N. Balachander, and C. N. Sukenik, *Langmuir*, **6**, 1621 (1990).
13. S. K. Bhatia, J. J. Hickman, and F. S. Ligler, *J. Am. Chem. Sci.*, **114**, 4432 (1992). N. Ichinose, H. Sugimura, T. Uchida, N. Shimo, and H. Masuhara, *Chem. Letter*, 1961 (1993).

14. J. K. Yee, D. B. Parry, K. D. Caldwell, and J. M. Harris, *Langmuir*, **7**, 307 (1991). M. J. Zalewski, P. Chu, P. N. Tutnijian, and J. H. Luns Ford, *Langmuir*, **5**, 1026 (1989).

15. A. H. Carim, M. M. Dovek, C. F. Quate, R. Sinclair, and C. Vorst, *Science*, **237**, 630 (1987).

16. R. Iler, The Chemistry of Silica, Wiley: New York, 1979, Chapter 6.

17. R. Maoz, and J. Sagiv, *Langmuir*, **3**, 1034 (1987).

18. L. H. Lee, *J. Colloid, Surf. Sci.*, **27**, 751 (1968).

Chapter 5

Self-Assembled Multilayers of Ionic Polymers on Sulfonate- and Thiol-Functionalized Siloxane-Anchored Substrates

5.1 Abstract

A monolayer film of (3-mercaptopropyl)trimethoxysilane (MPS) was deposited onto silica substrates to yield a photoreactive thiol-functionalized surface. Irradiation of the surface with UV light at the atmosphere of ozone converts the thiol groups of MPS completely to sulfonates. XPS and contact angle measurements indicate that polycation molecules (PAH) adsorb exclusively onto the sulfonate surfaces, whereas polyanion molecules (PDYE) adsorb exclusively onto the thiol surfaces. A novel self-assembly processing technique has been developed for the fabrication of ultrathin films of ionic polymers with angstrom-level control over thickness and multilayer architecture on sulfonate- and thiol functionalized siloxane-anchored substrates.

5.2 Introduction

In Chapter III, we reported that well-ordered, uniform molecular self-assembled ionic polymer films can be build up on oxide/hydroxide-bearing substrates (negatively charged) and N-2-Aminopropyltrimethoxysilane (APS) modified (positively charged) oxide/hydroxide-bearing substrates [1-6]. In Chapter IV, we demonstrated that highly-ordered and well-anchored siloxane monolayers of (3-mercaptopropyl)trimeothxy- silane (MPS) can be deposited onto surfaces of single crystal silicon, quartz, and glass substrates. Also in Chapter III, deep UV irradiation of MPS modified surface was reported to completely oxidize thiol groups and provide sulfonate-functionalized

(negatively charged) surfaces. In this chapter, we will further our study of thiol surface photooxidation by addressing organic templates and surface patterning strategies.

Masked UV exposure of a MPS monolayer film can be used to create patterned regions of sulfonate (negatively charged) and thiol functioanlity. This kind of patterned surface can be used to create a self-assembling three-dimensional structure using biomolecules as building blocks. The process begins with a two-dimensional template which has the ability to direct the construction of subsequent layers. The first and basic step for making patterns of biomolecules, such a patterned template must include areas which resist nonspecific adsorption completely. The studies of Ligler and co-workers [7] have established that such patterned biomolecular assemblies can be produced by photooxidation of self-assembled monolayers, but the selectivity of the their patterned surface was not very high. They report about 14% of unwanted adsorption due to their incompletely photooxidation of thiols. Here we report the fabrication of high quality patterned surfaces of sulfonate- and thiol-functioalized self-assembled monolayers. XPS and contact angle measurements show that an anionic polyelectrolyte, poly s.119 (PDYE), does not adsorb on solfonated self-assembled monolayer (MPS) surface but on thiol-terminated MPS monolayer surface; While a cationic polyelectrolyte, poly(allylamine hydrochloride) (PAH), can be deposited on sulfonated self-assembled monolayer (MPS) surfaces but not on thiol-terminated MPS monolayer surfaces. Patterned surface functionalization has found extensive application as we have described in chapter IV. Furthermore, patterned surfaces can also be used as a basis for growth of patterned ionic polymer films. Therefore, such approaches can be expected to help to bridge the interaction between different materials and composites such as plastics, ceramics, metals and inorganic solids.

These investigations have depended heavily on comparisons of X-ray photoelectron spectroscopy (XPS), UV/Vis spectroscopy and contact angle measurements. It is well known that wetting is one of the most surface-sensitive techniques currently available [8-10]. Optical absorbance is one of the most appropriate instrument for probing the amount adsorbed on the surface. The two main advantage of the technique are its extreme surface specificity and nonrestrictive nature. XPS is an ideal tool for the surface analysis of thin films due to its non-destructive nature, extreme sensitivity and its shallow depth. Here, XPS was employed to characterize the chemical changes which occur on the thin films as a result of molecular adsorption. The experimental section of XPS, UV/Vis spectroscopy and contact angle measurements have been reported in detail in Chapters III and IV.

5.3 Experimental

5.3.1 Photochemical Patterning of Siloxaned Surface

The procedure for photo-oxidation of MPS monolayers has been described in Chapter IV. Macroscopic patterns were formed by using an aluminum foil to cover some regions of an MPS modified surface as shown in Fig. 5.1. The substrate and aluminum foil were positioned in a close mechanical contact. The MPS monolayer was irradiated by a 2W ozone-producing mercury lamp for 30 minutes. After the irradiation, the aluminum foil was carefully removed from the assembly, and the contact angle measurements were made within 30 min.

5.3.2. Construction of a Multilayer System

Self-assembled multilayer films were built up on photo-oxidized MPS surfaces, patterned MPS (sulfonate/thiol surfaces), and intact MPS surfaces. The substrates were

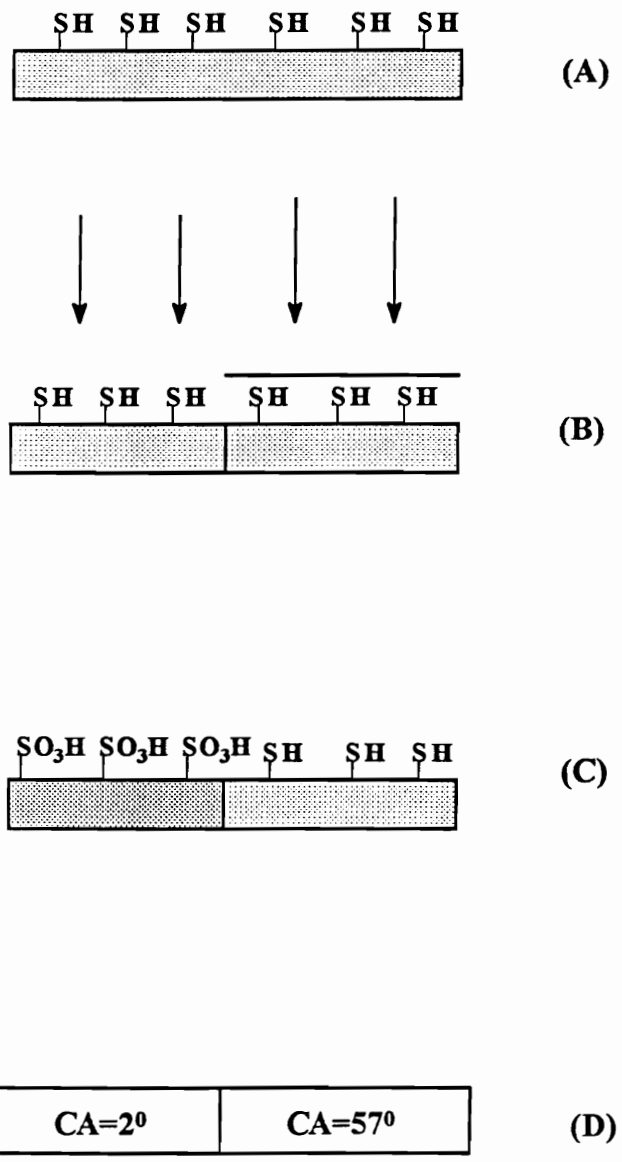

Fig. 5.1. Procedures for preparation of patterned surfaces. (A) MPS monolayer film on silica. (B) An UV exposed pattern on MPS monolayer film. (C) The patterned regions of sulfonate and thiol groups. (D) The contact angles of the patterned regions: CA=57^0 for protect regions (MPS film) and 2^0 for exposured regions (sulfonated MPS film).

alternately dipped into polycationic and polyanionic solutions for 15 minutes each. The film-coated substrates were extensively rinsed after adsorption of each layer. The dipping was carried out at room temperature and pressure (for structures see Figs. 2.4 and 3.2). In order to maintain the protonated state of the cationic molecules, the pH of all deposition solutions was kept at 4.0.

5.4 Results and Discussion

5.4.1 Patterning and Characterization of the Surfaces.

Patterns were formed in self-assembled monolayers (SAMs) of MPS on silica or silicon by using the masked UV exposure technique. The procedure for the preparation of the patterned surface is shown in Fig. 5.1. Irradiation through a mask produced a patterned SAM: the unexposed regions terminate in thiol and the irradiated areas terminate in sulfonate. The average contact angle for the protected regions is 57 ± 3^0, whereas the contact angle for the exposured areas is $<4^0$ which indicates a completely wetted surface. Based on the discussion in Chapter IV, the results clearly show that the unexposed area is well protected and that the thiol groups in the exposed area of the slides are converted to sulfonate groups. Although only a simple pattern of MPS and sulfonated MPS has been produced, it would be straight forward to make a high resolution (μm-scale) pattern using the same procedures with a high resolution mask. Thus, a high-contrast pattern, alternating sulfonates and a thiol surface can be produced.

5.4.2 Adsorption of Polyelectrolytes on sulfonated MPS and MPS.

Up to today, only mica and bare Si have been reported as negatively charged substrates for the buildup of self-assembly films through physisorption [11-12]. The new approach to employ the sulfonated SAM surface as an organic template comes from our

assumption that the sulfonate-functionalized SAM face is a better candidate of negatively charged template than the bare Si and mica, since it can play a role to promote the adsorption of caionic polyelectrolyte by providing anionic reaction center and/or by providing a lower local pH at the solid-solution interface [11], such surface also represents a more uniform and complete array of anionic sites, leading to adherent films with uniform thickness.

In order to assess the sulfonated surface as a substrate for the build-up of multilayer ionic polymer films, we dipped the photo-oxidized MPS substrate into a solution of polycation, poly(allylamine hydrochloride) (PAH). It is generally agreed that the interaction parameters governing the adsorption of polyelectrolyte on the charged surface indicate the adsorption energy parameter χ_S, the solvency parameter χ, the surface charge density σ_O, the polymer charge q_m, and the ionic strength c_s. However, in the low-salt limit, the electrostatic interaction is the main driving force. For simplicity, the salt-free solutions were used in our case, so only the surface charge density and the polymer charge govern the adsorption. Since the polymer and the surface have the opposite charges, the polyvalent ions have to assume the role of the counterions and are kept in the double layer, the electrostatics drive the adsorption process but at the same time limit it because the accumulation of charge at the surface is unfavorable. The surface charge is compensated entirely by the polymer charge, so a monolayer of PAH is adsorbed on the sulfonated SAM surface. As expected, the aqueous contact angle of sulfonated SAM changed from $<4^0$ to 24^0 after the immersion. This value is consistent with our previous results in which the PAH adsorbed on negatively charged glass slides (Chapter III). The XPS results also confirm the adsorption of polycation on sulfonated MPS surface as shown in Fig. 5.2. There is an obvious increase in the N1s peak intensity after the UV-

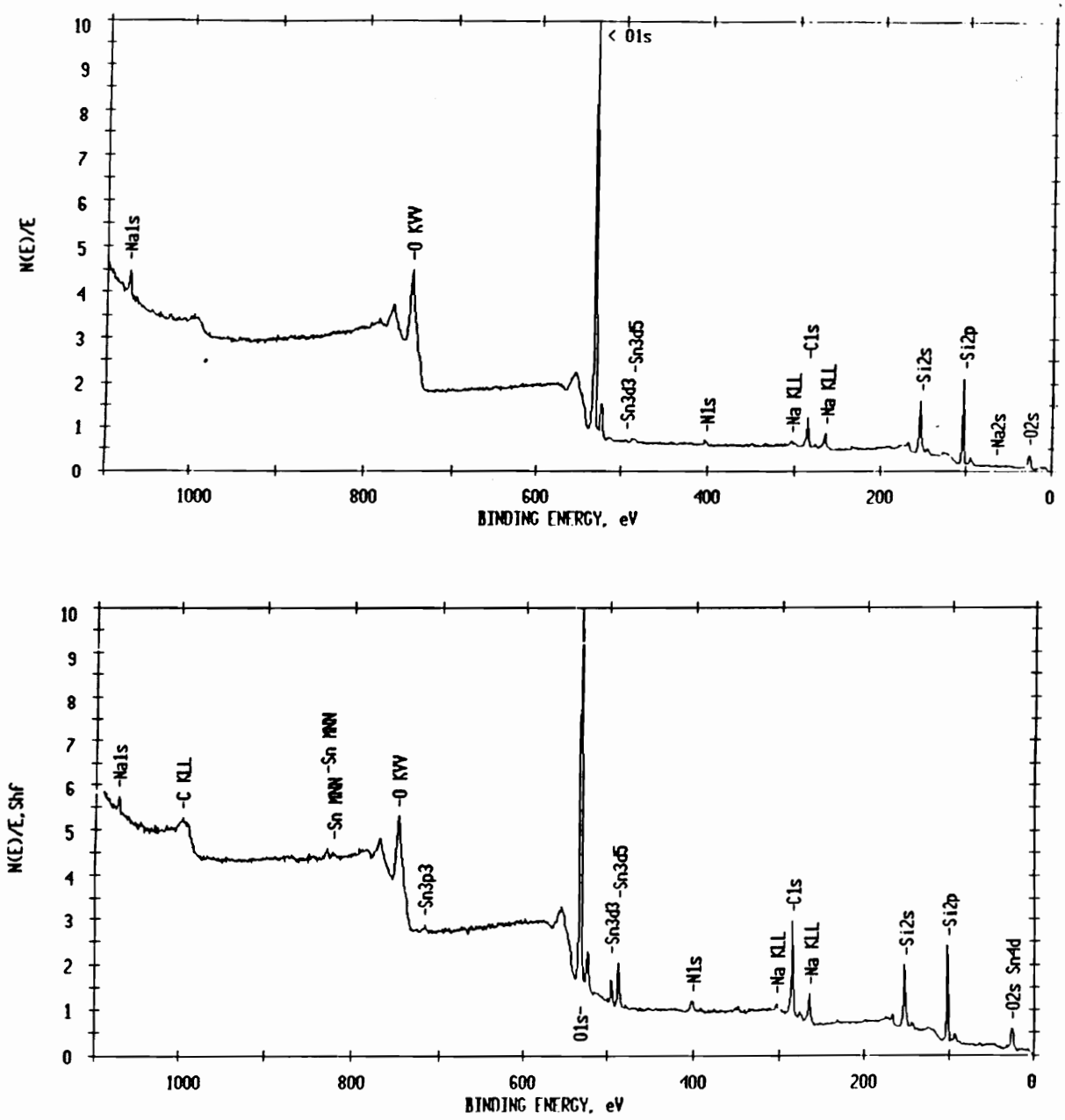

Fig. 5.2. The XPS spectra of MPS monolayer films. (a). After UV irradiation. (b). After immersed in aqueous PAH solution.

exposed MPS film slide was dipped into the solution of PAH, indicating that PAH adsorbed on the SO_3^- sites.

Conversely, there is no change in the peak intensities of XPS after the unirradiated MPS substrate (intact thiols) is immersed in the PAH solution as shown in Fig. 5.3. The aqueous contact angle of this latter sample remains 58 $\pm 1^0$ following exposure to the PAH solution. For the latter case, the adsorption of positively charged polymer on the uncharged surface is prevented by a lack of electrostatic contribution to the adsorption energy. The only electrostatic effect is the strong mutual repulsion among the segments at low c_s, preventing their accumulation on the surface and leading to a negative increment to the solvent parameter χ. Since no salt was added to screen the electrostatic interactions, the "chemical" (Van der Waals *et al.*) interactions among the PAH and SAM molecules are too weak to overcome the physical interactions. Therefore, there is no adsorption of PAH on the sulfonated SAM surface. Fleer *et al.* reported the similar results about poly(styrene sulfonate) (PSS) on essentially uncharged surface [14-15]. At low ionic strength (<0.05 M), there is little adsorption of PSS. As the ionic strength increases, the segment-segment repulsion is screened, and the adsorption increase, tending towards the behavior for the neutral polymers on uncharged surfaces in relatively poor solvents.

When the intact thiol-covered substrate was dipped into the polyanion (poly s.119) solution, the contact angle dropped from 58 $\pm 1^0$ to 44 $\pm$ 2^0. The change in contact angle indicates that some negatively charged polymer dye has been adsorbed on the MPS modified silica surface. More vigorous characterization of the adsorption of polyanion on unirradiated SAM is provided by X-ray photoelectron spectroscopy (XPS) as shown in Fig. 5.4. There are obvious increases in the intensities of the photopeaks associated with the N1s, S2p and C1s photoelectrons. These results strongly suggest that polyanion molecules have been adsorbed on the intact thiol-covered silica surface. Table 5.1 shows

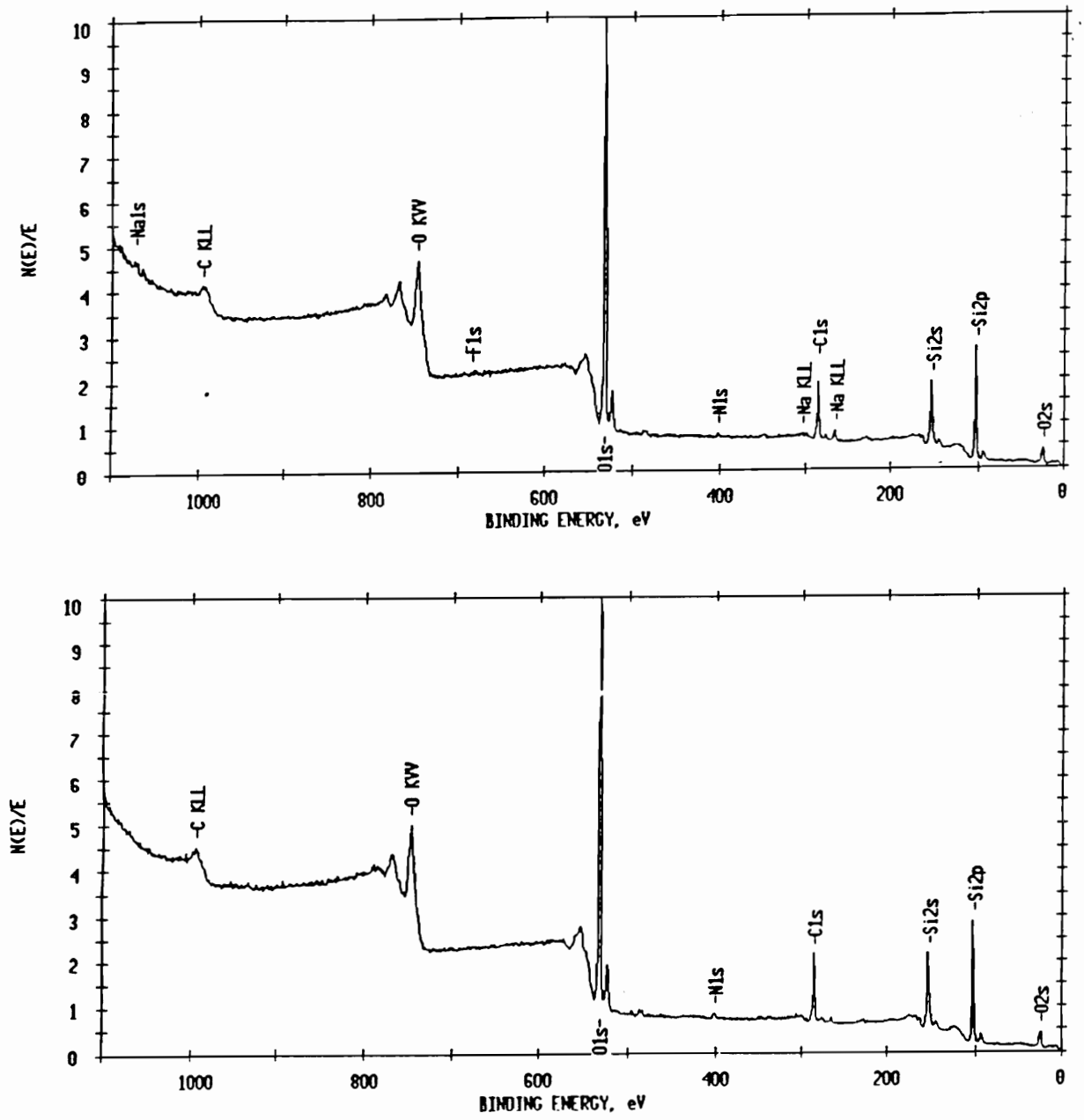

Fig. 5.3. The XPS spectra of MPS monolayer films. (a). Before the adsorption of PAH molecules. (b). After immersed in aqueous PAH solution.

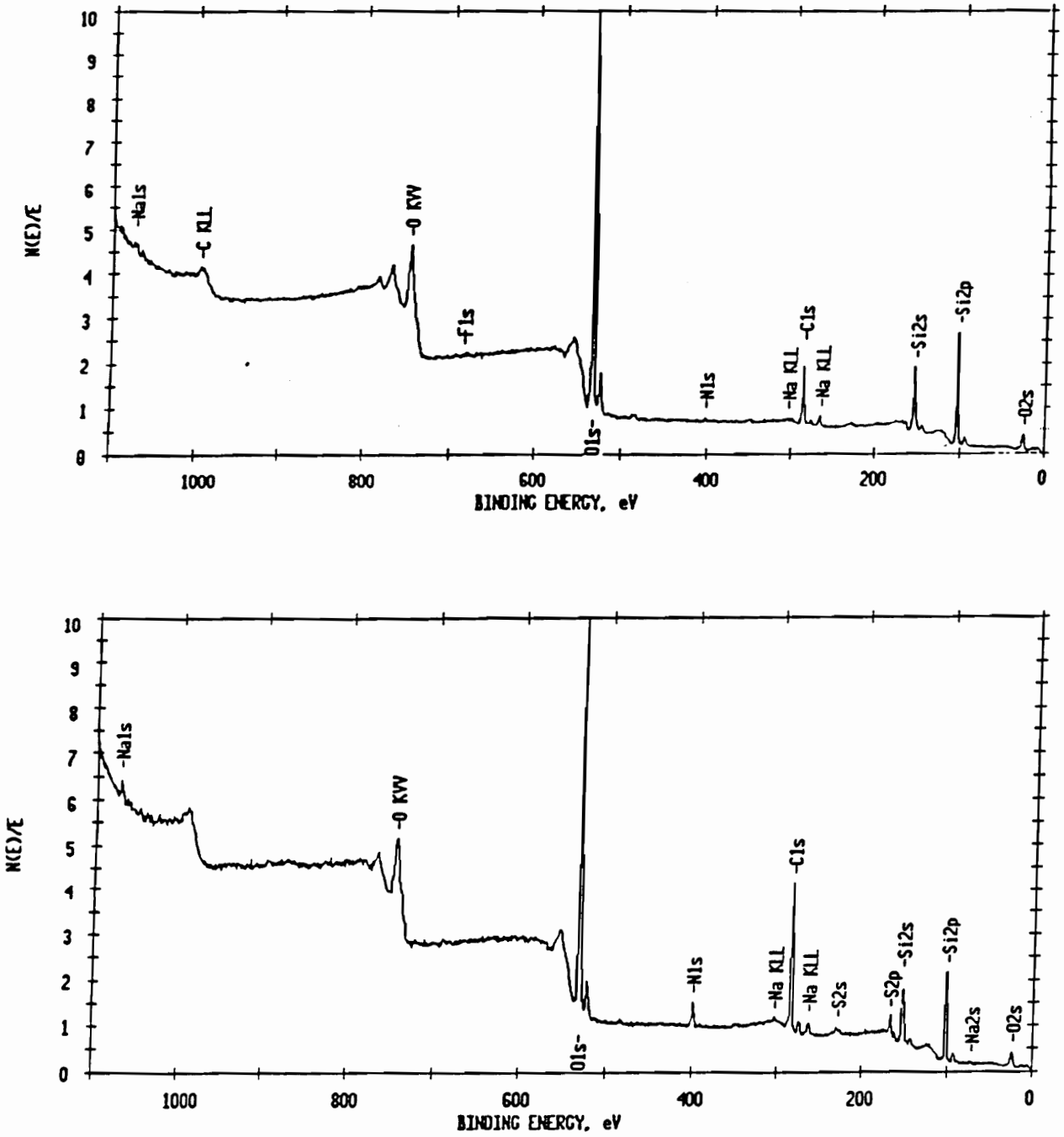

Fig. 5.4. The XPS spectra of MPS monolayer films. (a). Before the adsorption of PDYE molecules. (b). After immersed in aqueous PDYE solution.

Table 5.1: XPS atomic concentrations of MPS modified silicon and adsorption of PDYE on MPS modified silicon.

Element	Concentration (%) MPS film	Concentration (%) (after dipping in PDYE)
C1s	18.56	38.48
O1s	52.69	41.86
N1s	0.11	3.40
Si2p	26.04	14.51
S2p	2.61	1.75

relative surface concentration data derived from the C1s, O1s, N1s, Si2p, and S2p photopeaks. It can be seen that the relative nitrogen concentration on the surface increased dramatically from 0.11 to 3.40, and the relative carbon concentration increased from 18.56 to 38.48. Even though a clear increase in the S2p photopeak has been observed in Fig 5.4, the relative sulfur concentration dropped from 2.61 to 1.75 since there are many carbon atoms and only one sulfur atom in the monomer of PDYE. It is reasonable to see the relative oxygen and silicon concentrations to decrease from 52.69 to 38.48 and 26.04 to 14.51, respectively, because another monolayer has covered the silica surface. Thus, a relatively smaller amount of silica was detected by XPS.

The adsorption of polyanions to the thiol surface was initially unexpected. Our original idea was to use patterned thiol surfaces as templates for the selective buildup of self-assembled multilayers through physisorption. Yet, as described previously, adsorption of polyelectrolytes from salt-free aqueous solutions onto uncharged surfaces is negligible [14-16]. Thus, there might be some special mechanism governing this adsorption process.

In order to elucidate the adsorption mechanism, the adsorption of anionic polymers PDYE and PSS on quartz and glass (negatively charged) slides, and PDYE on sulfonated SAM surface were carried out, and the UV/Vis spectroscopy, XPS and contact angle measurements were utilized to probe the adsorption. The observation that no adsorption of anionic polyelectrolytes occurred onto a negatively charged surface is not surprising (Table 5.2). Neither contact angle measurements nor absorbance indicate any change from before to after the immersion of the slides in the anionic solutions. Similar results are obtained for the immersion of PDYE on photo-oxidized MPS monolayer film. This conclusion is verified by the XPS spectra shown in Fig. 5.5. There is no any change in the peak intensities of N1s and S2p following the deposition attempt. This indicates that the

Table 5.2. Dependence of water contact angle of the different film systems on quartz slides.

Samples	Contact Angles (^{0})	Absorbance
PDYE/quartz	<3	No signal
PSS/quartz	<3	No signal
PDYE/(-SO_3-)MPS	<3	No signal

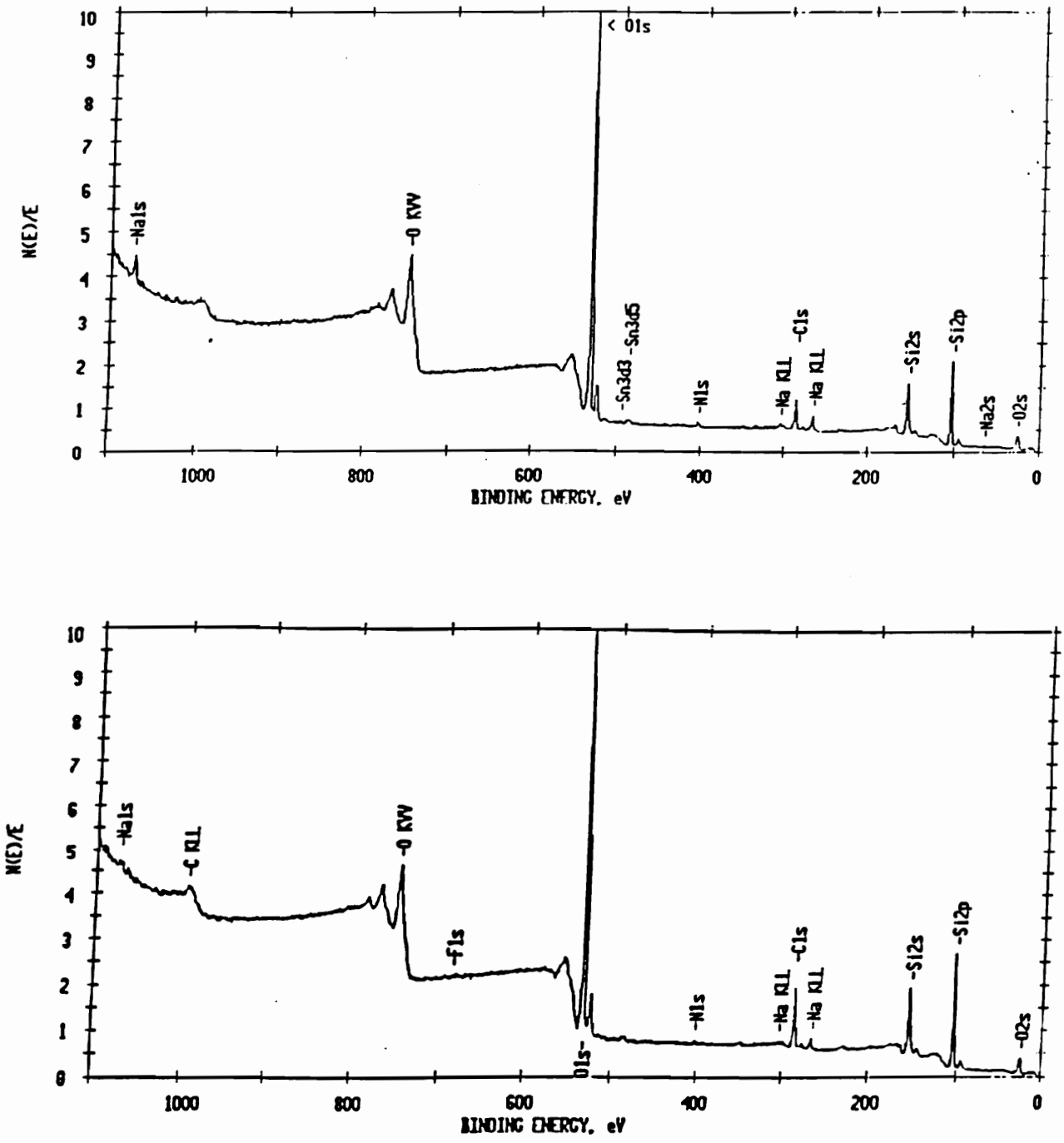

Fig. 5.5. The XPS spectra of MPS monolayer films. (a) After UV irradiation ; (b) After immersed in aqueous PDYE solution.

Columbic energy is dominant in the adsorption of polyelectrolyte in the salt-free aqueous solution.

On the other hand, the adsorption of anionic polymer PSS on a freshly prepared MPS film surface was also carried out to investigate the mechanism as shown in Table 5.3. The contact angle measurements, and optical absorbance spectra show that there is hardly any adsorption occurring on the MPS film surface, since there is no change upon immersion in the PSS solution. The difference of adsorption of PSS and PDYE on thiol terminated SAM surface must arise from different mechanism. A possible explanation for the adsorption of PDYE on the neutral MPS film is that the thiol has a lone pair of electrons and can behave as an electron donor; whereas PDYE has a high degree of conjugation, so it acts as an electron acceptor. When they are brought together, the interaction of electron-donor and electron-acceptor may result in a formation of a complex which is strong enough to withstand the electrostatic repulsion among the PDYE molecules. The absorbed amount is very low because it is unfavorable to accumulate many charged segments at the surface. Only in the surface layer, where there is a compensating adsorption energy (the interaction of donor and acceptor), is such an accumulation possible. As a result, the chains lie essentially flat, with only very short loops and hardly any tails. That is, a monolayer of PDYE is deposited on the neutral MPS monolayer surface.

So, from our results, polycation molecules can be adsorbed on sulfonated MPS surfaces and polyanion molecules PDYE can and PSS cannot adsorb on neutral thiol-functioalized SAM surfaces. Since the ionic attraction between the oppositely charged polymers promotes strong interlayer adhesion and thus, based on our previous results from Chapter III, it is expected that the multilayer ionic polymer films can be buildup on either sulfonated MPS surface or MPS surface.

Table 5.3. Dependence of water contact angle of the adsorption of PSS freshly prepared MPS modified quartz slides.

Sample	Contact Angles (^{0})	Absorbance
PSS/MPS/quartz	< 3	No signal

5.4.3 Buildup of Multilayer Ionic Polymer Films on Sulfonate and Thiol Functionalized Substrates.

In order to understand the deposition behavior of multilayer films of the PAH/PDYE system, we first studied the adsorption of PAH/PDYE system on sulfonated MPS surface and MPS surface, respectively. In the first case, adsorption was carried out on photo-patterned MPS substrates as shown in Fig. 5.2. The concentrations of the PAH and PDYE solutions for both cases were $1.5x10^{-3}$ mol L^{-1} and $1.0x10^{-3}$ mol L^{-1}, respectively. These solutions were adjusted to a pH of 4 with HCl. The dipping time was about 15 minutes for each of polycation and polyanion adsorption.

Fig. 5.6 shows the XPS spectra of 5 bilayers of PDYE/PAH system adsorbed on a sulfonated MPS surface. The results clearly show that PDYE/PAH molecules have adsorbed on sulfonated MPS surface in a layer-by-layer fashion. The XPS of 5 bilayer of PDYE/PAH system adsorbed on MPS modified thiol silicon surface is displayed in Fig. 5.7. As expected, an obvious increase of C1s, N1s, S2p is observed and indicates that the layer-by-layer molecular film of PDYE/PAH has been successfully buildup on the MPS surface. Since the adsorption of either PDYE or PAH will result in the change of surface wettability, contact angle measurements were employed to characterize the multilayer ionic polymer adsorption on the patterned surface as shown in Fig. 5.1. Fig. 5.8 shows the contact angle of PAH/PDYE system as a function of number of layers adsorbed on sulfonated MPS and MPS surfaces. It can be seen in this figure that the contact angle drops from 57^0 to 43^0 upon immersion of the MPS modified substrate in the solution of PDYE, and then systematically alternates with the cation/anion deposition around 400. For the sulfonated MPS surface, the contact angle increases from 4^0 to 19^0 after one adsorbed PAH monolayer, and after 5 bilayers, the contact angle has increased to about 40^0, approaching the value for the corresponding thiol substrate.

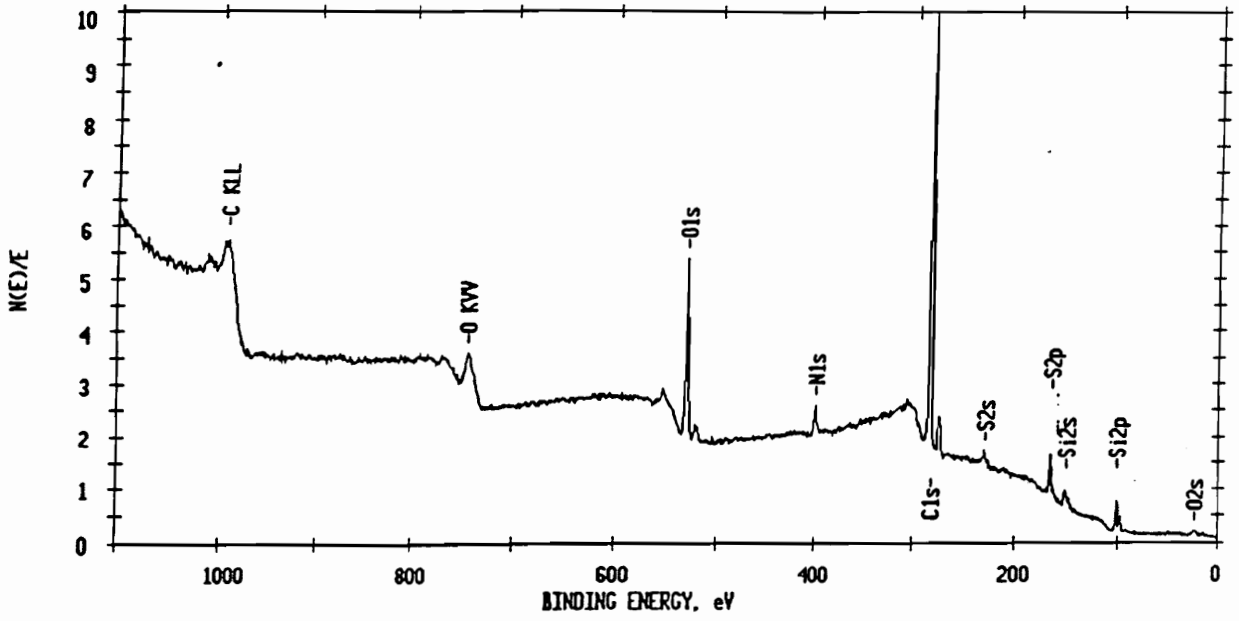

Fig. 5.6. The XPS spectrum of 5 bilayers of PAH/PDYE adsorbed on photo-oxidized MPS monolayer film.

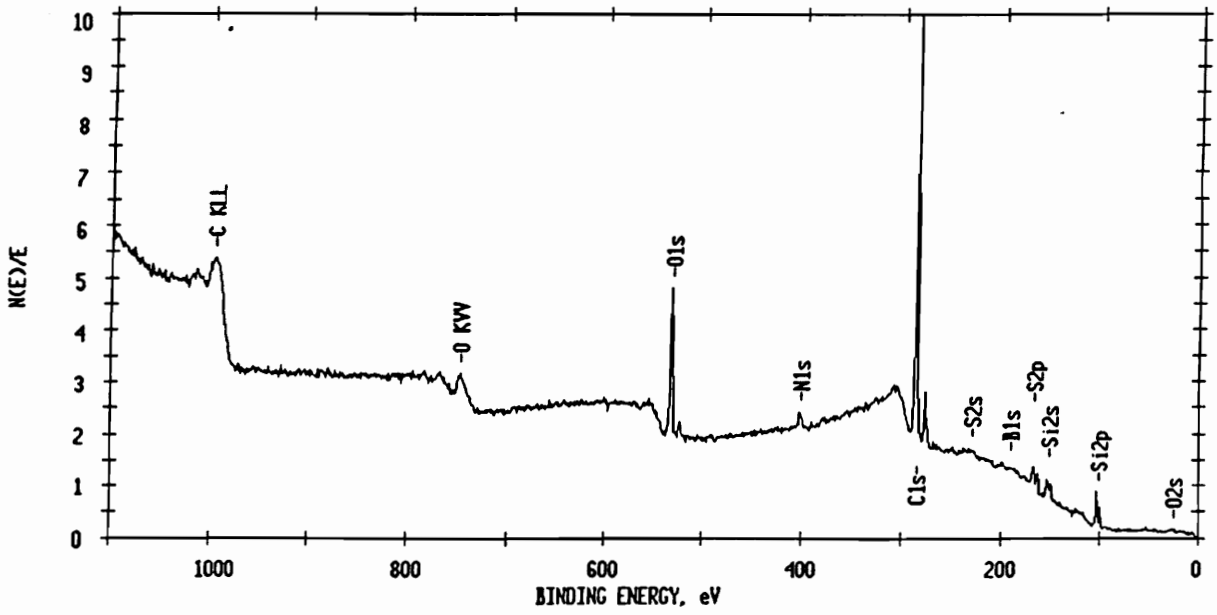

Fig. 5.7. The XPS spectrum of 5 bilayers of PAH/PDYE adsorbed on an intact MPS monolayer film.

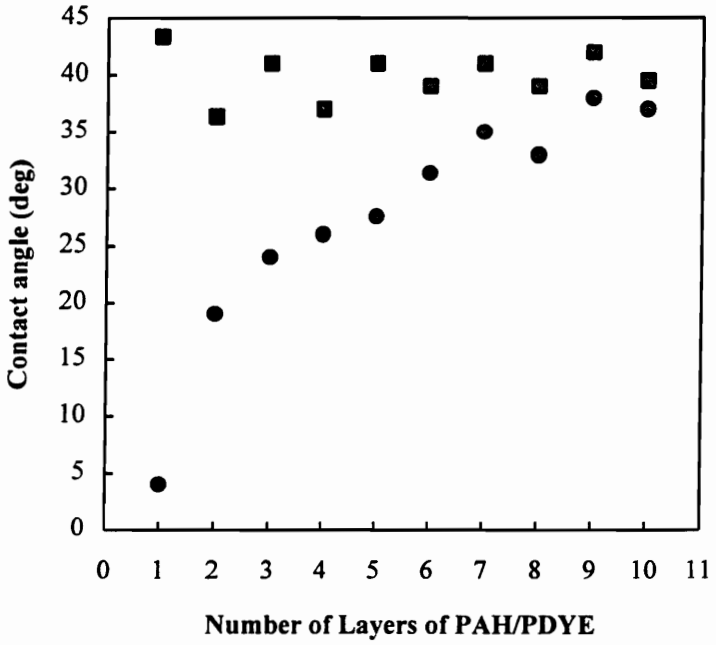

Fig. 5.8. Contact angle as a function of number of layers of PAH/PDYE system buildup on sulfonated MPS surface and MPS surface.

5.5 Conclusions

In summary, it has been demonstrated that molecular level multilayer film of PAH/PDYE system can be successfully buildup on sulfonated and sulfide modified surfaces using only dilute aqueous solutions of these materials. Since sulfonated and sulfide surface can be found in many materials such as polymer composites, ceramics and organic and inorganic solids, and Along with the techniques presented in the other chapters, layer-by-layer self-assembly films really open up vast new possibilities in the fabrication of complex, multicomponent heterostructure which can be usde in microelectronics, electroluminescence and optics.

5.6 References

1. G. Decher, and J. D. Hong, European Patent, application number 91 113 464.1.
2. G. Decher, and J. D. Hong, *Ber. Bunsenges. Phys. Chem.*, **95**, 1430 (1991).
3. G. Decher, and J. Schmitt, *Prog. in Colloid & Polymer Sci.*, **89**, 160 (1992).
4. G. Decher, Y. Lvov, and J. Schmitt, *Thin Solid Films*, **244**, 772 (1994).
5. J. H. Cheung, A. F. Fou, and M. F. Rubner, *Thin Solid Films*, **244**, 985 (1994).
6. M. Ferreira, J. H. Cheung, and M. F. Rubner, *Thin Solid Films*, **244**, 806 (1994).
7. K. S. Bhatia, J. J. Hickman, and F. S. Ligler, *J. Am. Chem. Soc.*, **114**, 4432 (1092).
8. F. M. Fowkes, Ed., *Contact Angle, Wettability and Adhesion*, Advance in Chemistry 43, American Chemical Society, Washing D. C., 1964.
9. S. R. Holmes-Farley, R. H. Reamey, T. J. McCarthy , J. Deutch, and G. M. Whitesides, *Langmuir*, **1**, 725 (1985).
10. N. Balachander, C. N. Sukenik, and J. E. Zull, *Langmuir*, **9**, 3009 (1993).
11. J. H. Cheung, A. F. Fou, and M. F. Rubner, *Thin Solid Films*, **244**, 985 (1994).

12. G. Mao, Y. Tsao, M. Tirrell, H. T. Davis, V. Hessel, and H. Ringsdorf, *Langmuir*, **9**, 3461 (1993).

13. H. Shin, R. J. Collins, M. R. De Guire, A. H. Heuer, and C. N. Sukenik, *J. Mater. Res* **10**, 692 (1995).

14. J. Papenhuijzen, G. J. Fleer, and B. H. Bijsterbosch, *J. Colloid, Interface Sci.*, **104**, 530 (1985).

15. J. Marra, H. A. van der Schee, G. J. Fleer, and J. Lyklema, *Adsorption from Solution*, Eds, R. H. Ottewill, C. H. Rochester, and A. L. Smith, Academic Press, 245, 1983.

16. G. J. Fleer, M. A. Cohen Stuart, J. M. H. M. Scheutjens, T. Cosgrove, and B.Vincent, *Polymers at Interfaces*, Chapman & Hall, New York, 1993.

Chapter 6

Patterning of Ultrathin Ionic Polymer Films by A Self-Assembly Process And Photolithography

6.1 Abstract

A recently developed self-assembly technique has been used to form novel and unique patterns in layer-by-layer polymer films. In this chapter, three different methods of micropatterning fabrication will be discussed and characterized by scanning electron microscopy (SEM). In order to selectively grow a second type of patterned film regions, several functional molecules were utilized to block further deposition over previous deposited regions. The UV/Vis absorbance and contact angle measurements were employed to investigate such end-capping effects. Dodecyltrimethylammonium bromide (DTAB) exhibits the desired blocking effects on self-assembled multilayers, the effectiveness of which depends on the concentration of DTAB and the orientation and quality of the underlying polymer film.

6.2 Introduction

In the first section, we report the development of three novel micropatterning methods for the deposition of patterned polymer. The distinguishing characteristic of our method over those previously reported that our layer-by-layer method forms the pattern first. Then the thick multilayer films are selectively adsorbed onto the patterned regions without using any etchants. Masked UV irradiation of silicon supported photoresist material is used to create a patterned surface of bare silica. In the first method, a chemisorbed SAM film of Octadecyltrichlorosilane (OTS) was deposited on such a

surface. Since the patterns in the conventional photoresist limits the initial adsorption of the SAM film, the monolayer of Octadecyltrichlorosilane (OTS) was adsorbed inly onto the irradiated areas of the substrate. After solvent stripping the remaining photoresist, the unexposed regions can then be modified with a second SAM film, terminated by an ionic group such as the negatively charged sulfonate or positively charged ammonium. The alternating deposition of polyionic materials will be directed into these charged areas [1-4], since the long unreactive chain of OTS will resist adsorption of ionic polymers. This kind of patterning methodology could provide for numerous applications of patterned polymeric materials.

Few experts deny the growing importance of advanced display technologies. Their uses range from lightweight flat-panel screens for portable computers to equipment for projecting wall-size high-definition television images [5]. For technologists, designing and building flat-planel and projection displays constitute major challenges. Many activites such as materials processing and lithography need to be developed in order that full-color (RGB) molecular pixels can be aligned on the substrates.

In the second section of this Chapter, we report progress toward such a purpose by using a novel self-assembly technique and photolithography. The characteristic of distinguishing this method from that above is that a second film type, with a different function (color, conductivity, magnetism, optical properties etc.), can easily be deposited onto different areas of the substrate after blocking films are introduced atop the pre-existing polyion multilayers. In this process, masked UV irradiation of photoresist produces patterns of bare silicon surrounded by photoresist. Then the multilayer ionic polymer films can be deposited onto the bare hydroxy silicon surface by self-assembly. After the sequential buildup of film regions, the photoresist is removed by a chemical wash. Thus, a self-assembled monolayer pattern is fabricated by selective deposition of

polyion multilayers using the photoresist/mask method. Dodecyltrimethylammonium bromide (DTAB) has been employed to block the further growth of the second film type on the sites of the first film type. From the results of UV/Vis spectroscopy and contact angle measurements, we find that the blocingk efficiency depends and on the concentration of DTAB and the orientation and quality of the polymer films.

6.3 Experimental

6.3.1 Materials

Poly(sodium 4-styrenesulfonate) (NaPSS, MW=70,000), and Poly(allylamine hydrochloride) (PAH, MW=50,000-65,000) and Dodecyltrimethylammonium bromide (DTAB) were obtained from Aldrich. Octadecyltrichlorosilane (OTS) and N-2-Aminoethyl-3-Aminopropyltrimethoxysilane (APS) were purchased from Huls America Inc. Stearylamine (octadecanamine), p-toluenesulfonic acid and chloroform were obtained from Sigma. All the above materials were used without further purification.

6.3.2 Characterization of the Multilayer Film Systems

6.3.2.1. Ellipsometry

Ellipsometric measurements were made using a variable angle spectroscopic ellipsometer (J. A. Woollam Co.) with a xenon source. The measurement details have been reported in chapter III.

6.3.2.2. Scanning Electron Microscopy (SEM)

The SEM technique employs the intensity of the secondary electrons. Some of these electrons recombine with ions at the interface, and as a result, photons are released which are the basis for the SEM imaging capability. The contrast in the image is a result of

deferences in scattering from different surface regions. SEM is an ideal tool to confirm the patterns of polymer films and has been utilized widely in the study of surface morphology, domains, pinholes, and defects .

In our study, the patterned surface was examined using an ISI SX-40 scanning electron microscope. The samples were sputter-coated with approximately 30-40 nm of gold to prevent surface charging by the electron beam and mounted onto the sample holder with double-sided tape. Two drops of silver paint were employed to make an electrical connection between the aluminum mount and the gold-coated surface, so that excess surface charge could be dissipated.

6.3.3 Preparation of Substrates

Single crystal Si substrates were cleaned to insure that photoresist adhered to the surface and that the chemical processing steps occurred to completion. Greasy materials were removed by rubbing the surface with filter paper saturated with Micro detergent (International Products Corp.), followed by a rinse in Milli-Q water. Then, the substrates were cleaned again according to the RCA standard cleaning procedure [6]. The substrates were finally baked in the atmosphere for 60 min at 130^{0}C.

6.3.4 Photolithography Techniques [22].

Positive photoresist Microposit 1450J (Shipley, PA) was spun at 4000 rpm for 30 sec. Then, the resist coating was cured for 30 min at 90^{0}C. A high resolution pattern was transferred to the resist by forming a contact print to the substrate with a mask containing the lithographic pattern (step 2 in Fig. 6.1). The resist was exposed to UV light from a low pressure mercury lamp for 14 min. The exposed surface was developed for 90 sec in

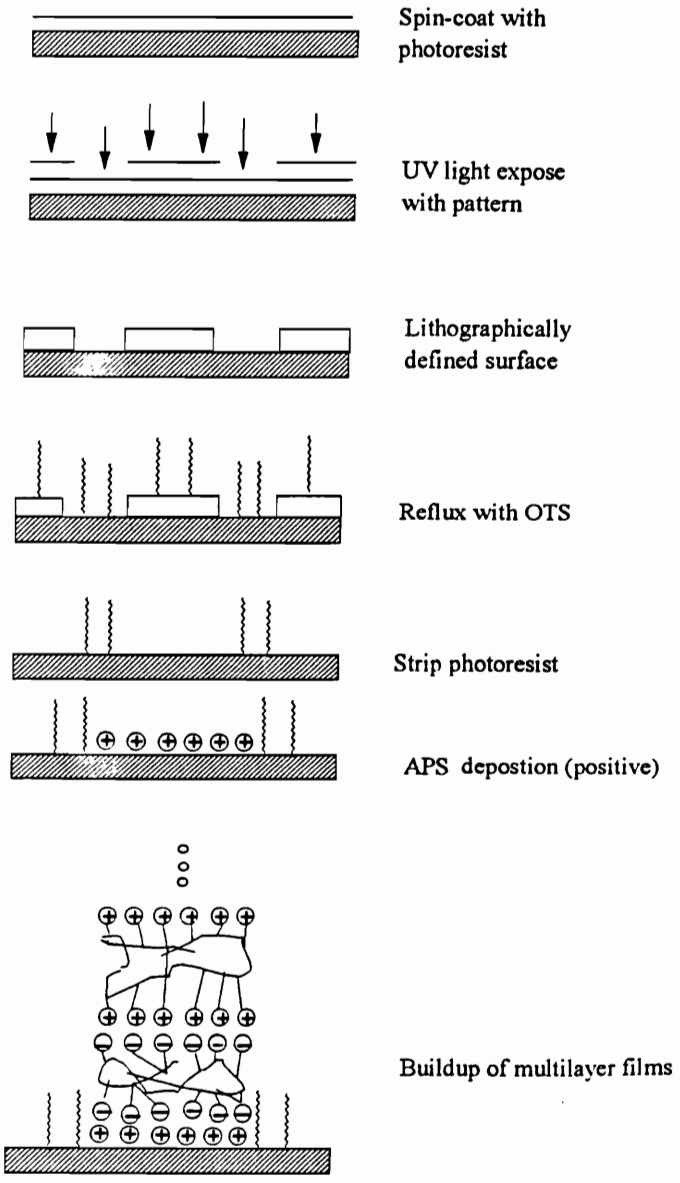

Fig. 6.1. A schematic representation of the steps required for the patterning of multilayer films with polycation and polyanion molecules.

Microposit MF-314 developer (Shipley, PA), followed by rinsing with water and blown dry with nitrogen gas. It was then baked at 100°C for 30 min.

6.3.5 Micropatterning of Surfaces (I)

Alkane chains were covalently bonded to the lithographically exposed substrate areas ($2.1x10^{-4}cm^2$) by refluxing the substrate in a solution containing an alkyltrichlorosilane (step 4 in Fig. 6.1).The substrate was refluxed for 20 hr in a 5% (vol/vol) solution of OTS dissolved in hexane, followed by 2 1-hr reflux steps in pure hexane to remove unbound OTS material.

The remaining photoresist was removed by ultrasonic aggitation in acetone (step 5 in Fig. 6.1). Two agitation cycles of 10 min each were used, each followed by a brief rinse in propanol. The substrate was dried under a stream of nitrogen gas. At this stage, the surface contained a pattern of alkylated regions on freshly cleaned silicon.

The amino functionality was introduced to the unmodified regions of the surface by reacting the substrate with APS, an aminotrihydroxysilane (step 6 in Fig. 6.1). The deposition solution was 1.0 % (vol/vol) APS in 95% methanol and 5% Milli-Q water, adjusted to pH 5.0 with acetic acid. The solution was used within 30 min of preparation to minimize cross linking between the silanols. The substrate was exposed to the solution for 5 min, washed 4 times with methanol, dried under a nitrogen gas stream, and baked in an air atmosphere at 110°C for 10 min. The resulting surface contained patterns of alkylated domains (OTS) surrounded by a monolayer terminated with an ammonium salt (APS).

All deposition solutions were maintained at pH 3.5 to assure protonation of the APS surface. The sulfonate groups of PAH are completely deprotonated at this pH value. The substrate was immersed for 15 min in an aqueous solution containing 80 mg of PSS at pH 3.5 (HCl), followed by vigorous washing in Milli-Q water. The first layer of PSS

adsorbs only to the positively charged ammonium regions. The substrate was then immersed in an aqueous solution containing 80 mg of PAH at pH 3.5 (HCl) for 15 min, followed by extensive washing 25 times with Milli-Q water. The monolayer film of PAH adsorbted to the first layer of PSS due to the electrostatic attraction between these oppositely-charged polyions. As the above procedure was repeated, multilayers of PSS/PAH were built up on the patterned regions.

6.3.6 Micropatterning of surfaces (II)

Another procedure for fabricating patterned layer-by-layer polyion films is shown in Fig. 6.2. In this process, masked UV irradiation of photoresist produces patterns of bare silicon surrounded by photoresist. Then the multilayer ionic polymer films can be deposited by self-assembly onto the bare hydroxy silicon surface (and also possibly the regions of photoresist). After the buildup of the films, the photoresist is removed by a chemical wash. Thus, a self-assembled monolayer pattern is fabricated by selective deposition of polyion multilayer using the photoresist/mask method.

6.3.7 Micropatterning of surfaces (III)

The third procedure for fabricating patterned layer-by-layer polyion films is shown in Fig. 6.3. In this process, when the bare silicon surfaces were patterned by removal of photoresist, N-2-aminopropyltrimethoxysilane (APS) molecules were covalently bonded to the bare regions by a self-assembly process (Chapter II and III). The substrates are kept in an acidic aqueous solution so that the amino groups of APS are protonated and the regions become positively charged. Here, the layer-by-layer polyion build up was initiated by deposition of PSS and continued in the same fashion as before (Chapter II and III).

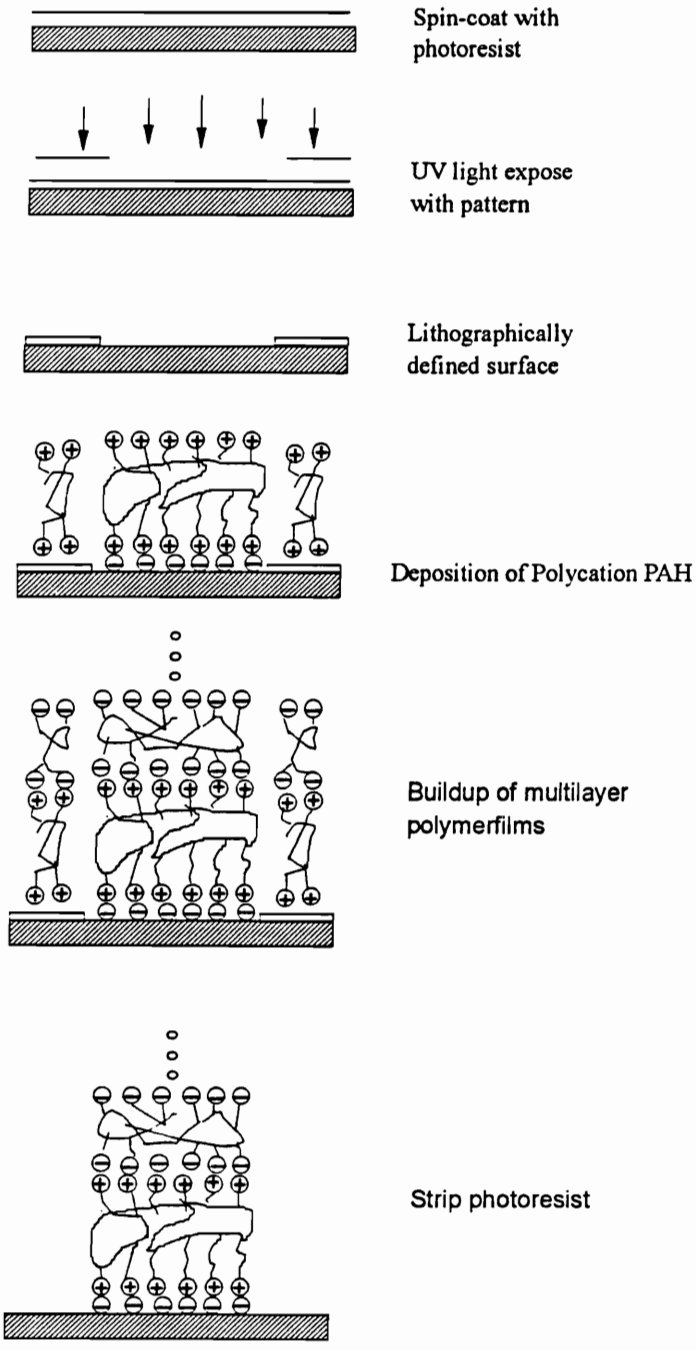

Fig. 6.2. A schematic representation of the steps required for the patterning of multilayer films with polycation and polyanion molecules.

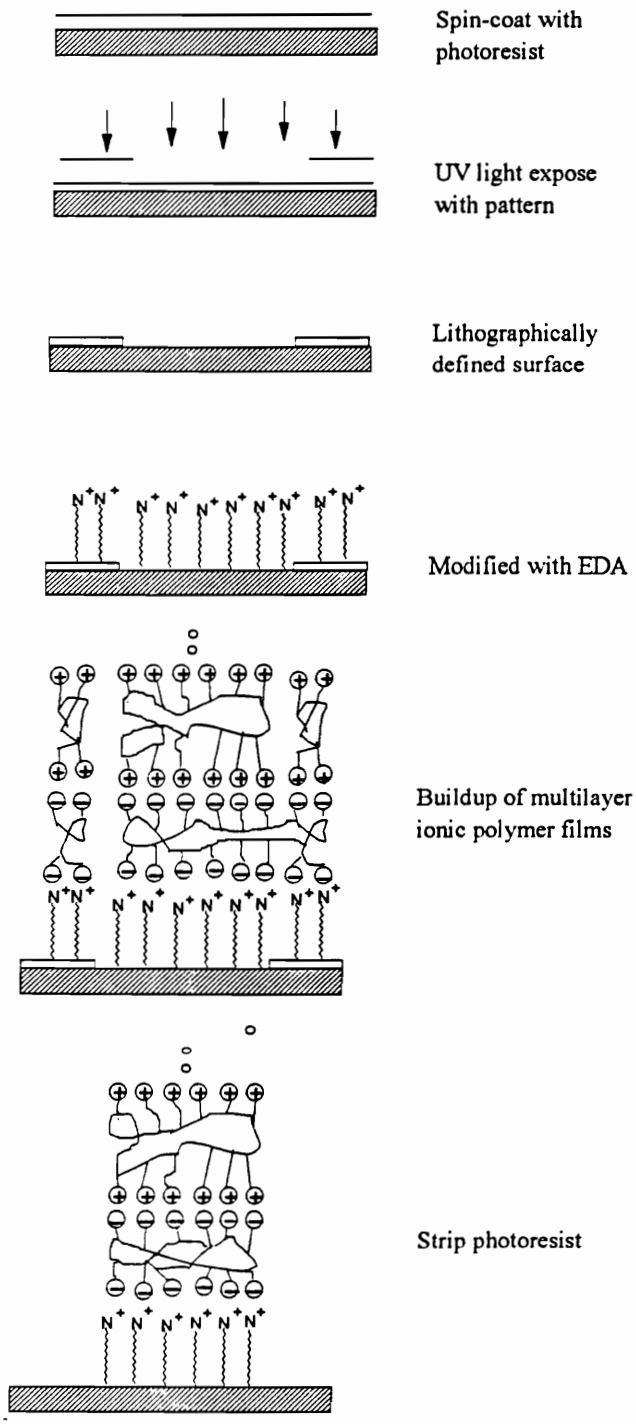

Fig. 6.3 A schematic representation of the steps required for the patterning of multilayer films with polycation and polyanion molecules.

6.4 Results and Discussion.

6.4.1. Micropatterning of surfaces (I)

The principle of this patterning technique is to sequentially buildup SAM's in defined areas by alternating adsorption of two polyelectrolytes of opposite charge after we have patterned a silicon substrate a different function. Neutral, hydrophobic alkalized regions and positively charged amino areas are created, so polyion adsorption is directed only to the charged regions. The desired thickness of these features can be reached by repeating the deposition steps as many times as needed [1-3]. The thickness of each ionic polymer monolayer ranges from 0.6 to 3.3 nm [23]. The larger thicknesses are obtained when salts (conterions) are added to the aqueous polyelectrolyte solutions, whereas the smaller thicknesses are obtained from dilute solutions and low salt concentrations.

Patterned film deposition was confirmed by Scanning Electron Microscopy (SEM). There was a distinct contrast observed between the round alkylated regions and their surrounding polymer multilayers, as shown in Fig. 6.4. The area of a given round region is about 2.1×10^{-4} cm^2. These regions contain only alkane (OTS) chains bound to the underlying surface. Only weak interaction occur between OTS and NaPSS or PAH, so frequent washes with water prevent any buildup of material onto the OTS surface. Thus, there is only a monolayer of OTS in the round areas, which are observed to be relatively bright in Fig. 6.4. The multilayer regions consisting of 29 bilayers of polyanion/polycation were prepared by consecutive adsorption steps of NaPSS and PAH. Ellipsometry measurements indicate that the average thickness of a bilayer of NaPSS and PAH is about 1.28 nm. The thickness of the total ionic polymer film is therefore 37.12 nm. These regions appear relatively dark in Fig. 6.4. It is clear that the ionic polymer molecules have selectively deposited on the charged regions. At this level of resolution, we observe excellent reproduction of the mask features. However, close inspection reveals that the

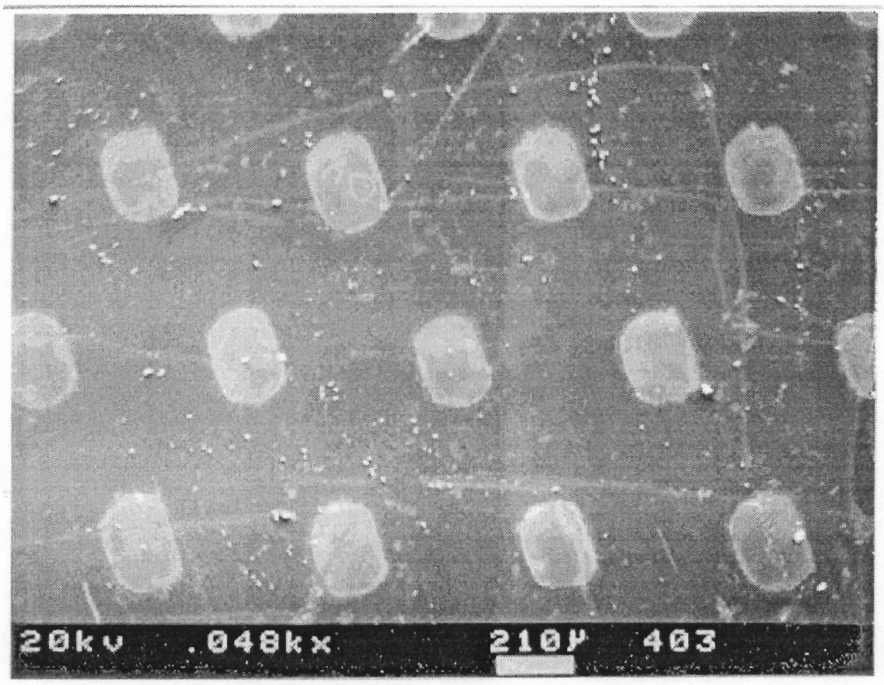

Fig. 6.4 SEM image of patterning (I) of ultrathin ionic polymer films by a self-assembly process and photolightgraphy.

lateral dimensions of the round regions are somewhat less than the mask edges, this might come from some photoresist that has not developed well and therefore remains on the substrate. It is also possible that the polyion adsorption starts to fill-in the holes by adsorbing to the inside walls of the OTS pits. In principle, all polyelectrolytes (including conjugated polymers, and metal oxides) can be used for this adsorption process, so the patterning strategy described here promises to be generally applicable. Perhaps of greater technological .interest, this process provides a very easy and low cost method for automation of patterned polymer film deposition. As the resolution of photolithography reaches sub-micron dimension, there is no foundamental limitation to fabricating the micron-scale patterns of ionic polymer films.

6.4.2. Micropatterning of surfaces (II) and (III)

In this method, we pattern a silicon substrate with different functionalized regions that are either negatively charged (most inorganic solids have negatively charged surfaces in the weak acidic and basic solutions) or positively charged (amino groups) and buildup multilayers in the selected areas by alternating adsorption of two polyelectrolytes. Using this methodology, the polymer films are also deposited on the remaining photoresist. However, the remaining film-covered photoresist is eventually removed by a chemical wash (Figs. 6.2 and 6.3). In contrast to the micropatterning of surfaces (I), the multilayers are built-up into the round regions, whereas the surrounding areas remain unchanged (bare silicon).

Patterned film deposition by micropatterning method II was confirmed by Scanning Electron Microscope (SEM) as shown in Fig. 6.5. There was a distinct contrast observed between the round film regions and the surrounding bare silica area, as shown in Fig. 6.5. The area of a given round region is about 2.1×10^{-4} cm^2, 50 bilayers of PAH/PSS

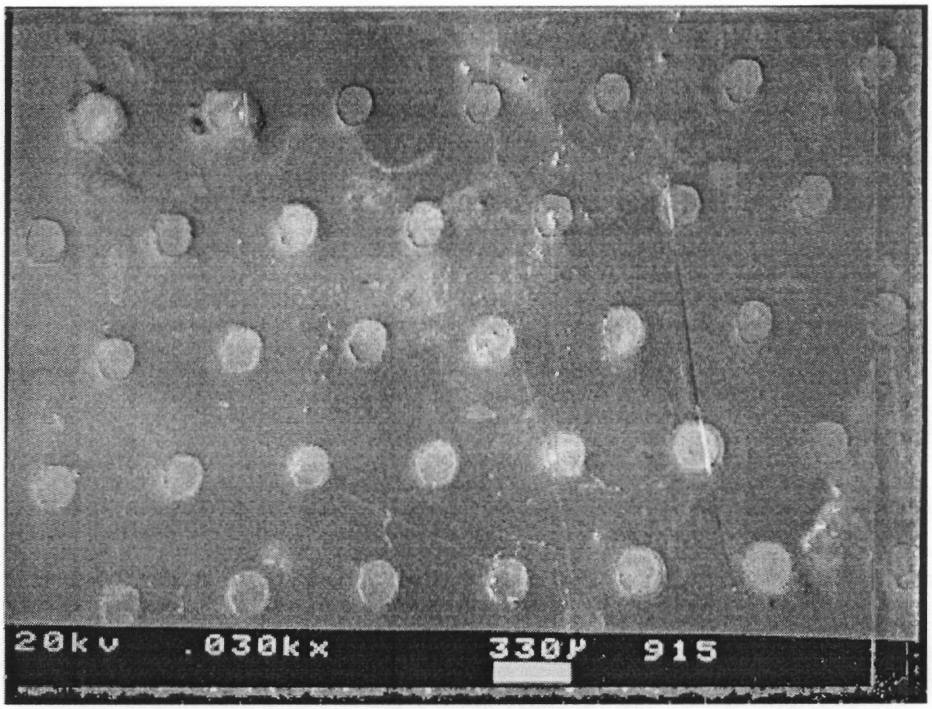

Fig. 6.5 SEM image of patterning (II) of ultrathin ionic polymer films by a self-assembly process and photolithography.

films with a thickness of about 64 nm were deposited onto these round regions by consecutive adsorption steps of NaPSS and PAH. The distinct convex shapes of the round regions can be seen from Fig. 6.5. It is clear that the ionic polymer molecules have selectively deposited into the charged regions. At this level of resolution, we observe excellent reproduction of the mask features.

A similar patterning process (micropatterning of surfaces III) is shown in Fig. 6.3. In this case, when the bare silicon surfaces were patterned by removal of photoresist, N-2-aminopropyltrimethoxysilane (APS) molecules were covalently bonded to the bare round regions by a self-assembly process (Chapter III). The substrate was then immersed in an acidic aqueous solution so that the amino groups of APS were protonated and the regions were positively charged. Here, the layer-by-layer polyion buildup was initiated by deposition of PSS and continued in the same fashion as before. Again, the pattern of 50 bilayer columns of PSS/PAH was confirmed by SEM as shown in Fig. 6.6.

By using the above procedures, we have demonstrated that we can direct the deposition of polyion multilayers onto any charged surface and that the polymer film is stabled with respect to removal of the surround photoresist templates. With our work discussed in the previous section, these results provide the basis of a new sequence for multilayer patterning in which the patterns are formed first, and selective adsorption is utilized.

6.4.3. Blocking Effects of Functional Molecules on Ionic Polymer Films

In order to deposit a second film in regions neighboring the first film, the first type of film must be "capped" in order that the deposition of a second film is directed only to the newly defined areas and not to previously deposited ones. To accomplish this, an inert

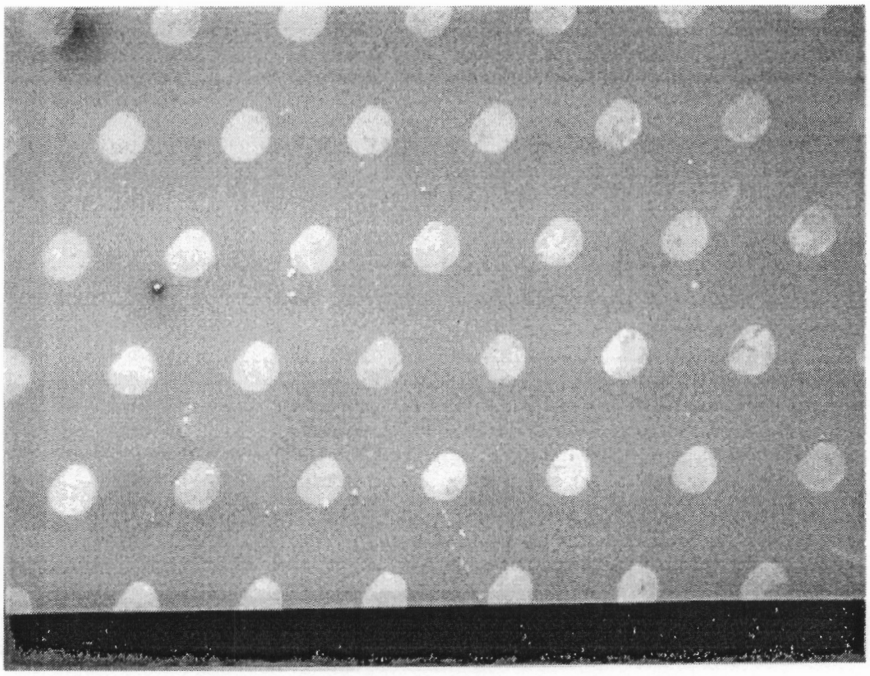

Fig. 6.6 SEM image of patterning (III) of ultrathin ionic polymer films by a self-assembly process and photolithography.

saturated alkane chain is introduced atop the pre-existing polyion multilayer through ionic attraction.

Several long alkane chain molecules which have an amine group on one end have been investigated. Six glass slides were immersed in a solution containing 16.2 mg of stearylamine (octadecanamine), 11.4 mg of *p*-tulenesulfonic acid, and 60 mL of chloroform at room temperature for different time intervals. Afterwards, the substrates were sonically washed with chloroform three times each for 3 min, followed by air drying. The water contact angle measurements give values of $32^0 \pm 2^0$ for all those time intervals (from 5 min to 35 min) as shown in Table 6.1. The samples were then dipped into the solution containging 80 mg of PSS and 40 mL ultrapure water for 15 min, followed by a vigorous rinse with ultrapure water. The water contact angle goes up to $43^0 \pm 2^0$. The substrate was then immersed in a solution containing 90 mg of PAH, and 40 mL of ultrapure water for 15 min. After the excess absorbant was washed away with ultrapure water, the contact angle reached $53^0 \pm 2^0$. These results indicate that these molecules do not work well to prevent further adsorption of ionic polymers probably due to a limited solubility in water which precludes the deposition of a well ordered film. The observed contact angle of only 30^0 is far below the expected value of 70^0 [7].

In order to study the effects of concentrations on the formation of a capping monolayer, two glass slides were immersed in a lower (1/16) concentration solution containing 1 mg of stearylamine, 0.7 mg *p*-tulenesulfonic acid, and 60 mL of chloroform for 15 min and 40 min, respectively. The slides were then ultrasonically rinsed with pure chloroform 3 times each for 3 min. The water contact angle was 17^0 for the two samples. These results show that a worse coverage has been obtained from the lower concentration.

Based on this previous experience, it seems that C-12 to C-14 length chains might be appropriate for our purpose, since they are not only soluble in the aqueous solution, but

Table 6.1. Contact angles of octadecanamide solution adsorbed on glass slides as a function of the deposition time.

Time (min)	5	10	15	20	25	30
Contact Angle (^{0})	31± 2	32± 2	33± 2	31± 2	32± 2	32± 2

also are long enough to provide the level of protection necessary to block the further adsorption. The adsorption of cationic surfactants by silica samples, particularly in relation to the medical and pharmaceutical applications of these systems, has been studied by Rupprecht et al. [7-9], their results support a model proposed by Rupprecht: At low surfactant concentrations a monolayer is formed due to interactions between opposite charges on the silica surface and the surfactant ions. At higher concentrations a different mechanism (probably hydrophobic bonding) causes a bilayer to be built up. In our case, dodecyltrimethylammonium bromide (DTAB) has been employed to block further growth of a second system of film on the sites of the first system. Fig. 6.7 shows the contact angle of DTAB on the silica surface as a function of its concentration in aqueous solution at pH 4. It is obvious that only partial coverage occurs for concentrations below 10^{-5} M, since the contact angles continue to increase as the concentration increases. The contact angle then reaches a plateau for the concentration range about 10^{-5} to 10^{-2} M, indicating that a monolayer is formed. As the concentration continues to increase to near its CMC point of $1.2\text{-}1.4\text{x}10^{-3}$ mmole/l [10], the contact angle suddenly falls down from 60^0 to 18^0, suggesting that bilayer has been formed at the interface as depicted in Fig. 6.8. The general character of our curves is consistent with those of Rupprecht *et al* [7]. The DTAB layer is adsorbed via an electrostatic mechanism with the ionic groups associated with SiO^- groups on the surface. Such an arrangement implies coverage of the surface with the hydrophobic tails directed upward for multilayers adsorbed from the lower concentration of solution (Fig. 6.8b). At the higher concentrations, bilayers are formed (Fig. 6.8c). Gaudin and Fuerstenau describe this process as hemi-micelle formation [11]. Therefore, optimal adsorption of the cation is reached just below the CMC.

We observe, in some cases that even at concentrations around 10^{-4} M to 10^{-3} M, the contact angles of DTAB monolayers are about 40^0 rather than 60^0. This might indicate

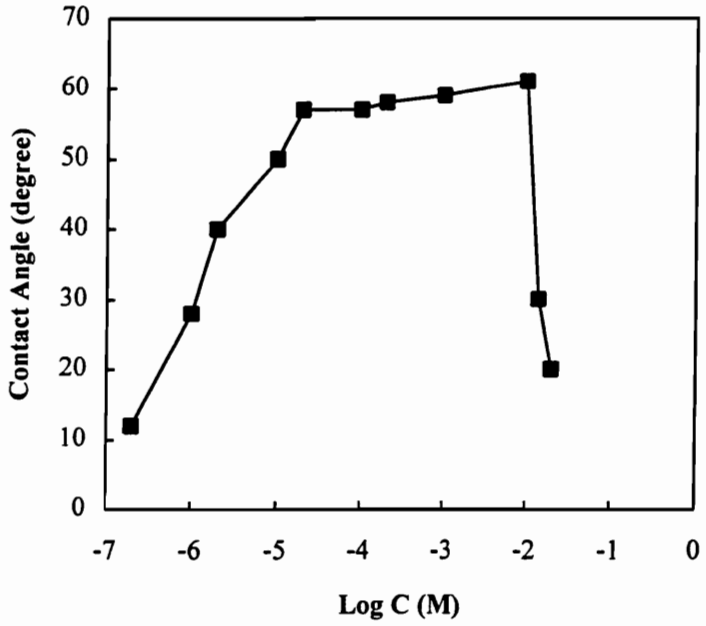

Fig. 6.7. Contact angle on the surface of DTAB film adsorbed on the silicon surface as a function of concentration of DTAB.

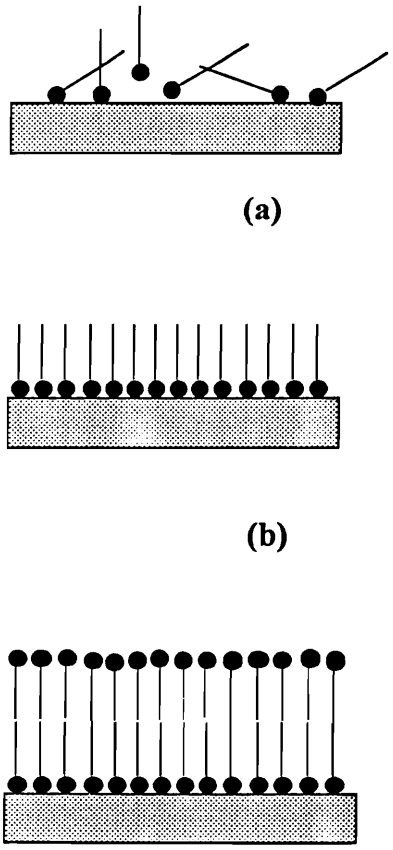

Fig. 6.8. Schematic representation of the adsorption of DTAB molecules at different concentrations on a negatively charged surface. (a) at dilute solution; (b) at moderate concentration; (c) at high concentration.

that a partial second layer of DTAB has been adsorbed. A similar model has been proposed for DTAB adsorption onto a crystalline silica [12-13] and for negatively charged dodecylsulfate ions onto positively charged $BaSO_4$ [11]. This might also arise from the quality and orientation of the top ionic film, so a partial (or a bad film) coverage of DTAB has been formed atop the ionic multilayers.

In order to check the blocking effect of DTAB, the concentration of 10^{-3} M was choosen. UV/Vis absorption spectroscopy was employed to monitor adsorption of PSS. Typical adsorption times for DTAB on the PSS film were 30 min. The results are shown in Fig. 6.9. Upon adsorption of DTAB, the UV/Vis absorbance intensities do not increase significantly, indicating that DTAB can prevent further adsorption of the ionic polymers onto the films. Even though there might be some weak adsorption of the ionic polymer onto the methyl-terminated DTAB film, the washing cycles appear to remove any such buildup.

From the above results on the blocking effects of DTAB, it can be concluded that DTAB monolayer films atop the PSS/PAH ionic polymer films work well to prevent the further growth of polyelectrolyte films.

6.5. Conclusions

In summary, we have demonstrated that the selective deposition of multilayer polymer films to specific functionalized regions can be used to form bottom-up (vertical) patterning of polymer films on silicon substrates. We hope to use this technique to tailor micro-fabricated structures with different functional groups. The importance of this method results from the fact that unique electronic and photonic properties of certain polymeric materials might be integrated into Si-based devices by using this simple patterning technique.

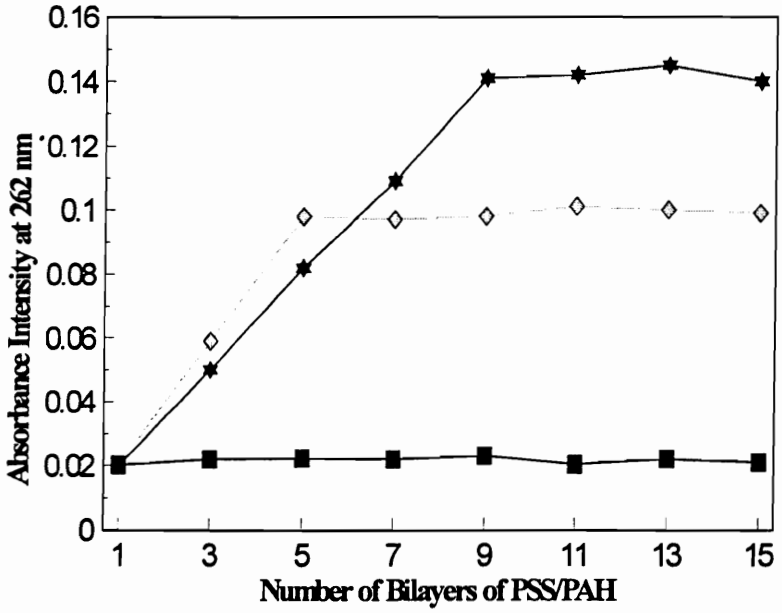

Fig. 6.9. Optical absorption of block efficiencies of DTAB film vs. number of bilayers of PSS/PAH multilayer films on quartzs.

6.6. References:

1. G. Decher, J.D. Hong and J. Schmitt, *Thin Solid Films,* **210/211**, 831(1992).
2. G. Decher and J. D. Hong , *European Patent,* application number 91 113 464.1.
3. G. Decher and J.D. Hong , *Ber Bunsenges. Phys. Chem.* **95**, 1430(1991).
4. J. H. Cheung, A.F. Fou and M. F. Rubner, *Thin Solid Films*, **244**, 985(1994).134
5. D.A. McGillis, Lithography, In *VLSI Technology,* S.M. Sze ed., McGraw-Hill, New York, P267, 1983.
6. W. Kern ed. *Handbook of Semiconductor Wafer Cleaning Technology,* Noyes Publications, 1993.
7. H. Rupprecht, E. Ulmann, and K. Thoma, *Fortschr, Kolloide Polymere*, **55**, 45 .(1971).
8. H. Rupprecht, *Kolloid-Z, Z. Polum.*, **249**, 1127 (1971).
9. H. Rupprecht, *J. Pharm. Sci.*, **61**, 700 (1972).
10. B. H. Bijsterbosch, *J. Colloid Inter. Sci.*, **47**, 1, 186 (1974).
11. A. M. Gaudin, and D. W. Fuerstenau, *Ann. Un. Sci. Budapestinensis, Sect. Chim.*, **11**, 19 (1969).
12. D. J. O'Connor, and A. S. Buchanan, *Trans. Faraday Soc.*, **52**, 397 (1956).
13. B. Tamaushi, *Kolloid-Z*, **150**, 44 (1957).

Chapter 7

Summary and Future Work

7.1 Summary

Heterostructure multilayer thin films comprised of chromophore polymer, poly s.119 (PDYE) with poly(allylamine chloride) (PAH), and poly(sodium styrenesulfonate) (PSS) have been successfully fabricated on different substrate surfaces such as single crystal silicon, quartz, hydrophilic glass, as well as sulfonate- and thiol-functioal surface via self-assembly process through physisorption (SAMp). The process involves the alternate dipping of a substrate into an aqueous solution of a polycation followed by dipping an aqueous solution of polyanion. UV/Vis absorbance, contact angle and ellipsometry measurements revealed that in all cases the bilayer deposition process was linear and highly reproducible from layer to layer and film thickness of up to 1 μm can be easily obtained by repeating the deposition process. The typical thickness of bilayer film depends on the solution concentration. Our results also demonstrated that the mechanical stability of SAMp film is remarkably high and can only be removed from the surface by scraping. SAMp films are stable in common organic solvents and even in high acidic media (6 M HCl aqueous solution). The conformation of the films are thermally stable up to at least 150 ^{0}C. The deposition time for a full monolayer coverage of PDYE and PAH is about 20 seconds.

An novel and effective photochemical conversion of thiol groups into sulfonate ones has been developed. We show that close-packed, well-ordered 3-mercaptopropyl)trimethxysilane (MPS) monolayer can be found on the surface of single crystal silicon, quartz and glass by allowing hydrolyzed silane to self-assemble from a dilute hydrocarbon solution. The films of MPS were irradiated with the UV output of an ozone-producing Hg pencil lamp to photo-oxidize thiols to sulfonates. From contact angle

measurements and X-ray photoelectron spectroscopy, a complete oxidation of thiols on a silane-anchored surface can be seen to occur in as short as 15 minutes, and a complete wetting of the sulfonated substrate can be achieved. Moreover, masked UV exposure of a MPS monolayer film can be used to create patterned regions of sulfonate and thiol functionality. Such patterned template is the first and basic step for making patterns of biomolecules adsorption for various application. Such approaches can be expected to help to bridge the interaction between different materials and composites such as plastics, ceramics, metals and inorganic solids.

SAMp technique combined with photolighography was employed to develop two novel methods of micropatterning fabrication in an attempt to first achieve the goal of "bottom-up" approach for the nano-patterning technique. The characteristic of distinguishing our methods from the existed ones is that the patterning is done first and then the vertical multilayers are built-up on the patterned areas *i.e.* "bottom-up". In our methods, SAMp films are used as active species. Scanning electron microscopy (SEM) was utilized to confirm the patterning technique. Because of the unique characteristic of our patterning methods and SAMp technique, there is no doubt such patterning methods are ready for the nano-patterning fabrication. In order to block the further growth of the second film type on the sites of first film type, several molecules with inert function groups were tried. UV/Vis absorbance and contact angle measurements showed that dodecyltrimethylammonium bromide (DTAB) atop the SAMp film could prevent further adsorption of the ionic polymers.

7.2 Recommendations for Future Work

Since the SAMp technique has emerged as a powerful tool of processing and integrating various materials into ultrathin multilayer films with controlled thickness and

controlled molecular architecture. There are a lot of important and new chances existed. The following is suggested for the future study:

1. Low cost fabrication of nanocomposite film of polymer/TiO_2. In this system, anionic polymers such as polyimide, polystyrene, conjugated polymers is sandwiched between cationic TiO_2 complexes. The thickness of TiO_2 colloid is 2 nm (confirmed by TEM) and that of polymers vary from 6 to 31 Å depending on solution chemistry. Such film system can be fabricated on plastics, glass and metal substrates used as UV filter, membrane, high refractive index coating, waveguide, nonlinear optical device, quantum-sized p-n junction, p-n-p, n-p-n or p-n1-n2-p junction.

2. Fabrication of multilayer magnetic film of γ-Fe_2O_3 by a molecular-level layer-by-layer assembly process. First, Commercial nanosized γ-Fe_2O_3 particles are coated with bolaamphiphile molecules. The basic idea is to self-assemble bolaamphiphile on γ-Fe_2O_3 in such a way that one functioal group (-COOH) anchors to the surface through chemical bond formation and other ($-NH_2$) remains active for the formation of cationic amine. Then, in a similar way, the multilayer magnetic film is assembled by the SAMp technique.

3. .Patterned, multilayered magnetic , optical and electrical units. Combined our patterned technique, patterned thiol-and sulfonate-functioality, colloid chemistry, and SAMp technique, magnetic units of γ-Fe_2O_3 , conducting polymer units, and optical matrix (including light emitting device, waveguide, coupler, etc.) can be aligned and integrated into one device.

VITA

Yanjing Liu was born on June 19, 1956 in Beijing County, People's Republic of China to Huiying Qin and Wenzao Liu. His college began in 1978 when he was admitted to Department of Physics in Henan University in Kaifeng, Henan Province. In 1982, he received his B.S. degree and then worked as an instructor at the same University. In 1987, he was promoted to be Assistant Professor. He enrolled in Jilin University in 1986 and received his M.S. degree in physical chemistry in 1989. Then, he went back to Henan University to continue his teaching and research career as Assistant Professor. .

In order to continue his graduate study, he was admitted to Virginia Tech in 1992. His interest in nanotechnology led him to study under Dr. G. Alan Schick in Department of Chemistry. His current research interest includes the nanocomposite polyimide/TiO_2 and conducting polymer/γ-Fe_2O_3 multilayer films from self-assembly physisorption process. He has accepted a research associate position in Fiber & Electro-Optics Research Center at Virginia Tech.